2012

Genetic regulation of aleurone cell fate in Zea mays

Gibum Yi
Iowa State University

Genetic regulation of aleurone cell fate in *Zea mays*

by

Gibum Yi

A dissertation submitted to the graduate faculty

in partial fulfillment of the requirements for the degree of

DOCTOR OF PHILOSOPHY

Major: Plant Biology

Program of Study Committee:

Philip W. Becraft, Major Professor

Diane Bassham

Erik Vollbrecht

Paul Scott

Yanhai Yin

Iowa State University

Ames, Iowa

2012

TABLE OF CONTENTS

CHAPTER 1. General Introduction……..**1**

Thesis Organization……...7

References ……...8

CHAPTER 2. High-Throughput Linkage Analysis of Mutator Insertion Sites in Maize. ……**11**

Abstract……11

Introduction……..12

Results……..16

Discussion……23

Materials and methods……..……28

Acknowledgement……..31

References……..……32

Figure Legends……..……32

Tables and Figures……35

CHAPTER 3. The *thick aleurone1* Mutant Defines a Negative Regulation of Maize Aleurone Fate that Functions Downstream of *dek1*……..……**46**

Abstract…..……46

Introduction……..……...47

Results……..……..50

Discussion……59

Materials and methods……67

Acknowledgement……69

References……70

Figure Legends……77

Tables and Figures……83

CHAPTER 4. The *naked endosperm* genes encode duplicate ID domain transcription factors required for maize aleurone differentiation……**98**

Abstract……98

Introduction……99

Results……103

Discussion……113

Materials and methods ……117

Acknowledgement……121

References……121

Figure Legends……125

Table and Figures……129

CHAPTER 5. General Conclusions……**137**

References……140

ACKNOWLEDGEMENTS……**141**

CHAPTER 1. General Introduction

Cereal grains are essential for human society as food, animal feed, and industrial raw material such as biofuels and plastic. The triploid endosperm is the main tissue of cereal grains. The endosperm is composed of four different cell types; starchy endosperm, aleurone, basal endosperm transfer layer (BETL) and embryo surrounding region (Olsen, 2001; Sabelli and Larkins, 2009). Starchy endosperm is the main storage tissue containing most of the starch and proteins. Aleurone which is the epidermal cell layer of starchy endosperm contains vitamins, minerals and high quality proteins which are not included in starchy endosperm. The dietary benefits of cereal bran mostly come from the aleurone cells (Harris et al., 2005). Many studies support the dietary benefits of aleurone such as anti-obesity and anti-cancer activities (Fenech et al., 2005; Stewart and Slavin, 2009; Borowicki et al., 2010). As consumers gain more interest in eating a healthy diet, the research interest for the aleurone will also increase. Recently wheat aleurone extract has been commercialized for use as food additives.

Basically aleurone functions as a digestive tissue. Aleurone produces hydrolases to digest starch in the endosperm to produce nutrients for the germinating embryo. In some species, it is also known that aleurone is related with seed dormancy and seed germination which are also important agronomic traits. Aleurone provides amylase which is of major importance to the malting process to make recreational beverages. Maize is one of the three major crops

along with wheat and rice to serve as a model system to study endosperm development, especially aleurone. The maize kernel is the biggest among cereals. Furthermore, maize has many progenies on a single ear, and the kernels do not have glumes which makes it easy to screen for aleurone mutants. Because the aleurone is in the peripheral layer it is more accessible than any other cell type in the endosperm. Transient assays using aleurone cells make it easy to test in vivo activities. The maize aleurone and anthocyanin maker have long been used for transposon and other genetic studies.

Aleurone development

The cereal grain has three parts; endosperm and embryo are both enclosed within maternal tissue, pericarp. Four different cell types in the endosperm originate from the single 3n primary endosperm cell and each has specialized functions. The basal endosperm transfer layer (BETL), which is the basal layer close to the maternal pedicel and characterized by its extensive cell wall invaginations, helps to absorb nutrients from the maternal plant when seeds are developing (Hueros et al., 1995; Hueros et al., 1999a; Hueros et al., 1999b). Embryo surrounding region (ESR) cells, which show specific *ESR* gene expression early in the endosperm development, surround the young embryo and are proposed provide communication between the embryo and endosperm (OpsahlFerstad et al., 1997; Bonello et al., 2000; Bonello et al., 2002). Starchy endosperm functions as storage cells, which are full of starch granules and

protein bodies. Starchy endosperm fills the entire internal parts of the endosperm mass. The peripheral layer of the endosperm is the aleurone layer which remains alive during desiccation when starchy endosperm undergoes programmed cell death. Aleurone is a digestive tissue that produces enzymes such as amylase when the seed is germinating to break down the nutrients of starchy endosperm. This provides sugars and free amino acid to the germinating embryo. Generally cereal grains have a single layer of aleurone but there are some exceptions; barley has two to four layers of aleurone, some varieties of rice have variable number of aleurone and one of maize landrace, Coroico, has multiple layers of aleurone (Wolf et al., 1972a). Aleurone cells undergo a different development program from starchy endosperm.

Upon double fertilization, one sperm nucleus and two polar nuclei in the central cell undergo karyogamy to produce triploid primary endosperm. The endosperm cell then undergoes mitotic nuclear divisions without cytokinesis to produce multi nuclei within a common cytoplasm, otherwise known as a syncytium or coenocyte. At 128-256 cell stage the nuclei are arranged on the periphery of the central cell. Cell walls form to produce alveoli which are tube like cell wall structures with one side open to the central vacuole (Olsen, 2004c). These cells undergo cellularization to fill the central vacuole. The peripheral cells, which are the aleurone initials, actively divide periclinally and anticlinally, maintaining meristematic function. These meristematic peripheral endosperm cells produce both aleurone cells and starchy endosperm cells. Aleurone appears about 7-9DAP at the peripheral endosperm when aleurone granules can

first be detected. Preferential anticlinal cell division also supports the aleurone cell identity (Morrison et al., 1978). The presence of preprophase bands (PPBs) in peripheral layer and absence in internal starchy endosperm suggests different cell fates have been established at the onset of cellularization. However the aleurone cell identity seems to be plastic until the very end of the cell division (Becraft and Asuncion-Crabb, 2000b). It is still unknown what the determinant of aleurone cell fate is.

Genetic control of aleurone formation

Several aleurone mutants have been reported. It was suggested that positional signaling and a subsequent genetic hierarchy control aleurone cell fate specification and differentiation (Becraft and Asuncion-Crabb, 2000b; Olsen, 2004b; Wisniewski and Rogowsky, 2004b; Gruis et al., 2006b). *Dek1* is a positive regulator of aleurone cell fate. The loss of function mutant has no aleurone which suggests DEK1 is required for aleurone cell fate. The *dek1* gene encodes a transmembrane protein with a cytoplasmic calpain protease domain suggesting a possible role as an aleurone cell fate signal transducer (Lid et al., 2002a; Wang et al., 2003b; Johnson et al., 2008). *Mu* induced revertant sectors or *Ds* induced chromosome breakage can produce transdifferentiated single cells. From the single cell revertants, it can be inferred that the peripheral cells have plasticity throughout development. Transdifferentiation from starchy endosperm cell to aleurone cell has only been observed in the surface cell suggesting a positional

cue is required for aleurone cell fate (Becraft and Asuncion-Crabb, 2000b). *Crinkly4* (*cr4*) is also a positive regulator of aleurone cell fate. The mutant shows a similar phenotype with *dek1*. The weak allele produces mosaic aleurone formation. CR4 is a receptor-like kinase which is thought to be another transducer of aleurone cell fate signaling (Becraft et al., 1996a; Becraft et al., 2001a). The *supernumerary aleurone layer1* (*sal1*) mutants are multilayered aleurone mutants (Shen et al., 2003b). *Sal1* encodes a class E vacuolar sorting protein which is similar to human CHMP1 which is involved in vesicle trafficking. It was proposed that SAL1 functions upstream of DEK1and CR4 by controlling their retrograde cycling. These three proteins were shown to be co-localized in endocytic vesicles (Tian et al., 2007a). *Vp1* is the most upstream known regulator of the anthocyanin biosynthesis pathway. VP1 is an orthologue of ABI3 in *Arabidopsis* and is one of the regulators for seed maturation. VP1 is controlled by ABA (Cao et al., 2007). ABA and gibberellic acid (GA) play major antagonistic roles in switching phase from seed maturation to germination and seed dormancy to vivipary. VP1 is a transcription factor containing a B3-domain which binds a DNA element (Suzuki et al., 1997). *Vp1* is specifically expressed in the embryo and aleurone cells thus *Vp1* promoter derived GUS serves as an aleurone specific marker (Cao et al., 2007). Several aleurone development mutants were reported and studied to reveal the aleurone differentiation pathway. Variation in the number of aleurone layer in barley, rice and one landrace of maize suggests that there is a natural variation in aleurone cell number and somehow it was domesticated to a single layer. Until now, only several genes for

aleurone differentiation were studied and much is still unknown about aleurone development. One of the best approaches to studying an unknown developmental pathway is mutant screening.

Genetic screening for mutants

Mutant analysis is a promising approach to study anuncharacterized genetic pathway such as aleurone development pathway. The anthocyanin marker provides convenience for large scale genetic screening for aleurone mutant. Insertional mutagenesis is one of the most powerful tools for gene identification because it is relatively easy to clone the gene directly from sequencing of the insertion flanking region. In maize, using endogenous transposable elements (TEs) is the most useful and practical insertional mutagenesis and *Ac/Ds* and *Mu* are the two most widely used (Brutnell, 2002b). The maize genome has 50-200 copies of *Mu* (Walbot et al., 1988). Even though *Mu* transposon has higher level of mutation frequency subsequent insertion identification is more difficult than *Ac/Ds*. There are several strategies to obtain an insertion flanking sequences. These strategies are base on enriching TE and flanking sequence by PCR with known TE primer and unknown flanking primers. One approach use adapter primers after restriction enzyme digestion and following adapter ligation in AIMS (amplification of insertion mutagenized sites) (Frey et al., 1998b; Wang et al., 2008b) and another approach use arbitrary

degenerate primers Mu-TAIL (thermal asymmetrically interlaced) (Liu et al., 1995b; Settles et al., 2007a).

Dissertation Organization

The general introduction (Chapter 1), three journal papers (Chapters 2, 3, 4), and the general conclusions (Chapter 5) are included in this dissertation.

Chapter2, in this chapter an improved approach for cloning the mutant gene from *Mu* insertional mutagenesis is described. MuTA is developed for high throughput screening of *Mu* inserted mutant screening. The basis of this method and application to the endosperm mutant identification is described. My contribution included confirmation of candidate Mu insertions by genotyping and phenotyping for each of the mutants.

Chapter3, in this chapter the multiple aleurone layer mutant *thick aleurone1* phenotypes and genetic interaction with *dek1* was studied. The epistatic interaction of *thk1* to *dek1* was demonstrated with double mutant analysis and *Ds* induced chromosome breakage sector analysis. My contributions included designing and conducting mapping, genotyping and some of the microscopy analyses.

Chapter4, in this chapter gene cloning and molecular characterization of the *nkd* mutant is described. Positional cloning and following complementation test and transgenic assay reveals that the *nkd* phenotype was caused by

duplicated transcription regulators which are members of the IDD gene family. My contributions included designing and conducting the experiments and writing the manuscript.

References

Becraft, P.W., and Asuncion-Crabb, Y. (2000). Positional cues specify and maintain aleurone cell fate in maize endosperm development. Development **127,** 4039-4048.

Becraft, P.W., Stinard, P.S., and McCarty, D.R. (1996). CRINKLY4: A TNFR-like receptor kinase involved in maize epidermal differentiation. Science **273,** 1406-1409.

Becraft, P.W., Kang, S.H., and Suh, S.G. (2001). The maize CRINKLY4 receptor kinase controls a cell-autonomous differentiation response. Plant Physiology **127,** 486-496.

Bonello, J.F., Opsahl-Ferstad, H.G., Perez, P., Dumas, C., and Rogowsky, P.M. (2000). Esr genes show different levels of expression in the same region of maize endosperm. Gene **246,** 219-227.

Bonello, J.F., Sevilla-Lecoq, S., Berne, A., Risueno, M.C., Dumas, C., and Rogowsky, P.M. (2002). Esr proteins are secreted by the cells of the embryo surrounding region. Journal of Experimental Botany **53,** 1559-1568.

Borowicki, A., Stein, K., Scharlau, D., Scheu, K., Brenner-Weiss, G., Obst, U., Hollmann, J., Lindhauer, M., Wachter, N., and Glei, M. (2010). Fermented wheat aleurone inhibits growth and induces apoptosis in human HT29 colon adenocarcinoma cells. British Journal of Nutrition **103,** 360-369.

Brutnell, T.P. (2002). Transposon tagging in maize. Functional & integrative genomics **2,** 4-12.

Cao, X.Y., Costa, L.M., Biderre-Petit, C., Kbhaya, B., Dey, N., Perez, P., McCarty, D.R., Gutierrez-Marcos, J.F., and Becraft, P.W. (2007). Abscisic acid and stress signals induce viviparous1 expression in seed and vegetative tissues of maize. Plant Physiology **143,** 720-731.

Fenech, M., Noakes, M., Clifton, P., and Topping, D. (2005). Aleurone flour increases red-cell folate and lowers plasma homocyst(e)ine substantially in man. British Journal of Nutrition **93,** 353-360.

Frey, M., Stettner, C., and Gierl, A. (1998). A general method for gene isolation in tagging approaches: amplification of insertion mutagenised sites (AIMS). Plant Journal **13,** 717-721.

Gruis, D., Guo, H., Selinger, D., Tian, Q., and Olsen, O.A. (2006). Surface position, not signaling from surrounding maternal tissues, specifies aleurone epidermal cell fate in maize (vol 141, pg 898, 2006). Plant Physiology **142,** 1771-1771.

Harris, P.J., Chavan, R.R., and Ferguson, L.R. (2005). Production and characterisation of two wheat-bran fractions: an aleurone-rich and a pericarp-rich fraction. Molecular Nutrition & Food Research **49,** 536-545.

Hueros, C., Gomez, E., Cheikh, N., Edwards, J., Weldon, M., Salamini, F., and Thompson, R.D. (1999a). Identification of a promoter sequence from the BETL1

gene cluster able to confer transfer-cell-specific expression in transgenic maize. Plant Physiology **121,** 1143-1152.

Hueros, G., Varotto, S., Salamini, F., and Thompson, R.D. (1995). MOLECULAR CHARACTERIZATION OF BET1, A GENE EXPRESSED IN THE ENDOSPERM TRANSFER CELLS OF MAIZE. Plant Cell **7,** 747-757.

Hueros, G., Royo, J., Maitz, M., Salamini, F., and Thompson, R.D. (1999b). Evidence for factors regulating transfer cell-specific expression in maize endosperm. Plant Molecular Biology **41,** 403-414.

Johnson, K.L., Faulkner, C., Jeffree, C.E., and Ingram, G.C. (2008). The Phytocalpain Defective Kernel 1 Is a Novel Arabidopsis Growth Regulator Whose Activity Is Regulated by Proteolytic Processing. Plant Cell **20,** 2619-2630.

Lid, S.E., Gruis, D., Jung, R., Lorentzen, J.A., Ananiev, E., Chamberlin, M., Niu, X.M., Meeley, R., Nichols, S., and Olsen, O.A. (2002). The defective kernel 1 (dek1) gene required for aleurone cell development in the endosperm of maize grains encodes a membrane protein of the calpain gene superfamily. Proceedings of the National Academy of Sciences of the United States of America **99,** 5460-5465.

Liu, Y.G., Mitsukawa, N., Oosumi, T., and Whittier, R.F. (1995). EFFICIENT ISOLATION AND MAPPING OF ARABIDOPSIS-THALIANA T-DNA INSERT JUNCTIONS BY THERMAL ASYMMETRIC INTERLACED PCR. Plant Journal **8,** 457-463.

Morrison, I.N., Obrien, T.P., and Kuo, J. (1978). INITIAL CELLULARIZATION AND DIFFERENTIATION OF ALEURONE CELLS IN VENTRAL REGION OF DEVELOPING WHEAT-GRAIN. Planta **140,** 19-30.

Olsen, O.A. (2001). Endosperm development: Cellularization and cell fate specification. Annual Review of Plant Physiology and Plant Molecular Biology **52,** 233-+.

Olsen, O.A. (2004a). Dynamics of maize aleurone cell formation: The "surface-"rule. Maydica **49,** 37-40.

Olsen, O.A. (2004b). Nuclear endosperm development in cereals and Arabidopsis thaliana. Plant Cell **16,** S214-S227.

OpsahlFerstad, H.G., LeDeunff, E., Dumas, C., and Rogowsky, P.M. (1997). ZmEsr, a novel endosperm-specific gene expressed in a restricted region around the maize embryo. Plant Journal **12,** 235-246.

Sabelli, P.A., and Larkins, B.A. (2009). The Development of Endosperm in Grasses. Plant Physiology **149,** 14-26.

Settles, A.M., Holding, D.R., Tan, B.C., Latshaw, S.P., Liu, J., Suzuki, M., Li, L., O'Brien, B.A., Fajardo, D.S., Wroclawska, E., Tseung, C.W., Lai, J.S., Hunter, C.T., Avigne, W.T., Baier, J., Messing, J., Hannah, L.C., Koch, K.E., Becraft, P.W., Larkins, B.A., and McCarty, D.R. (2007). Sequence-indexed mutations in maize using the UniformMu transposon-tagging population. Bmc Genomics **8**.

Shen, B., Li, C.J., Min, Z., Meeley, R.B., Tarczynski, M.C., and Olsen, O.A. (2003). sal1 determines the number of aleurone cell layers in maize endosperm and encodes a class E vacuolar sorting protein. Proceedings of the National Academy of Sciences of the United States of America **100,** 6552-6557.

Stewart, M.L., and Slavin, J.L. (2009). Particle size and fraction of wheat bran influence short-chain fatty acid production in vitro. British Journal of Nutrition **102,** 1404-1407.

Suzuki, M., Kao, C.Y., and McCarty, D.R. (1997). The conserved B3 domain of VIVIPAROUS1 has a cooperative DNA binding activity. Plant Cell **9,** 799-807.

Tian, Q., Olsen, L., Sun, B., Lid, S.E., Brown, R.C., Lemmon, B.E., Fosnes, K., Gruis, D.F., Opsahl-Sorteberg, H.G., Otegui, M.S., and Olsen, O.A. (2007).

Subcellular localization and functional domain studies of DEFECTIVE KERNEL1 in maize and Arabidopsis suggest a model for aleurone cell fate specification involving CRINKLY4 and SUPERNUMERARY ALEURONE LAYER1. Plant Cell **19,** 3127-3145.

Walbot, V., Britt, A.B., Luehrsen, K., McLaughlin, M., and Warren, C. (1988). Regulation of mutator activities in maize. Basic life sciences **47,** 121-135.

Wang, C.X., Barry, J.K., Min, Z., Tordsen, G., Rao, A.G., and Olsen, O.A. (2003). The calpain domain of the maize DEK1 protein contains the conserved catalytic triad and functions as a cysteine proteinase. Journal of Biological Chemistry **278,** 34467-34474.

Wang, Y., Yin, G., Yang, Q., Tang, J., Lu, X., Korban, S.S., and Xu, M. (2008). Identification and isolation of Mu-flanking fragments from maize. Journal of Genetics and Genomics **35,** 207-213.

Wisniewski, J.P., and Rogowsky, P.M. (2004). Vacuolar H+-translocating inorganic pyrophosphatase (Vpp1) marks partial aleurone cell fate in cereal endosperm development. Plant Molecular Biology **56,** 325-337.

Wolf, M.J., Zuber, M.S., Cutler, H.C., and Khoo, U. (1972). MAIZE WITH MULTILAYER ALEURONE OF HIGH PROTEIN CONTENT. Crop Science **12,** 440-&.

CHAPTER 2. High-Throughput Linkage Analysis of Mutator Insertion Sites in Maize.

Gibum Yi[1,2], Diane Luth[3], Carolyn Lawrence[2,3,4] and Philip W. Becraft[1,2,3*]

A paper published in *Plant Journal* in 2009

[1] Plant Biology Program, Iowa State University, Ames, IA 50011

[2] Genetics, Development & Cell Biology Department, Iowa State University, Ames, IA 50011

[3] Agronomy Department, Iowa State University, Ames, IA 50011

[4] USDA-ARS, Iowa State University, Ames, Iowa 50011-2207, USA.

* For correspondence (phone 1-515-294-2903; fax 1-515-294-6755; becraft@iastate.edu)

Abstract

Insertional mutagenesis is a cornerstone of functional genomics. High copy transposable element systems such as *Mutator* (*Mu*) in maize afford the advantage of high forward mutation rates but pose a challenge in identifying the particular element responsible for a given mutation. Several large mutant collections have been generated in *Mu*-active genetic stocks, but current methods limit the ability to rapidly identify the causal *Mu* insertions. Here we present a method for rapidly assaying for *Mu* insertions that are genetically linked

to a mutant of interest. The method combines elements of Mu-TAIL and AIMS protocols and is applicable to analysis of a single mutant or high throughput analysis of a mutant collection. Briefly, genomic DNA is digested with a restriction enzyme and adapters ligated. PCR is performed with TAIL cycling parameters, using a fluorescently labeled *Mu* primer, resulting in the preferential amplification and labeling of *Mu* containing genomic fragments. Products from a segregating line are analyzed on a capillary sequencer. To recover a fragment of interest, PCR products are cloned and sequenced to identify an insert of the size corresponding in size to the desired band. We demonstrate the utility of the method by identifying Mu insertion sites linked to seed-lethal mutations with a preliminary success rate of nearly 50%.

Introduction

Insertional mutagenesis is a powerful method for gene identification. In plants, T-DNAs and several transposable element (TE) systems have been extensively used. In maize, endogenous TEs are the most effective and widely used insertional mutagens. Mutant screens are conducted in strains containing active TEs of known sequence and the TE is then used to isolate genomic DNA flanking the insertion site, corresponding to the disrupted gene of interest. Several TE systems have been extensively used, and each has advantages and disadvantages. The two systems most commonly used in maize are Activator/Dissociation *(*Ac/Ds*) and* Mutator *(*Mu*) (Brutnell, 2002a).*

Activator *(*Ac*) is a low copy system; forward mutation rates are low making mutant generation difficult, but subsequent identification and isolation of the mutated gene is relatively easy.* Ds *is a non-autonomous element that requires the transposase encoded by* Ac *for its transposition. This provides convenient control of* Ds *activity. Both* Ac *and* Ds *transpose preferentially to linked sites so genes in proximity to one of these elements may experience a relatively high mutation rate (Dooner and Belachew, 1989).*

Mu *is a high copy system with typically 50 to 200 copies per individual genome (Walbot and Warren, 1988). Forward mutation rates are high making mutant generation efficient. For example, when* Mu *activity was introduced into the W22 inbred line, plants contained an average of 57* Mu *elements and generated new seed mutants with a frequency of 7% per generation (McCarty et*

al., 2005). Transpositions were randomly scattered throughout the genome. However, subsequent identification of the particular Mu *element responsible for the mutation of interest is challenging.*

Efficient means of analyzing *Mu* elements would greatly facilitate their utility in gene isolation efforts. Several PCR strategies have been developed to allow the identification and recovery of genomic sequences flanking *Mu* insertion sites. A method called AIMS (amplification of insertion mutagenized sites) is a ligation-mediated method (Frey et al., 1998a; Wang et al., 2008a). Briefly, genomic DNA is digested with a restriction enzyme and an adapter is ligated to the ends of the restriction fragments. PCR is then performed using a *Mu* primer that recognizes conserved sequences in the terminal inverted repeats (TIRs) of *Mu* elements, and a primer that recognizes adapter sequences. In the first round of amplification, the *Mu* primer is biotinylated, and the products are purified with strepavidin beads to enrich for *Mu* containing fragments. In the second round of PCR, the *Mu* primer is labeled with radioisotope or a fluorescent tag. Fragments are run on a sequencing gel and if a fragment cosegregates with the mutant phenotype of interest, it is cut from the gel and cloned. This approach is generalizable to other transposable element families as well (Yephremov and Saedler, 2000).

Another strategy to amplify sequences flanking insertion sites is TAIL (thermal asymmetrically interlaced) PCR (Liu et al., 1995a). MuTAIL is a recent adaptation of this approach to the analysis of *Mu* insertion sites (Settles et al., 2004; Settles et al., 2007b). This approach relies on nested specific primers to

Mu TIRs in combination with arbitrary degenerate primers to amplify unknown flanking sequences. Preferential amplification of fragments containing *Mu* insertions is achieved by using primers of differential melting temperatures. The *Mu* TIR specific primers have a high melting temperature while the degenerate primers have low melting temperatures. Multiple cycles run at high annealing temperatures allow linear amplification only from the *Mu* specific primers. Interspersed cycles at low annealing temperatures allow exponential amplification from the degenerate primers.

While the AIMS approach has proven successful, the drawback for implementing this approach in a high-throughput manner is the amount of labor involved. Genomic DNA must be digested and ligated, then after a set of PCR cycles, the biotinylated *Mu*-containing fragments are purified with strepavidin beads. After segregation analysis, fragments of interest must be excised and recovered from the sequencing gel, reamplified and finally cloned and sequenced. Another limitation is that fragment sizes generally were small, ranging from 100-400 base pairs (Frey et al., 1998a), although with the preference of *Mu* elements for genic sequences (McCarty et al., 2005, and references therein) and the advent of a fully sequenced maize genome, the small fragment size will no longer pose a significant problem.

The TAIL approach is amenable to high-throughput in that the DNA requires no manipulations prior to PCR. Additionally, the TAIL-PCR regimen strongly enriches for *Mu*-containing fragments, allowing amplification products to be directly cloned and sequenced. *Mu* TAIL also produces a greater range of

fragment sizes, up to 2000 base pairs (Settles et al., 2004). TAIL has been used effectively for extensive analysis of *Mu* insertion sites in maize lines (Settles et al., 2004; McCarty et al., 2005). In principle, *Mu* TAIL could be adapted to undertake cosegregation analyses of mutants of interest, but the large fragments go beyond the size that can be readily resolved on standard sequencing equipment, and the complexity is too great to be resolved on agarose gels. Furthermore, a battery of up to 12 different degenerate primers are required to achieve an estimated 80% representation of the *Mu* insertions present in a genome.

Here we combine elements of both MuTAIL and AIMS into a procedure we call MuTA, which is an efficient method for co-segregation analysis of *Mu*-induced mutants and is suitable for high throughput.

Results

Overview of the method

Like AIMS, MuTA is based on the principles of AFLP (Vos et al., 1995; Frey et al., 1998a; Wang et al., 2008a). The genomic DNA is digested with a restriction enzyme to generate fragments and an adapter is ligated onto the ends of the fragments. PCR is then performed using one primer to the *Mu* terminal inverted repeats (MuTIRs) and one to the adapter. However, to enrich for *Mu*-containing fragments, instead of using a biotinylated MuTIR primer and strepavidin purification, we incorporated principles of TAIL PCR (Liu et al., 1995a). The MuTIR primer used had a melting temperature of 65^{o}C while the

adapter primer had a TM of 50^{o}C. The PCR protocol consists of multiple cycles with annealing temperature of 60^{o} interspersed with a single cycle at 47^{o} (Figure 1). The high annealing temperatures allow linear amplification from *Mu* elements while the low temperature allows annealing of both primers and exponential amplification.

To detect the *Mu*-containing products, the MuTIR primer used in the second round of PCR contains a fluorescent label. Products are analyzed on a capillary sequencer, such as an ABI3100, and the chromatograms are analyzed with genotyping software such as the publicly available Genographer, or other commercial packages. For example, fragments can be conveniently visualized on a pseudogel image (Figures 3, 5).

Cosegregation with the mutant of interest is used to identify candidate fragments that are genetically linked to the mutation. If a transposon is responsible for a mutation, absolute linkage between the transposon insertion and the mutant phenotype is expected. A PCR product that is present in all the mutants and none of the wild types is a candidate for a causal insertion site (Figure 3). We identified candidate fragments by analyzing small segregating families consisting of four mutant and four homozygous wild type individuals. The genotyping software provides an accurate size estimate of the candidate fragment.

To recover a candidate fragment, a library of cloned PCR products from one of the reactions containing the desired target is generated. We use a

commercial topoisomerase cloning kit and then pick 96 clones and sequence the inserts. The target clone is recognized by comparing the number of sequenced bases to the size estimate of the desired fragment provided by the genotyping software. The candidate sequence is then used for database searches and to design gene-specific PCR primers to verify the genetic linkage between the insertion and the mutant of interest.

Identifying a Mu insertion genetically linked to a mutant phenotype

We initially developed the method using an empty pericarp mutant, *emp*02S-0422* (Figure. 2), obtained from the UniformMu collection (McCarty et al., 2005; Settles et al., 2007b). Because the mutation is homozygous lethal, it must be maintained as a heterozygote. We crossed a heterozygous mutant to the wild type W22 inbred line to generate a family segregating 1:1 heterozygous mutants and homozygous wild types. Tissue was isolated from progeny plants, which were then self-pollinated to determine the genotypes; the heterozygotes segregated *emp*02S-0422* mutant kernels on their ears.

DNA was isolated from four heterozygous mutants and four wild types and subjected to the MuTA analysis. Six PCR templates were prepared by digesting the DNA with *AseI*, *BstBI*, *NdeI, BsaHI*, *BfaI*, or *HinP1I* (6, 6, 6, 5, 4 and 4-cutters, respectively). All these enzymes produce either a 5’ TA or a 5’ CG overhang. Two sets of adapters were prepared that were identical except for the TA or CG overhang. Adapters were ligated to the ends of genomic restriction fragments

and PCR was performed as described. The PCR reactions on the *NdeI* and *HinP1I* templates were performed with FAM labeled MuTIR primers, *BsaHI* and *BstBI* with HEX, and *AseI* and *BfaI* with NED. Following PCR, portions of the *NdeI, BsaHI* and *AseI* reactions from a given individual were combined in a well of a 96-well plate. Thus, these samples occupied one column (eight wells) of the plate. The *HinP1I*, *BstBI* and *AseI* reactions were likewise combined to occupy a second column of the plate. The samples were analyzed on an ABI3100 at the Iowa State Univesity DNA Facility. Pseudogel images were produced from the resultant chromatograms using Genographer software. As shown in Figure 3, the *BsaHI* reactions produced a band that was observed in all four mutants and none of the wild types, as would be expected for a *Mu* insertion responsible for causing the mutant phenotype. The band associated with the mutants was estimated by Genographer to be 176 base pairs.

To recover the desired DNA fragment, PCR products from mutant individual 2 were shotgun cloned using the Strataclone topoisomerase cloning kit (Stratagene). Transformed bacteria were plated on LB medium containing ampicillin and X-gal. Ninety-six white colonies were picked and the plasmid inserts sequenced. One clone contained an insert of 176 bases.

Another PCR experiment was performed to verify that the recovered clone corresponded to the PCR product associated with the mutant individuals. The clone sequence was used in database searches and showed a 100% match to a maize EST (NCBI accession number DV491867). A gene-specific primer was designed against the EST and used for PCR on DNA from additional segregants

of the mutation. In combination with a MuTIR primer, only mutant individuals produced a product, while in combination with a second gene-specific primer, all individuals produced a product (Figure 3 c,d). This demonstrated that both the recovered clone and the EST correspond to the Mu insertion associated with the mutation. To date, we have assayed over 80 segregants and have observed complete linkage between this *Mu* insertion and the mutant phenotype. This demonstrates the feasibility of this approach for identifying *Mu* elements tightly linked to mutant genes of interest.

High-throughput identification of linked Mu insertion sites

To test the adaptability of this method to high throughput analysis, we assembled twelve seed-lethal mutants for which we had sufficient segregating material. Because efficient amplification of a *Mu* insertion site is dependent on the proximity of the restriction site used for template preparation, the likelihood of identifying a linked *Mu* insertion for a given mutant is maximized by performing multiple restriction digests and PCR reactions. For high-throughput, this must be balanced with the increased labor and cost of performing additional reactions on a given mutant. We decided on three digests per mutant *BfaI*, *Csp6I* and *MspI*. Each digest was used as template for MuTA PCR using a MuTIR primer labeled with a different fluorophore, NED, FAM or HEX. Multiplexing was used to reduce lane costs in the genotyping analysis; the products of the three separate reactions were combined in a single lane for analysis on the ABI3100. When the products of the three reactions are combined, each mutant occupies one column

of a 96-well plate, allowing the electrophoretic analysis of twelve mutants per plate (Figure 4).

Of the twelve mutants we analyzed, we were able to identify a band associated with the mutant individuals for six (Figure 5). In three cases, a cosegregating product was identified in two of the different enzyme digests (Figure. 5 A) and in one case a linked product was detected in all three digests.

To recover the candidate linked DNA fragment for a given mutant, the PCR products from one mutant reaction were cloned and 96 clones sequenced. For example, for mutant 2, we cloned the products from the reaction displayed in lane 2 of the *BfaI* reactions (Figure 5). In every case, we were able to recover a correctly sized fragment by sequencing 96 cloned products. For five cases, there was a unique product of the correct size. For mutant 12, the estimated size of the linked product was 240 bp and three different candidate clones had sizes of 242, 244 and 245 bp.

The sequences of all the candidate fragments were used in database searches to identify genomic sequences from which gene-specific primers were designed. When the gene-specific primers were used in combination with a MuTIR primer, a product was produced from mutant individuals of lines 2, 6, 8, 10 and 11, but not wild type individuals. This confirmed that the recovered clone corresponded to the cosegregating PCR product observed on the pseudogel image. In the case of mutant 12, PCR primers were designed against all three

candidate clones and only the 244 base sequence produced a product specific to the mutant DNA samples.

Verification of linkage between isolated Mu insertions and mutant phenotypes

Further analysis of linkage in larger segregating populations was undertaken. For each mutation, DNA was isolated from individuals in lines segregating 1:1 homozygous wild type and heterozygous mutants, and PCR was performed using the same gene-specific primer and MuTIR primer pairs described. Each plant was also self-pollinated to determine whether the plant carried the mutant allele. Linkage was verified for all seven insertions. In six of the lines, there was perfect correspondence between mutant phenotype and the candidate Mu insertion (Table 3; Supplemental Figure 1). A total of 88, 37, 39, 42, 40 and 56 segregants were analyzed for each of these six lines, indicating the identified Mu insertions were tightly linked to all these mutations.

Mutant 11 showed several discrepancies between the presence of the *Mu* insertion and the mutant phenotype. Of 53 segregants analyzed, 3 displayed a mutant phenotype but did not contain the candidate *Mu* insertion. Two segregating lines were analyzed for this mutant and all the discrepancies occurred in the same line. We suspect this line might actually carry a second empty pericarp mutation that could account for the discrepancies, but this

remains to be tested. Existing evidence indicates that this *Mu* insertion is genetically linked to the respective mutation, but does not support it being causal.

Analysis of cloned sequences

For each mutant with a candidate band, a micro library of 96 clones was sequenced. A quality measure of the protocol is provided by the analysis of all the sequences. 95.5% of the sequences were “good”, where good was defined as high quality sequence that included a MuTIR and an adapter at the termini. “Bad” included colonies that failed to grow, empty vectors, failed reactions, multiple clones per reaction, and clones with two adapters and no MuTIR. Among the 550 “good” sequences represented in the latter six libraries, all but 17 had hits when used in BLAST searches of maize sequence databases. Of those that failed, 14 were too short to perform a search. Of the searchable sequences, all but 10 had matches in the maize HTGS database. Only three sequences of sufficient length to perform a search had no matches among the maize HTGS, GSS or EST Genbank accessions.

The analysis of the sequenced insertion sites among the latter 6 libraries is summarized in Tables 1 and 2. Most clones had multiple isolates. An average of 21 independent insertion sites was identified per library, with an average of 5 represented by both flanks. A total of 93 unique insertion sites were identified, with 21 shared among multiple libraries and 72 unique to a given library. Some of the shared insertions reflect the common parentage among the lines in that four

were derived from the Uniform *Mu* population. However, mutants 11 and 12 were derived from different materials and surprisingly, 11 insertion sites from these two libraries were shared with the other four Uniform Mu libraries.

Of the 93 insertions identified, 79 had hits in EST database searches. Of the six clones identified that were linked to mutant phenotypes, five had direct hits in ESTs (Table 1). For mutant 11, genomic sequence corresponding to the PCR product was identified and used to search the EST database. A 5' EST was identified that mapped 197 bp 3' to the *Mu* insertion site.

Discussion

The protocol described here is simple and reproducible. The method can be applied to either a single mutant of particular interest, or adapted to high throughput. Thus far, we have analyzed fifteen mutants with this method and cosegregating fragments have been identified and recovered for seven of them (Figures. 3, 5). In all seven cases, we were able to recover a correctly sized fragment by sequencing 96 cloned PCR products from one of the reactions containing the band of interest. Database searches identified maize genomic sequences for all seven clones. These were used to design PCR primers that were used in combination with a MuTIR primer to verify that the desired fragment was recovered from each reaction. Examination of a larger segregating population verified the linkage between the *Mu* insertion and the respective

mutation in all seven cases, and in six cases the linkage was perfect suggesting the insertion could be responsible for the mutation.

Factors affecting the identification of linked Mu insertion sites

Thus far we have experienced slightly less than a 50% success rate recovering insertions linked to mutations derived from *Mu* lines. Of the factors affecting success, the most critical is whether the mutation is caused by a *Mu* insertion. Mutants derived from *Mu*-active lines have been shown to be caused by other transposons (Patterson et al., 1991) or by deletions (Robertson and Stinard, 1987; Robertson et al., 1994; Das and Martienssen, 1995). Anecdotal evidence suggests that approximately half the mutants derived from *Mu* stocks might not be *Mu*-tagged. Thus, only a subset of mutants derived from *Mu* stocks are amenable to cloning by any *Mu*-tagging approach, including this one.

Whether a particular *Mu*-containing genomic region amplifies with MuTA depends on the proximity of the nearest site for the particular restriction endonuclease used in the template preparation, as well as the PCR conditions. Any enzyme that produces a constant overhang can be used and no one enzyme will work for every *Mu* insertion. In the case of a single mutant of particular interest, the likelihood of identifying a linked Mu insertion is maximized by performing the analysis with several different restriction enzymes. We created two adapters that differed only in their 5’ overhangs, TA versus CG (Table 4). These can be used in conjunction with any restriction enzyme that produces a

compatible overhang. There are at least 15 restriction enzymes that produce one of these two overhangs (although *Taq*I is not useful because it cleaves most MuTIRs and several other enzymes are too expensive to be practical). Thus, these adapters allow substantial versatility in template preparation.

The average fragment size is dependent on the size recognition site; enzymes with 4-base sites cut an average of once every 256 bases, 6-base sites cut an average of every 4096 bases. The upper limit of useful size PCR products in our system is 1200 bases, which is the upper limit of the available size standards for the capillary sequencer. The lower limit is determined by the ability to unequivocally identify the cognate sequence in a database search. Several variables influence this, including whether the Mu insertion site is in unique sequence. In our experience, 20 bases is sometimes sufficient but 50 has a good probability of identifying a unique target. The range of PCR products we have thus far obtained is generally below 700 bases, regardless of restriction endonuclease, suggesting that PCR conditions are currently limiting efficient amplification of longer fragments.

We recovered an average of 21 insertion sites from each 96 cloned PCR products sequenced. This appears consistent with the number of bands observed in the pseudogel images. Some of the genetic materials we used include isolates from the Uniform Mu population, which contains an average of 57 *Mu* elements per individual (McCarty et al., 2005). Assuming this value, we appear to amplify approximately 37% of the insertion sites with a given enzyme. To reduce the complexity of fragments displayed, AIMS adds a selective base to

the adapter primer (Frey et al., 1998a). We have not found this necessary, perhaps due to the outstanding resolution afforded by capillary sequencers.

The size of the segregating family affects the statistical ability to detect linkage, and 8 individuals is smaller than typical for linkage studies. Our experiments have been conducted on segregating families consisting of 4 heterozygous mutants and 4 wild types. Since we are interested in insertions showing absolute linkage to a mutant, any element showing linkage in a large sample will also be apparent in a small sample. But what is the likelihood of false positives? With the current sample size, the probability of a false positive (an element present in all 4 mutants and none of the wild types) for an unlinked element is $(0.5)^8$, or 0.004. However, the Uniform Mu lines contain an average of 57 Mu elements (McCarty et al., 2005). With that number, there is approximately a 50% chance of having an element within 20 cM of any given locus, and a 20% chance of having one within 5 cM (Briggs and Beavis, 1994). In these cases, a sample size of 8 would have a 0.08 or 0.13 chance of producing a false positive, respectively. For example, at 20 cM, the probability of not observing a recombinant and thus obtaining a false positive would be $(0.8)^8$, or 0.08. If we increased the sample size to 12, these likelihoods of false positives would drop to 0.03 and 0.11, respectively—not a dramatic improvement given the extra labor and expense. Since further analysis is required for verification of candidate insertion sites, this is an acceptable false positive rate for the first pass. Furthermore, the Poisson distribution of *Mu* elements in these lines (McCarty et

al., 2005) argues that the majority of cosegregating insertions will be responsible for the linked mutation.

Quality and Reproducibility

The analysis of sequenced PCR products indicated that this method is an effective means of reliably identifying Mu insertion sites. Approximately 95% of the products sequenced produced high quality sequences containing a Mu TIR and an adapter. Among the flanking sequences analyzed, only 3 showed no match in BLAST searches of existing maize database accessions. This reflects the efficacy of the method for amplifying bona fide *Mu* insertion sites from maize, and also reflects the degree of coverage in maize sequence databases. As database resources continue to improve, they will pose less of a limitation on methods such as this that rely on sequence searches.

The banding patterns generated in the pseudogel images clearly show products in common among related individuals of a segregating line, as well as bands unique to various individuals. The related banding patterns among related individuals demonstrates the reproducibility of the method. In summary we conclude that this is an effective method for rapidly identifying candidate *Mu* insertions linked to mutants of interest.

Materials and methods

Genetic Stocks

Plants of lines segregating seed lethal mutations (Figure. 2) were self pollinated for progeny tests to identify wild type and heterozygous mutant individuals.

Template Preparation

DNA was isolated from leaf tissue by the Iowa State DNA facility using an AutoGen 740 ™. 0.5 to 1 µg of genomic DNA was digested with an appropriate restriction endonuclease in a 10 µl reaction volume according to manufacturers' specifications. If the subsequent adapter ligation recreated the restriction site, the restriction enzyme was heat killed after the digestion was complete. 1 µl of the digested genomic DNA was added to 1 µl of 50 µM adapter DNA in a 10 µl ligation reaction. Adapter sequences are shown in Table 4. Ligations were performed overnight at 4^{o} C.

PCR

Two rounds of PCR were performed. For the first round, 1 µl of template DNA from the ligation reaction was added to a 20 µl PCR reaction containing 20pmol each of the MuTIR1 primer and adapter primer (Table 4), GoTaq polymerase and buffer (Promega), 1.5 mM $MgCl_2$ and 0.5 mM dNTPs. The PCR program is shown in Table 5.

For the second round, PCR products of the first round are diluted 1:1000 in water and 1 µl added to a 30 µl reaction containing 30 pmol each of MuTIR2 and the adapter primer (Table 4). Other components were identical to the first

round reaction mix. MuTIR2 is a 1:1 mix of labeled and unlabeled primer because the 5' fluorescent tag interferes with cloning. The PCR cycling is identical to the first round except the 60^{o} C annealing temperature in step 3 is reduced to 57^{o} C to accommodate the lower melting temperature of MuTIR2.

PCR Product Analysis

A total volume of 1.5 µl of the second reaction products was analyzed. When performing multiple analyses on a given sample (i.e. multiple restriction enzymes), the PCR for each digest was performed with a different fluorescent label on the MuTIR2 primer. We used FAM, HEX and NED fluorophores. 0.5 µl from each of three reactions were combined in a single well. Samples were submitted to the Iowa State University DNA Facility for analysis on an ABI3100. Chromatograms were downloaded and analyzed using Genographer software to produce pseudogel images. Images were scrutinized for cosegregating bands and size estimates of candidate bands of interest were provided by the software.

Fragment Recovery

To recover the desired DNA fragment, PCR products from one of the mutant individuals containing a fragment of interest were shotgun cloned using the Strataclone topoisomerase cloning kit (Stratagene). Transformed bacteria were plated on LB medium containing ampicillin and X-gal. Ninety-six white colonies were picked and the plasmid inserts sequenced by the Iowa State University DNA Facility. Sequences were analyzed either using Vector NTI.

Clone inserts corresponding in size to the fragment of interest represented candidates for the linked Mu. Sequences were searched to identify the MuTIR and the adapter. The sequence in between the MuTIR and adapter represented genomic sequences flanking the insertion site. Flanking sequences were used in BLAST (Altschul et al., 1990) searches of maize sequence databases.

Fragment Verification

Database sequences were used to design gene specific primers that were used in combination with the MuTIR3 primer to verify that the desired fragment had been recovered and was indeed linked to the mutation. The primers B2B-D11, C6D-A6, C8C-G10, M10B-E5, C11C-D3 and C12D-E3 (Table 4) were used with mutants 2, 6, 8, 10, 11 and 12, respectively.

Acknowledgements

This research was supported by funds from NSF Plant Genome Award 0077676, and from the Genetics, Development and Cell Biology Department at Iowa State University.

References

Altschul, S.F., Gish, W., Miller, W., Myers, E.W. and Lipman, D.J. (1990) Basic local alignment search tool. *J Mol Biol*, **215**, 403-410.

Briggs, S.P. and Beavis, W.D. (1994) How RFLP loci can be used to assist transposon-tagging efforts. In *The Maize Handbook* (Freeling, M. and Walbot, V. eds). New York: Springer-Verlag, pp. 653-659.

Brutnell, T.P. (2002) Transposon tagging in maize. *Functional & Integrative Genomics*, **V2**, 4.

Das, L. and Martienssen, R. (1995) Site-selected transposon mutagenesis at the hcf106 locus in maize. *Plant Cell*, **7**, 287-294.

Dooner, H.K. and Belachew, A. (1989) Transposition Pattern of the Maize Element Ac from the Bz-M2(ac) Allele. *Genetics*, **122**, 447-457.

Frey, M., Stettner, C. and Gierl, A. (1998) A general method for gene isolation in tagging approaches: amplification of insertion mutagenised sites (AIMS). *The Plant Journal*, **13**, 717-721.

Liu, Y.G., Mitsukawa, N., Oosumi, T. and Whittier, R.F. (1995) Efficient isolation and mapping of Arabidopsis thaliana T-DNA insert junctions by thermal asymmetric interlaced PCR. *Plant J*, **8**, 457-463.

McCarty, D.R., Settles, A.M., Suzuki, M., Tan, B.C., Latshaw, S., Porch, T., Robin, K., Baier, J., Avigne, W., Lai, J., Messing, J., Koch, K.E. and Hannah, L.C. (2005) Steady-state transposon mutagenesis in inbred maize. *Plant J*, **44**, 52-61.

Patterson, G.I., Harris, L.J., Walbot, V. and Chandler, V.L. (1991) Genetic Analysis of B-Peru, a Regulatory Gene in Maize. *Genetics*, **127**, 205-220.

Robertson, D.S. and Stinard, P.S. (1987) Genetic Evidence of Mutator-Induced Deletions in the Short Arm of Chromosome 9 of Maize. *Genetics*, **115**, 353-361.

Robertson, D.S., Stinard, P.S. and Maguire, M.P. (1994) Genetic evidence of Mutator-induced deletions in the short arm of chromosome 9 of maize. II. wd deletions. *Genetics*, **136**, 1143-1149.

Settles, A.M., Holding, D.R., Tan, B.C., Latshaw, S.P., Liu, J., Suzuki, M., Li, L., O'Brien, B.A., Fajardo, D.S., Wroclawska, E., Tseung, C.W., Lai, J., Hunter, C.T., 3rd, Avigne, W.T., Baier, J., Messing, J., Hannah, L.C., Koch, K.E., Becraft, P.W., Larkins, B.A. and McCarty, D.R. (2007) Sequence-indexed mutations in maize using the UniformMu transposon-tagging population. *BMC Genomics*, **8**, 116.

Settles, A.M., Latshaw, S. and McCarty, D.R. (2004) Molecular analysis of high-copy insertion sites in maize. *Nucleic Acids Res*, **32**, e54.

Vos, P., Hogers, R., Bleeker, M., Reijans, M., van de Lee, T., Hornes, M., Frijters, A., Pot, J., Peleman, J., Kuiper, M. and et al. (1995) AFLP: a new technique for DNA fingerprinting. *Nucleic Acids Res*, **23**, 4407-4414.

Walbot, V. and Warren, C. (1988) Regulation of Mu element copy number in maize lines with an active or inactive Mutator transposable element system. *Mol Gen Genet*, **211**, 27-34.

Wang, Y., Yin, G., Yang, Q., Tang, J., Lu, X., Korban, S.S. and Xu, M. (2008) Identification and isolation of Mu-flanking fragments from maize. *J Genet Genomics*, **35**, 207-213.

Yephremov, A. and Saedler, H. (2000) Technical advance: display and isolation of transposon-flanking sequences starting from genomic DNA or RNA. *Plant J*, **21**, 495-505.

Figure legends

Figure 1. Overview of the MuTA PCR strategy.

Figure 2. The seed lethal mutant *emp*02S-0422.*

Figure 3. Identification of a *Mu* insertion linked to mutant *emp*02S-0422.*

(a) Pseudogel image produced by Genographer™ from the chromatograms produced by running the MuTA PCR products on an ABI3100 capillary sequencer.

(b) Closeup of the inset shown in (a). A band cosegregates with the mutant. Genographer provided a size estimate of 176 base pairs.

(c) Diagram depicting the relation of the *Mu* insert, the cloned PCR product, the EST identified in database searches, and the primers used in PCR reactions to verify the identity of the recovered band and linkage of the Mu insertion site to the mutation.

(d) PCR results showing the presence of the *Mu* insertion in all individuals carrying the mutation. Genomic DNA from segregating individuals was used as template for PCR reactions using the primer pairs depicted in (c).

Figure 4. Multiplexing of three independent reactions into a single column of a 96-well plate.

Figure 5. Results of a high-throughput analysis of twelve mutants. Linked insertions were found for six.

(a) Typical output of three different reactions on samples of eight segregating individuals for seed-lethal mutant 2. Cosegregating bands were found in the *BfaI* and *MspI* reactions. Below are shown enlargements of the cosegregating fragments from the ABI3100 output. The ethidium bromide stained gel showing the PCR verification, similar to figure 3(c,d), that the desired fragment had been identified.

(b-f). Mu insertions cosegregating with five additional seed-lethal mutations. Fluorescent bands represent the ABI3100 output and the ethidium bromide gels verifying recovery of the linked fragment.

Supplemental Figure 1. Verification of genetic linkage.

Wild type and mutant segregants for the respective mutants were analyzed by PCR using a gene-specific primer in combination with a Mu primer. Only individuals with a Mu inserted in the respective gene will produce an amplification product. Lanes designated mutant showed segregation of the mutant phenotype upon self pollination. Only three discrepancies were observed, all in Mutant 11, shown in the lower gel image.

Table 1. Summary of the sequence analyses for the libraries associated with six seed lethal mutants.

Library	Mutant	# insertion sites sequenced	# isolates of linked site	Corresponding EST
2	*emp*02S-0288*	23	3	CF631304
6	*emp*02S-0254*	11	3	EB815794
8	*emp*02S-0089*	23	1	DY241608
10	*emp*02S-0390*	19	1	EB640046
11	*emp-msc*0285*	37	1	DY623734
12	*o5-PS3038*	18	2	EE189213

Table 2. Summary of the sequence analysis for all six libraries combined.

Total insertion sites	93
Mean # insertion sites per library	21
Insertion sites shared among >1 libraries	21
Insertion sites unique to a library	72
Insertion sites with both flanks recovered	27
Insertions per library with both flanks recovered	5.2

Table 3. Linkage data including original 8 segregants plus additional individuals sampled.

Mutant Line	WT lacking insertion / WT	Mutants with insertion / mutants
*emp*02S-0422*	42 / 42	46 / 46
2	16 / 16	21 / 21
6	20 / 20	19 / 19
8	20 / 20	22 / 22
10	21 / 21	19 / 19
11	28 / 28	22 / 25
12	28 / 28	28 / 28

Table 4. Primer and adapter oligonucleotide sequences.

Name	Sequence
Adapter 1	5’ TAGAAAGAATTCGGATCCAATTATAT 3’ 3’ CTTTCTTAAGCCTAGGTTAATATA 5’
Adapter 2	5’ CGGAAAGAATTCGGATCCAATTATAT 3’ 3’ CTTTCTTAAGCCTAGGTTAATATA 5’
Adapter primer	ATATAATTGGATCCGAATTCTTTC
MuTIR1	AGAGAAGCCAACGCCAWCGCCTCYATTTCGTC
MuTIR2	TCGTCGAATCCCBTYCBCTCTTCKTCYATAAT
MuTIR3	ATCCCGTCCGCTCTTCGTCTATAA
Net—for	AGCTCGCGGTACAGCTTTCCA
Net-rev	AAGCGGAGAAAGAAGCTCCTGA
B2B-D11	CAATCCTGCACGAGCACAAGC
C6D-A6	TGGCAGTCGATCAAGCTGTTG
C8C-G10	GCCCAGCACATCTAGCATCAA
M10B-E5	GATAGGGAAACCGTGGAAGGA
C11C-D3	CCGCTTGAAACGAAGACCTTTGGA
C12D-E3	TGGGCGTCCTTCTTCTCCAAT

Table 5. Cycling parameters for the first round of PCR.

Step	Condition	Time
1	95^{o}	3 min
2	94^{o}	20 sec
3	60^{o}	1 min
4	72^{o}	2 min 30 sec
5	Go to 2	2 times
6	94^{o}	20 sec
7	47^{o}	1 min
8	72^{o}	2 min 30 sec
9	Go To 2	12 times
10	72^{o}	7 min 30 sec
11	4^{o}	forever

Figure 1.

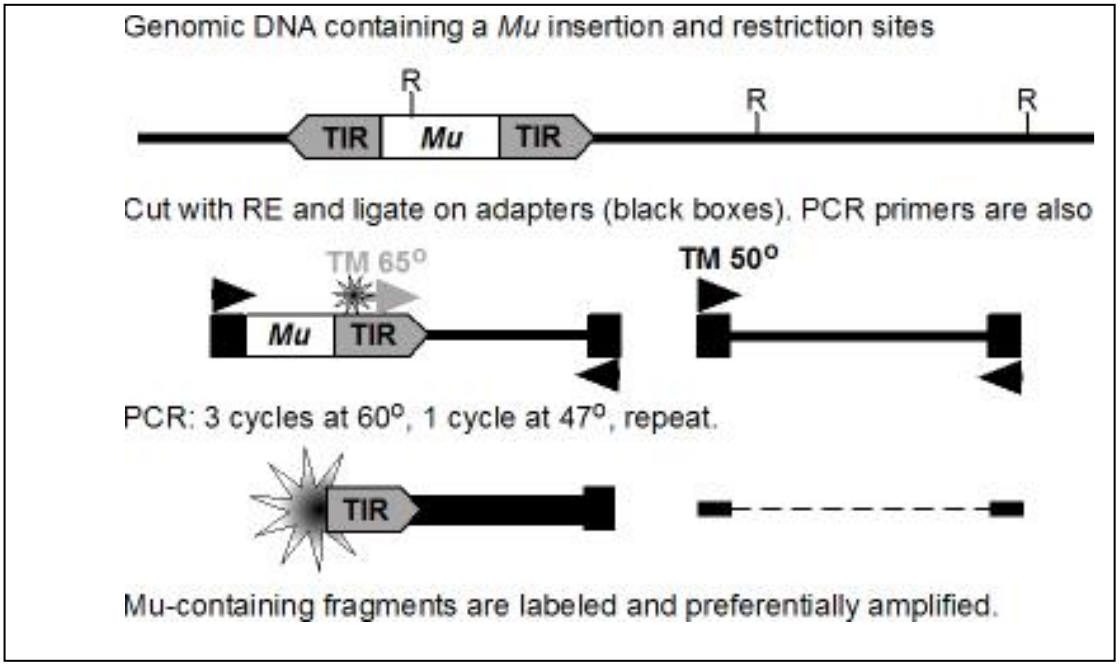
Genomic DNA containing a *Mu* insertion and restriction sites
R
R
R
TIR
Mu
TIR
Cut with RE and ligate on adapters (black boxes). PCR primers are also
TM 65°
TM 50°
Mu
TIR
PCR: 3 cycles at 60°, 1 cycle at 47°, repeat.
TIR
Mu-containing fragments are labeled and preferentially amplified.

Figure 2.

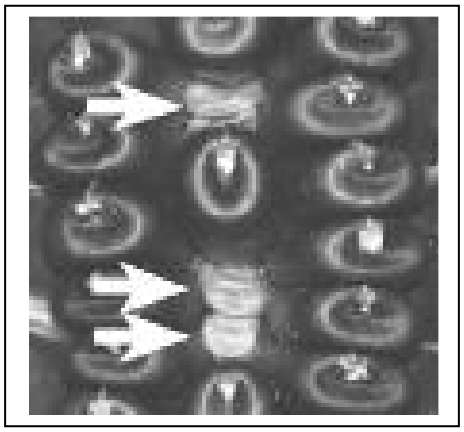

Figure 3.

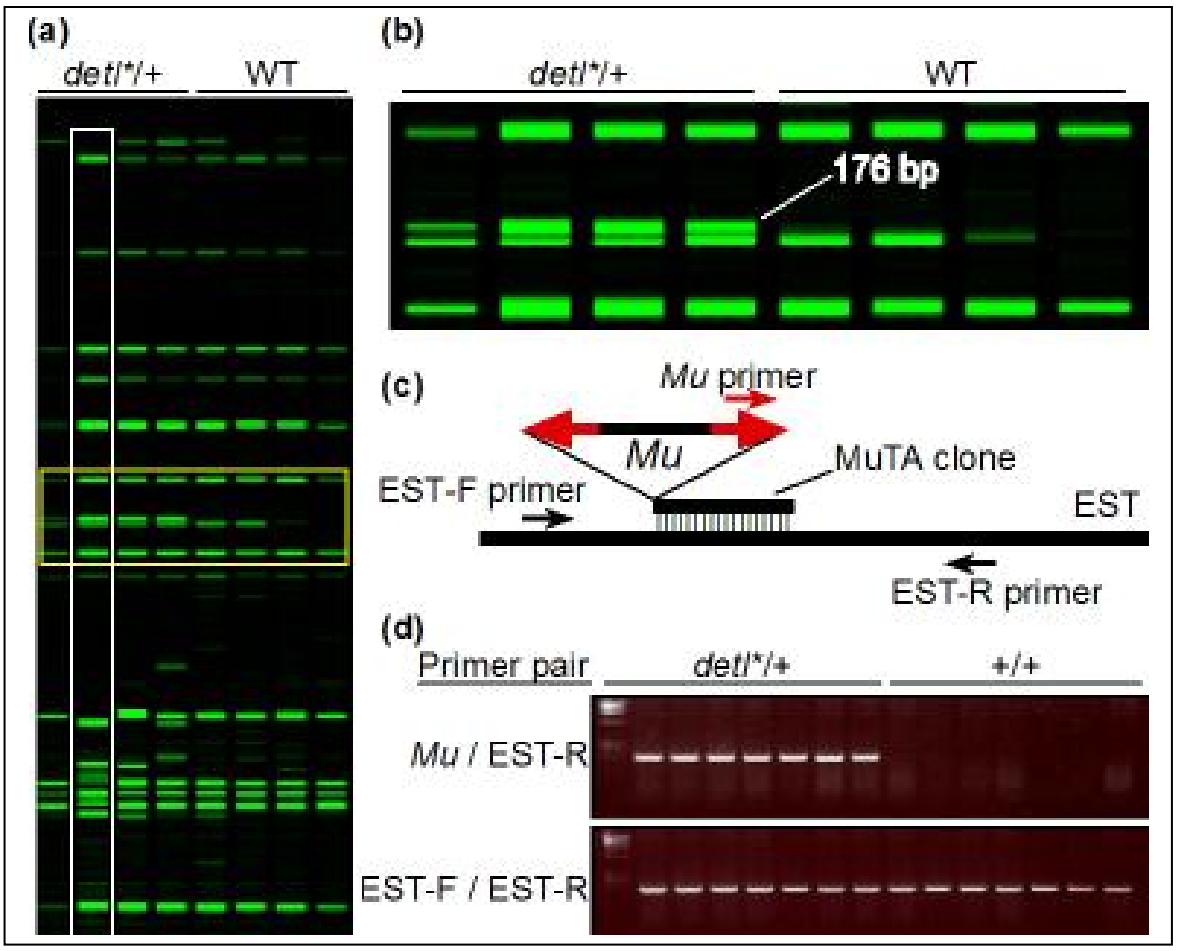
(a)
det1*/+
WT
(b)
det1*/+
WT
176 bp
(c)
Mu primer
Mu
MuTA clone
EST-F primer
EST
EST-R primer
(d)
Primer pair
det1*/+
+/+
Mu / EST-R
EST-F / EST-R

Figure 4.

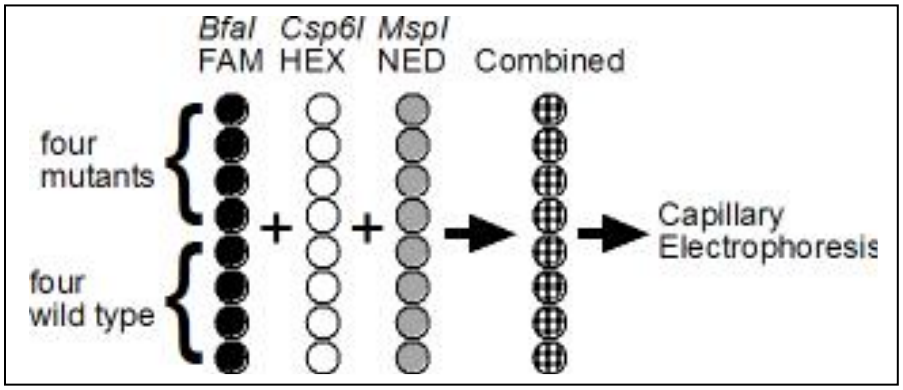
BfaI
FAM
Csp6I
HEX
MspI
NED
Combined
four
mutants
four
wild type
Capillary
Electrophoresis

Figure 5.

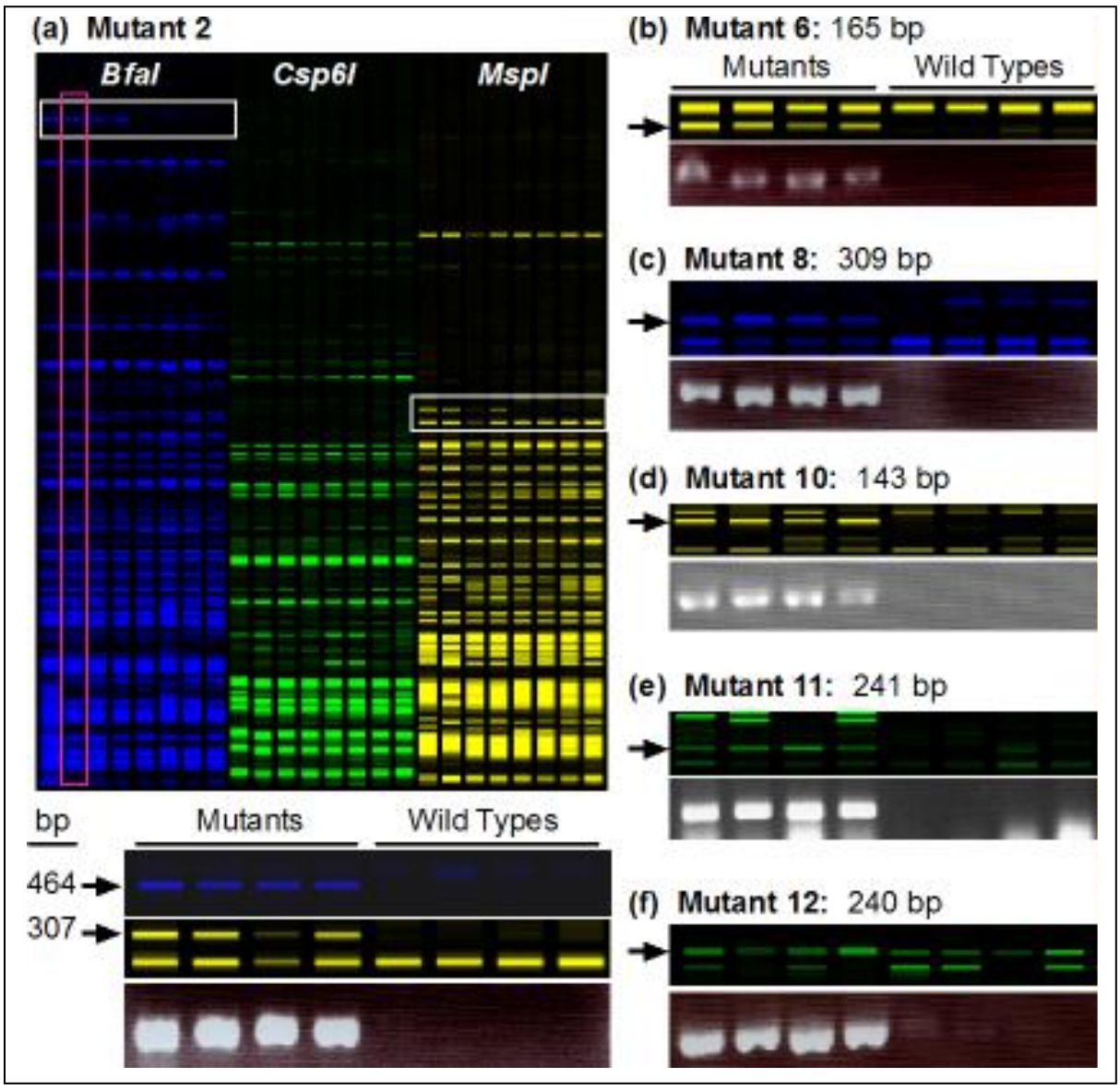
(a) Mutant 2
BfaI
Csp6I
MspI
bp
Mutants
Wild Types
464
307
(b) Mutant 6: 165 bp
Mutants
Wild Types
(c) Mutant 8: 309 bp
(d) Mutant 10: 143 bp
(e) Mutant 11: 241 bp
(f) Mutant 12: 240 bp

Supplemental Figure 1

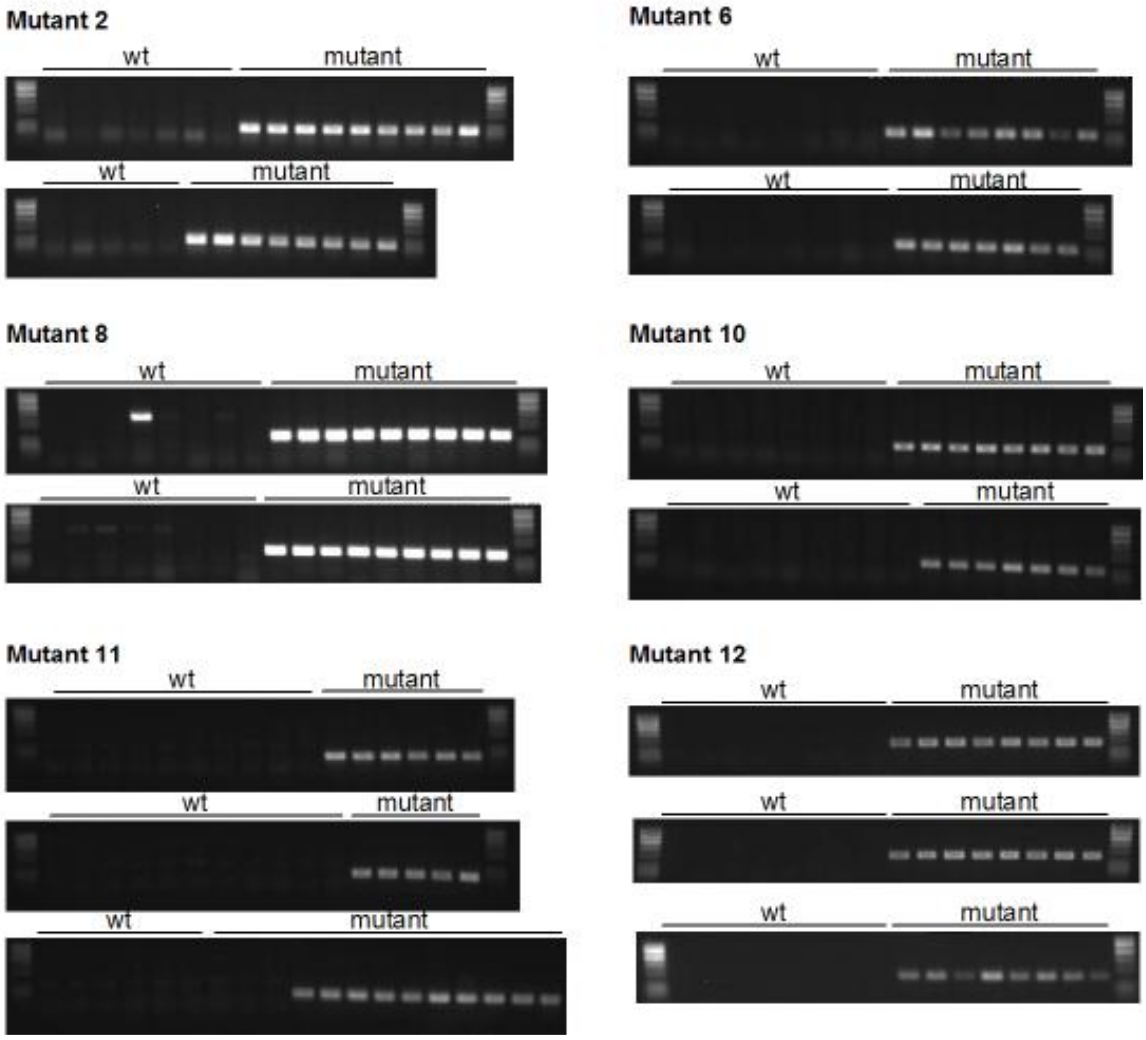

CHAPTER 3. The *thick aleurone1* Mutant Defines a Negative Regulation of Maize Aleurone Fate that Functions Downstream of *dek1*

Gibum Yi[1], Adrienne M. Lauter[2], M. Paul Scott[2,3] and Philip W. Becraft[1,2,3*]

A paper published in *Plant Physiology* in 2011

[1.] Genetics, Development and Cell Biology Dept. Iowa State University, Ames, IA 50011
[2.] USDA-ARS, Corn Insects and Crop Genetics Research Unit, Ames, IA 50011
[3.] Agronomy Dept., Iowa State University, Ames, IA 50011
* For correspondence (phone 1-515-294-2903; fax 1-515-294-6755; becraft@iastate.edu)

Abstract

The maize (*Zea mays*) aleurone layer occupies the single outermost layer of the endosperm. The *dek1* gene is a central regulator required for aleurone cell fate specification. *dek1* mutants have pleiotropic phenotypes including lack of aleurone cells, aborted embryos, carotenoid deficiency and a soft, floury endosperm deficient in zeins. Here we describe the *thick aleurone1* (*thk1*) mutant which defines a novel negative function in the regulation of aleurone differentiation. Mutants possess multiple layers of aleurone cells as well as aborted embryos. Clonal sectors of *thk1* mutant tissue in otherwise normal endosperm showed localized expression of the phenotype with sharp boundaries indicating a localized cellular function for the gene. Sectors in leaves showed expanded epidermal cell morphology but the mutant epidermis generally remained in a single cell layer. Double mutant analysis indicated that the *thk1* mutant is epistatic to *dek1* for several aspects of the pleiotropic *dek1* phenotype. *dek1* mutant endosperm that was mosaic for *thk1* mutant sectors showed localized patches of multilayered aleurone. Localized sectors were surrounded by halos of carotenoid pigments and double mutant kernels had restored zein

profiles. In sum, loss of *thk1* function restored the ability of *dek1* mutant endosperm to accumulate carotenoids and zeins and to differentiate aleurone. Therefore the *thk1* mutation defines a negative regulator that functions downstream of *dek1* in the signaling system that controls aleurone specification and other aspects of endosperm development. The *thk1* mutation was found to be caused by a deletion of approximately 2 megabases.

Introduction

The importance of cereal grain is increasing due to demands for food, feed, energy and other industrial applications. Different seed components contribute various biological functions as well as properties important for these diverse grain uses. The aleurone is important for mineral storage and the remobilization of storage compounds during germination. In *Arabidopsis,* the aleurone controls seed dormancy (Bethke et al., 2007). Aleurone is also the major source of amylase enzymes needed for the malting process and is thought to be responsible for many of the dietary benefits of cereal bran (Becraft and Yi, 2011a).

Most cereal grains including maize have a single cell layer of aleurone that forms at the periphery of the endosperm. Barley (*Hordeum vulgare*) and some varieties of rice (*Oryza sativa*) have multilayer aleurones (reviewed in Becraft et al., 2001b). In maize (*Zea mays*), the Coroico landrace was reported to have a multilayer aleurone (Wolf et al., 1972b). In barley, aleurone layer number is under genetic control and is inherited as a quantitative trait (Jestin et al., 2008).

Aleurone cell fate specification and differentiation has been recently reviewed (Becraft and Yi, 2011a). Plants such as cereals that undergo nuclear type endosperm development show distinct cellular behaviors in the peripheral cell layer compared to internal cells from the onset of cellularization (Brown et al., 1994; Brown et al., 1996; Brown et al., 1999). The peripheral cells assume a typical plant cell division cycle, including the formation of a preprophase band of microtubules that predicts the plane of mitotic cell division. In contrast, the internal cells do not form preprophase bands. This demonstrates a differential response to cellular position at the earliest cellular stages of endosperm development. Nonetheless, aleurone cell fate remains plastic throughout development. The *defective kernel1* (*dek1*) gene is required for aleurone cell identity indicating it is required for the response of endosperm cells to peripheral position. In *dek1* mutant kernels, the peripheral cell layer assumes starchy endosperm cell fate instead of aleurone (Becraft and Asuncion-Crabb, 2000a; Becraft et al., 2002a; Lid et al., 2002b; Wisniewski and Rogowsky, 2004a). Reversion of an unstable *dek1* mutant late in development results in the formation of somatic sectors of aleurone cells in a *dek1* mutant background lacking aleurone (Becraft and Asuncion-Crabb, 2000a). These represent transdifferentiation of starchy endosperm cells to aleurone. Conversely, somatic loss of *dek1* function late in development results in the transdifferentiation of aleurone cells to starchy endosperm. These results demonstrate that the positional cues which specify aleurone cell identity are present throughout endosperm development, that the cells retain the ability to respond to those cues

throughout development, and that the cues are required to maintain as well as specify aleurone cell identity (Becraft and Asuncion-Crabb, 2000a).

Mutant analyses suggest that aleurone cell differentiation is under a hierarchical genetic control (Becraft and Asuncion-Crabb, 2000a; Wisniewski and Rogowsky, 2004a). As described, the *dek1* gene is one of the key components in this regulatory system (Becraft and Asuncion-Crabb, 2000a; Becraft et al., 2002a; Lid et al., 2002b; Wisniewski and Rogowsky, 2004a). The *dek1* gene encodes a plasmamembrane protein with 21 predicted trans-membrane domains, an extracellular loop region, and a cytoplasmic domain containing a calpain protease (Lid et al., 2002b; Wang et al., 2003a). Mutants of *crinkly4* (*cr4*) show similar phenotypes to *dek1* suggesting they function in the same regulatory system (Becraft et al., 1996b; Becraft and Asuncion-Crabb, 2000a; Becraft et al., 2002a). CR4 is a receptor-like kinase (Becraft et al., 1996b; Jin et al., 2000), and as such, both CR4 and DEK1 could potentially function as receptors for the positional cues that induce and maintain aleurone cell fate.

The *supernumerary aleurone1* (*sal1*) mutant produces multiple aleurone layers, indicating it is a negative regulator of aleurone cell fate. The gene encodes a Class E vacuolar sorting protein suggesting it is involved in membrane vesicle trafficking (Shen et al., 2003a). SAL1 is proposed to negatively regulate CR4 and/or DEK1 by directing their retrograde cycling from the plasma membrane and thereby dampening their levels of signaling. Thus, the *sal1* mutant would have increased DEK1 or CR4 signaling, inducing extra layers of aleurone cells. SAL1, DEK1 and CR4 proteins all co-localize in endocytic

vesicles which is consistent with this hypothesis (Tian et al., 2007b). As such, it appears that SAL1 functions upstream of DEK1 and CR4.

Here we report a novel multilayer aleurone mutant, *thick aleurone1* (*thk1*). Genetic mosaic analysis indicates the gene functions locally to inhibit aleurone cell fate in sub-aleurone cells. Double mutant analysis demonstrates that the *thk1* mutant is epistatic to *dek1,* suggesting that *Thk1*+ functions downstream of *Dek1*+ to regulate cell layer number. We propose a model where *Dek1*+ functions as a negative regulator of *Thk1*+.

Results

The thk1 mutant causes specification of extra aleurone layers

In genetic backgrounds that confer anthocyanin pigmentation to the aleurone, recessive *thk1* mutant kernels can be recognized on a segregating ear by their dark pigmentation (Fig. 1, Supplemental Fig. S1). The *thk1* mutant is inherited as a recessive trait that shows complete penetrance and is fully transmissible through both male and female. Sectioning revealed that mutant kernels contain an abnormally thick aleurone layer, typically 4-6 cells thick, in contrast to the single cell layer of wild type (WT). The conclusion that these cells possess aleurone identity is based on their small cuboidal geometry, thick autofluorescent cell walls, accumulation of anthocyanin, lack of starch accumulation, and expression of a *Vp1-GUS* transgene, all markers of aleurone identity (Fig.1, Supplemental Fig. S1).

The thk1 gene is required for embryo development

Mutant kernels lack well developed embryos and fail to germinate when sewn. At the macroscopic level, normal kernels have a large embryo that occupies most of the adaxial face of the kernel. The embryo is greatly reduced or absent in *thk1* mutant kernels (Fig. 1B, C, Supplemental Fig. S1). Microscopic examination showed that mutant embryos are sometimes able to initiate basic embryonic structures, including shoot and root apical meristems and a scutellum. Other times variable morphological abnormalities manifest. Development always lags behind WT and arrests shortly after the transition stage. A novel aspect of the *thk1* mutant phenotype is the lack of a well developed embryo cavity in the endosperm. *Embryoless* (*emb*) mutants typically display a cavity in the endosperm at the site vacated by the aborted embryo (Clark and Sheridan, 1991). In *thk1* mutant kernels, the cavity is much less pronounced.

The thk1 locus maps to chromosome 1S

Recessive mutants can be mapped to chromosome arm using B-A translocations, which undergo non-disjunction in the second pollen mitosis (Beckett, 1978a). The *thk1* locus was localized to chromosome 1S when the mutant phenotype was revealed in segmental monosomic endosperms generated by nondisjunction of the B-A translocation, TB-1Sb. Bulk segregant SNP assays using Sequenom Mass Array™ (Liu et al., 2010b) confirmed the chromosomal location and suggested the locus mapped toward the distal end.

Further mapping was conducted in an F2 population generated by crossing *thk1*/+, in a W22 inbred background, to the B73 inbred. A summary of

markers and recombination frequencies is presented in Table S1 in the supplemental material. Tight linkage was detected with markers in the subdistal region of 1S, however nine markers to the distal most region did not amplify from the mutant, even though they amplified from W22, the background in which *thk1* arose, and B73 (Supplemental Tables S1 and S2). Among the markers tested, the distalmost to amplify from mutant DNA was 363D20-3,4 located at position 2.09 megabase pairs from the chromosome end, according to B73 genome assembly version 2.0. We interpret this to mean that the *thk1* mutant is likely caused by a deletion encompassing approximately 2 megabases. It is therefore formally possible that the phenotype is caused by loss of multiple genes.

The thk1 gene functions locally to regulate aleurone fate

Several potential mechanisms for the action of the *thk1* gene in aleurone cell fate specification give different predictions for the behavior of mutant sectors in genetic mosaics. For example, it is possible that the *thk1* mutant alters the concentration of a hormone or other morphogen that forms a gradient at the endosperm periphery. In such a case, then the gene would be expected to act cell non-autonomously and mutant sectors would show diffuse boundaries. On the other hand, if the *thk1* gene were involved in the interpretation or response to positional information, gene action would more likely be cell-autonomous and sector boundaries would be sharp.

The *Ds1S4* chromosome-breaking *Ds* transposable element was used to generate *thk1* mutant sectors in a background of WT tissue (Neuffer, 1995; Becraft and Asuncion-Crabb, 2000a). As shown in Figure 2, aberrant

transposition of the *Ds* element leads to chromosome breakage followed by loss of the acentric chromosome fragment carrying the WT *Thk1*+ allele. Daughter cells from such an event do not inherit the WT allele and therefore form a clonal sector of hemizygous *thk1* mutant cells. The *Ds1S4* line carrying *Ac* at the *P1* locus was crossed as a male to heterozygous *thk1*/+ mutant females. Among the F1 were kernels containing darkly pigmented sectors in an otherwise normally pigmented endosperm (Fig. 2, Table 1). Sectioning of these dark sectors revealed that they displayed the multilayered aleurone phenotype typical of *thk1* mutants.

Sector borders were sharp as would be expected for cell-autonomous gene action. A stringent test of cell-autonomy requires that sectors be marked with an independent marker. Sectors were generated that contained *thk1* marked with the linked *vp5* carotenoid-deficient mutant but unfortunately *vp5* sectors were not discernable in the endosperm. Therefore, it can be concluded that the *thk1* gene functions locally in a manner consistent with cell-autonomy but because sector boundaries could not be assessed independent of the *thk1* mutant phenotype, cell-autonomy remains equivocal.

It was of interest to test whether the *thk1* mutation could uncouple aleurone cell fate from surface position. Transpositions that occur late in development result in the formation of small sectors and the *Ds1S4* line has been shown to generate single-celled sectors (Becraft and Asuncion-Crabb, 2000a). Therefore, if *thk1* uncoupled aleurone fate from surface position, it should be possible to detect internally isolated aleurone cells. To explore this, 60 kernels

were sectioned and a total of 421 sectors examined. Late *thk1* sectors were readily observed in most mosaic kernels but none were observed where there was not a continuity of aleurone cell contacts to the surface of the endosperm (Fig. 2 and Supplemental Fig. S2). That is, no internal aleurone cells were observed where all their surrounding neighbors were starchy endosperm cells.

The thk1 deletion affects leaf epidermal cell size

These genetic stocks also afforded the opportunity to examine the phenotype of *thk1* mutant cells in sporophyte tissues, which cannot otherwise be studied because *thk1* mutants are embryo lethal. For these experiments, the *thk1* mutant allele was linked in coupling to *vp5*, which confers cell-autonomous albino sectors in leaves due to carotenoid deficiency (Becraft et al., 2002a). As a control, the *vp5* mutant linked to the normal *Thk1+* allele was used. These chromosomes were made heterozygous with the Ds1S4 chromosome-breaker and leaves were examined for *thk1* mutant sectors. In particular, we were interested in testing the hypothesis that the *thk1* mutant might confer multiple leaf epidermal layers because many genes such as *Extra Cell Layers (Xcl)* similarly affect the aleurone and leaf epidermis (Kessler et al., 2002a; Becraft and Yi, 2011a). Ds1S4 leaves carrying the *thk1* mutant allele showed prominent ridges that often caused the leaves to crease (Supplemental Fig. S3). These were not present in control *vp5*-sectored leaves, nor did they form in *dek1* sectors (Becraft et al., 2002a). Examination of these sectors revealed irregular epidermal cells that often appeared enlarged in section. In most instances, mutant epidermis was clearly a single cell layer, even when the sector covered an extensive area of the

epidermis (e.g. Fig 3B). Several instances were observed where internal cells displayed characteristics consistent with epidermal cell identities. Figure 3C shows an example where internal cells either showed features of sclerenchyma or bulliform-like cells. Sclerenchyma cells occur internally in localized foci associated with major and intermediate veins (Fig. 3A). In *thk1* mutant sectors, internal sclerenchyma cells were observed interveinally. Other internal cells were observed that did not have characteristics of mesophyll or other normal internal cell types but resembled bulliform cells.

The thk1 mutant is epistatic to dek1

Of the various mutants that disrupt aleurone cell fate specification, *dek1* is the strongest and most consistent. The weak *dek1-D* allele causes a partial and somewhat variable loss of aleurone identity while the severe *dek1-1394* allele causes a complete loss of aleurone (Becraft and Asuncion-Crabb, 2000a; Becraft et al., 2002a). To test the genetic relationship between the two genes, *thk1*/+ was crossed to *dek1-D*/+ and the resultant F1 plants were self pollinated to generate ears segregating F2 kernels. Six full ears were obtained that segregated both mutants.

A summary of the totals of each phenotypic class are presented in Table 2. Kernels with *dek1-D* phenotypes were examined for the presence of thick aleurone but none was found. Ears contained three major phenotypic classes, WT, *dek1-D* and *thk*, with a few malformed and aborted kernels of questionable phenotype with respect to *dek1* and *thk*. Notably, there was an excess of *thk* mutant kernels relative to *dek1-D*. A χ^2 test for goodness of fit of the data to a

9:3:3:1 ratio, expected for independent assortment, produced a value of 229.89 indicating that this hypothesis should be rejected. When tested for fit to a 9:4:3 ratio, a χ^2 value of 9.68 indicated that the data fit this hypothesis. The *thk1* mutant was then crossed to *dek1-1394* to test whether the same segregation ratios would hold for a strong *dek1* allele. Three ears were obtained that segregated both mutants, and again *thk1* mutants were in excess relative to *dek1* and the data fit a 9:4:3 ratio ($\chi^2 = 3.31$) but not 9:3:3:1 ($\chi^2 = 95.74$). Thus, segregation ratios suggested that the excess *thk1* mutants were in fact *thk1, dek1* double mutants and that *thk1* is epistatic to *dek1*.

Two alternative explanations other than epistasis were considered to explain the data. The first was linkage; both *thk1* and *dek1* loci are on chromosome 1S. However, *dek1* maps proximally and *thk1* maps distally, and in a cross of *thk1, dek1-1394* /+ + to B73, the mutants were transmitted to progeny independently, indicating that the loci are genetically unlinked. The second possibility considered was inefficient transmission of the *dek1* mutant alleles. The cross that generated the ears segregating both *thk1* and *dek1-1394* also generated ears segregating for each mutant individually. As summarized in Table 2, ears segregating only *dek1-1394* contained mutant kernels in a ratio that did not differ significantly from 3:1 (χ^2=1.91), indicating the mutant allele was transmitted with full efficiency.

Finally, kernels with a *thk1* mutant phenotype were selected from an F2 ear segregating for both the *thk1* and *dek1* mutants. These kernels were genotyped using a DNA marker, IDP112, located approximately 2 cM from the

dek1 locus (Fig. 4A). Among 18 kernels genotyped, 5 were homozygous *Dek1+*, 8 were heterozygous *Dek1+/dek1-1394* and 5 were homozygous mutant *dek1-1394* (barring recombination). Therefore, double homozygous mutants have a *thk1* phenotype and *thk1* is epistatic to *dek1-D* and *dek1-1394*.

The epistatic action of thk1 revealed in genetic mosaics

To further test the epistatic relationship of *thk1* to *dek1,* we generated genetic mosaics that contained *thk1* mutant sectors in a *dek1-1394* background (Fig. 5, Supplemental Fig. S4). More precisely, *thk1, dek1-1394*/-, - hemizygous sectors were generated in a *dek1-1394/dek1-1394* background. The epistatic action of *thk1* predicted that such mosaics should contain sectors of thick aleurone on kernels otherwise devoid of aleurone. The strategy for generating these mosaics is shown in Figure 5A and the cross used to generate the appropriate genotypes is described in Supplemental Fig. S4. Data are summarized in Table 1.

Figure 5 shows examples of clonal sectors of *thk1, dek1-1394/-,-* double mutant cells in otherwise *dek1-1394* single mutant kernels. Whereas *dek1-1394* kernels are devoid of aleurone cells, the loss of *Thk1+* function restored the ability of *dek1* mutant endosperm cells to form aleurone, and conferred the multilayered aleurone phenotype of *thk1* mutants.

In addition to the sector types described above, kernels were frequently observed that contained separate *dek1* and *thk1* sectors (Supplemental Fig. S4). Such kernels most likely result from interstitial chromosome deletions or rearrangements as has been described for chromosome-breaking double *Ds*

elements (English et al., 1995). Because the exact chromosomal position of the *Ds1S4* is not known, the experiment was repeated with two well characterized *fAc* derivatives of *P1-vv*. *P1-wwB54* has been shown to cause various chromosome rearrangements, including interstitial deletions and rearrangements, while *P1-vv9D9A* generates primarily distal deletions (Zhang and Peterson, 2004; Yu et al., 2011). Both are located at the *P1* locus, 1 cM proximal to *dek1*. Crosses with *P1-wwB54* generated the same array of kernel types as *Ds1S4* (data not shown). In contrast, *p1-vv9D9A* generated all the expected sector types but very few kernels with mixed *thk1* and *dek1*sectors. Among 5 ears from crosses to *dek1-1394*/+ females, 320 *dek1* mutant kernels were observed and none contained any aleurone cells. From 18 crosses to *thk1,dek1-1394*/+,+ females, 14 kernels were recovered that had *thk1* phenotypic sectors in *dek1* mutant kernels. Thus, for all three chromosome breakers, crosses to *thk1,dek1-1394*/+,+ females produced *dek1* mutant kernels with *thk1* sectors, while when crossed to *dek1-1394*/+ alone, no instance of a pigmented sector or aleurone cell was observed among 1586 *dek1* mutant kernels examined, validating the interpretation of sector types.

thk1 epistasis is pleiotropic

Mutant *dek1* kernels show a variety of phenotypic defects in addition to the lack of aleurone. These include a deficiency of carotenoid pigments as well as opaque endosperm with a soft floury texture. Mosaic kernels with isolated *thk1* sectors in a *dek1* mutant background showed yellow halos of carotenoid

pigments surrounding the *thk1* sectors (Fig. 5C) suggesting that *thk1* is epistatic to *dek1* for this trait as well.

Floury endosperm can result from a deficiency in zein storage protein accumulation. The double mutant kernels genotyped above did not show a floury texture. To test the hypotheses that the floury texture of *dek1* endosperm reflected a zein deficiency and that the *thk1* mutant suppressed this deficiency in double mutants, zein profiles were analyzed by HPLC (Fig. 4). Compared to wild type, *dek1* mutants showed dramatic reductions in gamma zeins including the 27kD gamma zeins. In contrast, the *thk1* mutant endosperms showed zein profiles very similar to wild type. The *dek1, thk1* double mutant endosperms also showed zein profiles remarkably similar to wild type. Thus, the *thk1* mutant is epistatic to *dek1* for the regulation of aleurone formation, carotenoid accumulation and gamma zein accumulation.

Discussion

We described a new recessive loss-of-function mutant that causes an increased number of aleurone layers in maize endosperm. In addition the mutant results in embryo lethality. Other than the effect on the aleurone layer, the overall morphology of the endosperm is generally normal. One aspect of the *thk1* mutant kernels that is novel compared to most *emb* mutants is that they do not form a prominent cavity in the region of the endosperm vacated by the aborted embryo (Clark and Sheridan, 1991).

The *thk1* mutant is likely caused by a deletion encompassing approximately 2 megabases. It is therefore formally possible that the phenotype

is caused by loss of multiple genes. Regardless of whether the *thk1* mutant phenotype results from loss of one or multiple genes, the analysis presented here clearly demonstrates a function in the aleurone signaling system encoded by the distal region of chromosome 1S.

The thk1 *gene functions locally in the cellular response to position*

The *thk1* gene functions locally within the endosperm as evident by the distinct sector boundaries. Similarly clear boundary delineations were observed both for *thk1* mutant sectors in fields of normal endosperm cells and for double mutant sectors in fields of *dek1* mutant cells. Because mutant sectors were not marked with an independent cell-autonomous marker, it cannot be definitely concluded that *thk1* function is cell-autonomous but this is likely the case.

The *dek1* gene produces similarly sharp sector boundaries and has been proposed to function in the cellular response to positional cues (Becraft and Asuncion-Crabb, 2000a; Becraft et al., 2002a; Lid et al., 2002b; Tian et al., 2007b). The results reported here strengthen that model. The sharp boundaries of *thk1,dek1* double mutant sectors in *dek1* mutant endosperm indicate that the epistatic relationship of *thk1* to *dek1* is likely to function at the cell-autonomous level. As such, the signaling system defined by these two genes would appear to function in the response of endosperm cells to position rather than in the generation of those positional cues.

Aleurone forms on the surface of endosperm that is isolated from contacts with surrounding kernel tissues either by in vitro culture or as a consequence of a mutant phenotype (Olsen, 2004a; Gruis et al., 2006a; Reyes et al., 2010). These

observations led to the proposal of the ‘surface rule’ which posits that the source of the positional information that specifies aleurone identity is intrinsic to the endosperm. The *Ds1S4* line generates late-occurring transposition events that produce sectors as small as a single cell (Becraft and Asuncion-Crabb, 2000a). Late *thk1* sectors were readily observed but interestingly, none were observed where there was not a continuity of aleurone cell contacts to the surface layer of the endosperm (Fig. 2 and Supplemental Fig. S2). That is, no internal aleurone cells were observed that where completely surrounded on all sides by starchy endosperm cell neighbors. In contrast, isolated single cells at the surface can be completely surrounded by starchy endosperm and still assume aleurone identity (Becraft and Asuncion-Crabb, 2000a). So while the *thk1* mutant produces aleurone cells in sub-peripheral cell layers, there still appears to be adherence to the surface rule. It may be that determinants of aleurone fate are transmitted from the surface only via aleurone cells. This transmission could potentially be through plasmodesmatal connections, which are distinct between aleurone cells compared to other endosperm cell types (Tian et al., 2007b), via lineage, or by an aleurone-specific signaling mechanism. These results imply that *Thk1+* function is normally required for the transdifferentiation event that occurs in the internal daughters of periclinal aleurone cell divisions. Such internal cells normally redifferentiate to starchy endosperm cells (Becraft and Asuncion-Crabb, 2000a) and this might be the primary site of action for *Thk1+*. The formation of small isolated *thk1* sectors in *dek1* kernels indicates there is no requirement for aleurone continuity in the lateral dimension (Supplemental Fig. S2).

Mutant sectors in leaves produced enlarged epidermal cells that resembled bulliform cells in morphology and histological staining characteristics. In most sectors observed, these cells occupied a single epidermal layer. In *cr4* mutants, cells with unmistakable epidermal identities, such as epidermal hair cells, were observed internally (Jin et al., 2000). A few examples were observed in *thk1* sectors where internal cells had characteristics consistent with epidermal identity, but not unequivocal. Thus, it seems possible that *thk1* may function to regulate leaf epidermal cell layer number, but this remains tenuous. It is clear that a *thk1* deficiency in epidermal cells does not directly cause them to form a multi-layered epidermis. Furthermore, because multiple genes are deficient due to the deletion, it is not possible to formally conclude that the gene(s) regulating leaf epidermal cells are the same as those regulating aleurone development, although this seems likely given the similar functions of other genes in aleurone and leaf epidermis (Kessler et al., 2002a; Becraft and Yi, 2011a).

The regulation of aleurone layer number

The genetic regulation of aleurone cell layer number does not appear to be simple. Typical barley cultivars contain 3-4 aleurone layers, with layer number inherited as a quantitative trait (Jestin et al., 2008). The recessive barley *des5* mutant possesses a single aleurone layer indicating this gene normally functions to increase layer number, opposite *Thk1+* (Olsen et al., 2008). The Multiple Aleurone Layer trait present in Coroico maize landraces is inherited as a partially dominant, but complex, trait (Wolf et al., 1972b, our unpublished observations). *Xcl* is another dominant maize mutant that produces double aleurone cell layers

(Kessler et al., 2002a). Transgenic knockdown of two rice transcription factors also affected aleurone layer number. RISBZ1 and RPBF are bZIP and DOF zinc finger transcription factors, respectively, that function together to regulate endosperm storage protein gene expression (Yamamoto et al., 2006). Knockdown of either factor singly had mild or no effects on the aleurone but the double knockdown of both genes produced a multilayered, disordered aleurone (Kawakatsu et al., 2009).

Maize, *sal1* mutants also produce extra layers of aleurone cells. The *sal1* gene maps to chromosome 9 and encodes a CHMP Class E vacuolar sorting protein. It appears to act upstream as a negative regulator of *dek1* (Shen et al., 2003a; Tian et al., 2007b). In contrast, the epistatic relationship of *thk1*over *dek1* suggests that *thk1* functions downstream of *dek1*. *dek1* encodes a plasmamembrane localized protein with a predicted extracellular domain and a cytoplasmic calpain protease domain (Lid et al., 2002b; Wang et al., 2003a). It functions in the signaling system that specifies aleurone fate (Becraft and Asuncion-Crabb, 2000a; Becraft et al., 2002a; Lid et al., 2002b; Tian et al., 2007b). As such, the *thk1* gene product represents a likely target of regulation by DEK1, potentially a direct target.

The calpain protease function of DEK1 suggests that targets of regulation would likely be proteolytic substrates, which could provide a clue to the identity of the *thk1* gene. However, substrate recognition by calpains is complex and involves three dimensional structures that are not easily recognized in primary sequences (reviewed in Goll et al., 2003; Croall and Ersfeld, 2007). Known

calpain substrates in mammalian systems include many membrane proteins including receptors, but also diverse other proteins such as cytoskeletal proteins and transcription factors. Therefore, it is not feasible to predict a candidate *thk1* gene from within the deleted region based on potential calpain substrates.

A model for the regulation of aleurone cell fate

The loss of function *thk1* mutant results in the specification of extra layers of aleurone cells indicating that the normal gene function is to negatively regulate aleurone fate in the sub-peripheral layers. The function of the normal *dek1* gene is to promote aleurone identity in the peripheral cell layer. The epistatic relationship of *thk1* over *dek1* suggests that the *thk1* gene functions downstream of *dek1* in the specification of aleurone fate (and in the control of other endosperm traits). As such, a model where *Dek1*+ promotes aleurone identity by negatively regulating *Thk1*+ accounts for all the available data. As shown in Figure 6, *Dek1*+ could normally function in the peripheral layer to inhibit *Thk1*+ function and thereby permit aleurone formation. In *dek1* mutants, *Thk1*+ function would be derepressed in the peripheral cell layer and block aleurone differentiation. In *thk1* mutants, there would be no repressive function regardless of whether *dek1* were functional. As discussed below, additional factors must be involved that limit aleurone fate to the peripheral regions of the endosperm.

Pleiotropic epistasis

DEK1 function is not restricted to the regulation of aleurone cell fate as is evident from the pleiotropy of the *dek1* mutant phenotype. Mutants are

carotenoid deficient, have floury, opaque endosperms and are embryo lethal. The opaque endosperm phenotype likely relates to a zein storage protein deficiency (Fig. 4). Carotenoid and zein content are important grain quality traits. Interestingly, *thk1* mutants appear to rescue these aspects of the *dek1* mutant phenotype indicating that *Thk1+* has functions in addition to aleurone regulation.

That *dek1* and *thk1* appear to function in a regulatory pathway that controls zein and carotenoid accumulation in internal starchy endosperm cells indicates that the function of this pathway to regulate aleurone specification is context dependent and only occurs in the peripheral few cell layers of the endosperm. It is therefore evident that additional factors are ultimately involved in patterning the endosperm. One possible source of positional information could be auxin, which was recently reported to be at highest concentrations in the periphery of maize endosperm and to possibly influence aleurone fate specification (Forestan et al., 2010b).

The relationship between protein content and aleurone cell layer number is not currently understood but several previous reports have hinted at it. The Coroico landrace with the Multiple Aleurone Layer trait is also high in protein content (Wolf et al., 1972b). While it was recently shown that zeins are expressed in aleurone cells (Reyes et al., 2011), such a minor fraction of the endosperm is unlikely to have a major impact on the overall endosperm protein content, and it was concluded that the aleurone layer and protein content traits of Coroico were likely controlled separately (Nelson and Chang, 1974). As mentioned, the rice RISBZ1 and RPBF transcription factors function to promote

prolamine storage protein gene expression in the endosperm as well as restrict aleurone layer number (Yamamoto et al., 2006; Kawakatsu et al., 2009). This relationship is different from *thk1* which appears to negatively regulate both aleurone layers and zein accumulation.

Signaling has previously been implicated in the regulation of zein accumulation. Protein levels and activity, as well as transcript levels of maize OPAQUE2 (O2), a bZIP transcription factor that promotes alpha-zein gene expression, are regulated diurnally (Ciceri et al., 1997; Ciceri et al., 1999). The protein undergoes cyclic phosphorylation and dephosphorylation, with unphosphoryated forms having higher DNA binding activity. Highest levels are present during the daytime phase of the diurnal cycles, but phosphorylation ratios do not appear to change during development. Genetic and cell biological evidence suggest that DEK1 functions in the same regulatory system as the CR4 receptor kinase to regulate aleurone cell fate as well as other aspects of development (Becraft and Asuncion-Crabb, 2000a; Becraft et al., 2002a; Tian et al., 2007b). Mutants of *cr4* show an opaque kernel phenotype, similar to *dek1*, consistent with the hypothesis that both genes may also function together to regulate storage proteins (Jin et al., 2000). The current study now places *thk1* in that system. It is not yet evident why the same signaling system responsible for aleurone cell fate specification would also be used to regulate zein accumulation. This will become clear when the regulatory networks of endosperm development are more completely understood.

Materials and methods

Genetic stocks

The *thk1* mutant arose in a *Mutator* transposon line in a maize (*Zea mays*) W22 inbred background and was a kind gift from Donald McCarty, University of Florida. The *dek1-1394* and *vp5* mutants and the Ds1S4 line were obtained from the Maize Genetics Cooperation Stock Center, Urbana, IL. The *dek1-D* mutant was a gift from Hugo Dooner, Waksman Institute. The *P1-WWB54* and *p1-vv9D9A* lines were gifts from Thomas Peterson, Iowa State University. The *thk1* and *dek1* mutants were backcrossed 5 generations into a B73 inbred background.

Microscopy and histology

For Figure 1 C-F, developing kernels were dissected from young ears, fixed in FAA (formaldehyde, alcohol and acetic acid) and embedded in Paraplast Plus according to standard procedures (Berlyn and Miksche, 1976). 10 µm sections were affixed to glass slides, deparaffinized, stained with fast green and mounted. Figure 1 G and H were 28 DAP kernels fixed in 2% paraformaldehyde and 3% gluteraldehyde buffered in 0.1M cacodylate (pH 7.2) and embedded in LR White resin. Samples were sectioned to 1 µm on a Leica EM UC6 ultramicrotome and stained with Periodic Acid Schiff's (PAS) and Toluidine blue. Leaf sections (Fig. 3) were prepared the same way except no PAS stain was applied. For Figure 1I and J, 24 DAP kernels were hand sectioned and incubated in GUS staining solution (50 mM sodium phosphate [pH 7.0], 0.5 mM potassium

ferricyanide, 0.5 mM potassium ferrocyanide, 10 mM EDTA, 0.05% [v/v] Triton X-100, 0.35 mg/ml 5-bromo-4-chloro-3-indolyl-b-D-glucuronide) for 24 h at 37^{o}C for several hours until blue precipitate was apparent (Jefferson et al., 1987). Figures 1K and L were hand sectioned mature kernels examined under epifluorescence using a narrow-violet filter (excitation 400–410 nm, dichroic mirror and barrier filter, 455 nm). Mosaic kernel sectors were examined using epi-illumination of hand sections. All micrography was performed with an Olympus BX-60 microscope equipped with a Jenoptik C-5 camera.

Genetic mapping and genotyping

Genomic DNA was extracted from mature dried kernels with modifications to a described protocol (Edwards et al., 1991). Briefly, kernels were cut with a razor blade and a half kernel was extracted for mutants and a quarter kernel for wild type (~100mg). Kernels were soaked in 200 µl extraction buffer for 3 to 12 hours at room temperature. Samples were then ground with a plastic pestle and a hand-held drill. Additional buffer was added to a total volume of 500 µl, followed by the addition of 400 µl chloroform. Samples were vortexed and then centrifuged 10 min at 13,000 rpm with a tabletop centrifuge. After transferring 250 µl of supernatant to a new tube, DNA was precipitated with an equal volume of isopropyl alcohol. Samples were centrifuged and the pellet was washed with 70% ethanol and air-dried. The pellet was then dissolved in 500 µl distilled water. 1 µl (20-50 ng genomic DNA) was used for PCR. All PCR was performed with Go Tag Green Mastermix (Promega) in 10 µl reactions containing 5 pmol of each primer. Cycling conditions were 94^{o}C for 4 min followed by 35 cycles of 94^{o}C for

30 sec, 55^{o}C for 30 sec, 72^{o}C for 1 min. After an additional 10 min at 72^{o}C, reactions were kept at 4^{o}C until visualized by agarose gel electrophoresis.

HPLC analysis of zein proteins

Alcohol-soluble proteins were extracted from 25 mg of flour using 1000 µL extraction buffer consisting of 70% EtOH, 61 mM NaOAc, and 5% β-mercaptoethanol. The mixture was vortexed briefly, shaken for 1 h at room temperature, and then centrifuged for 10 min at 13,000 rpm. An aliquot of 25 µL of each extract was injected into a C18 protein and peptide column heated to 55^{o}C in a Waters 2695 Separation Module, and absorbance at 200 nm was measured with a Waters 2487 Dual Absorbance Detector. Separation of distinct proteins based on hydrophobicity was achieved with a gradient of ultrapure water and acetonitrile, both containing 0.01% trifluoroacetic acid. The complex gradient ranged from 20 to 60% acetonitrile for a total of 75 min excluding equilibration steps before and after elution. Gradient slopes were optimized for separation of peaks. A flow rate of 1 mL/min was used.

Acknowledgments

The authors thank Donald R. McCarty for the gift of the *thk1* mutant and Thomas A. Peterson for the *fAc* lines. Amanda Ripley provided excellent technical assistance. The Iowa State University Microscopy and NanoImaging Facility assisted with some of the microscopic preparations. The Iowa State University Genomic Technologies Facility provided the mass array SNP genotyping service.

References

Ahern, K.R., Deewatthanawong, P., Schares, J., Muszynski, M., Weeks, R., Vollbrecht, E., Duvick, J., Brendel, V.P., and Brutnell, T.P. (2009). Regional mutagenesis using Dissociation in maize. Methods **49,** 248-254.

Altschul, S.F., Gish, W., Miller, W., Myers, E.W., and Lipman, D.J. (1990). Basic local alignment search tool. J Mol Biol **215,** 403-410.

Beckett, J.B. (1978a). B-A translocations in maize. I. Use in locating genes by chromosome arms. J. Heredity **69,** 27-36.

Beckett, J.B. (1978b). B-A TRANSLOCATIONS IN MAIZE .1. USE IN LOCATING GENES BY CHROMOSOME ARMS. Journal of Heredity **69,** 27-36.

Becraft, P.W. (2001). Cell fate specification in the cereal endosperm. Seminars in Cell & Developmental Biology **12,** 387-394.

Becraft, P.W., and Asuncion-Crabb, Y. (2000a). Positional cues specify and maintain aleurone cell fate in maize endosperm development. Development **127,** 4039-4048.

Becraft, P.W., and Asuncion-Crabb, Y.T. (2000b). Positional cues specify and maintain aleurone cell fate during maize endosperm development. Development **127,** 4039-4048.

Becraft, P.W., and Yi, G. (2011a). Regulation of aleurone development in cereal grains. J Exp Bot **62,** 1669-1675.

Becraft, P.W., and Yi, G. (2011b). Regulation of aleurone development in cereal grains. Journal of Experimental Botany **62,** 1669-1675.

Becraft, P.W., Stinard, P.S., and McCarty, D.R. (1996a). CRINKLY4: a TNFR-like receptor kinase involved in maize epidermal differentiation. Science **273,** 1406-1409.

Becraft, P.W., Stinard, P.S., and McCarty, D.R. (1996b). CRINKLY4: A TNFR-like receptor kinase involved in maize epidermal differentiation. Science **273,** 1406-1409.

Becraft, P.W., Li, K.J., Dey, N., and Asuncion-Crabb, Y. (2002a). The maize dek1 gene functions in embryonic pattern formation and cell fate specification. Development **129,** 5217-5225.

Becraft, P.W., Li, K., Dey, N., and Asuncion-Crabb, Y.T. (2002b). The maize *dek1* gene functions in embryonic pattern formation and in cell fate specification. Development **129,** 5217-5225.

Becraft, P.W., Brown, R.C., Lemmon, B.E., Opsahl-Ferstad, H.G., and Olsen, O.-A. (2001). Endosperm Development. In Current Trends In The Embryology Of Angiosperms, S.S. Bhojwani, ed (Dordrecht: Kluwer), pp. 353-374.

Berlyn, G.P., and Miksche, J.P. (1976). Botanical microtechnique and cytochemistry. (Ames, IA: Iowa State University Press).

Bethke, P.C., Libourel, I.G.L., Aoyama, N., Chung, Y.-Y., Still, D.W., and Jones, R.L. (2007). The Arabidopsis aleurone layer responds to nitric oxide, gibberellin, and abscisic acid and is sufficient and necessary for seed dormancy. Plant Physiol. **143,** 1173-1188.

Bomblies, K., Wang, R.L., Ambrose, B.A., Schmidt, R.J., Meeley, R.B., and Doebley, J. (2003). Duplicate FLORICAULA/LEAFY homologs zfl1 and zfl2 control inflorescence architecture and flower patterning in maize. Development **130,** 2385-2395.

Borowicki, A., Stein, K., Scharlau, D., Scheu, K., Brenner-Weiss, G., Obst, U., Hollmann, J., Lindhauer, M., Wachter, N., and Glei, M. (2010). Fermented wheat aleurone inhibits growth and induces apoptosis in human HT29 colon adenocarcinoma cells. British Journal of Nutrition **103,** 360-369.

Briggs, S.P., and Beavis, W.D. (1994). How RFLP loci can be used to assist transposon-tagging efforts. In The Maize Handbook, M. Freeling and V. Walbot, eds (New York: Springer-Verlag), pp. 653-659.

Brown, R.C., Lemmon, B.E., and Olsen, O.-A. (1994). Endosperm development in barley: microtubule involvement in the morphogenetic pathway. Plant Cell **6,** 1241-1252.

Brown, R.C., Lemmon, B.E., and Olsen, O.A. (1996). Development of the endosperm in rice (Oryza sativa L.): cellularization. J. Plant Res. **109,** 301-313.

Brown, R.C., Lemmon, B.E., Nguyen, H., and Olsen, O.-A. (1999). Development of endosperm in *Arabidopsis thaliana*. Sex. Plant Reprod. **12,** 32-42.

Brutnell, T.P. (2002). Transposon tagging in maize. Functional & Integrative Genomics **V2,** 4.

Cao, X.Y., Costa, L.M., Biderre-Petit, C., Kbhaya, B., Dey, N., Perez, P., McCarty, D.R., Gutierrez-Marcos, J.F., and Becraft, P.W. (2007). Abscisic acid and stress signals induce viviparous1 expression in seed and vegetative tissues of maize. Plant Physiology **143,** 720-731.

Ciceri, P., Locatelli, F., Genga, A., Viotti, A., and Schmidt, R.J. (1999). The activity of the maize Opaque2 transcriptional activator is regulated diurnally. Plant Physiology **121,** 1321-1327.

Ciceri, P., Gianazza, E., Lazzari, B., Lippoli, G., Genga, A., Hoschek, G., Schmidt, R.J., and Viotti, A. (1997). Phosphorylation of Opaque2 changes diurnally and impacts its DNA binding activity. Plant Cell **9,** 97-108.

Clark, J.K., and Sheridan, W.F. (1991). Isolation and characterization of 51 embryo-specific mutations of maize. Plant Cell **3,** 935-951.

Colasanti, J., Yuan, Z., and Sundaresan, V. (1998). The indeterminate gene encodes a zinc finger protein and regulates a leaf-generated signal required for the transition to flowering in maize. Cell **93,** 593-603.

Colasanti, J., Tremblay, R., Wong, A.Y.M., Coneva, V., Kozaki, A., and Mable, B.K. (2006). The maize INDETERMINATEI flowering time regulator defines a highly conserved zinc finger protein family in higher plants. Bmc Genomics **7**.

Croall, D., and Ersfeld, K. (2007). The calpains: modular designs and functional diversity. Genome Biology **8,** 218.

Das, L., and Martienssen, R. (1995). Site-selected transposon mutagenesis at the hcf106 locus in maize. Plant Cell **7,** 287-294.

Dash, S., Van Hemert, J., Hong, L., Wise, R.P., and Dickerson, J.A. (2012). PLEXdb: gene expression resources for plants and plant pathogens. Nucleic Acids Research **40,** D1194-D1201.

Dooner, H.K., and Belachew, A. (1989). Transposition Pattern of the Maize Element Ac from the Bz-M2(ac) Allele. Genetics **122,** 447-457.

Edwards, K., Johnstone, C., and Thompson, C. (1991). A simple and rapid method for the preparation of plant genomic DNA for PCR analysis. Nucleic Acids Res **19,** 1349.

Emrich, S.J., Barbazuk, W.B., Li, L., and Schnable, P.S. (2007). Gene discovery and annotation using LCM-454 transcriptome sequencing. Genome Research **17,** 69-73.

English, J.J., Harrison, K., and Jones, J. (1995). Aberrant Transpositions of Maize Double Ds-Like Elements Usually Involve Ds Ends on Sister Chromatids. Plant Cell **7,** 1235-1247.

Fenech, M., Noakes, M., Clifton, P., and Topping, D. (2005). Aleurone flour increases red-cell folate and lowers plasma homocyst(e)ine substantially in man. British Journal of Nutrition **93,** 353-360.

Feurtado, J.A., Huang, D.Q., Wicki-Stordeur, L., Hemstock, L.E., Potentier, M.S., Tsang, E.W.T., and Cutler, A.J. (2011). The Arabidopsis C2H2 Zinc Finger INDETERMINATE

DOMAIN1/ENHYDROUS Promotes the Transition to Germination by Regulating Light and Hormonal Signaling during Seed Maturation. Plant Cell **23,** 1772-1794.

Forestan, C., Meda, S., and Varotto, S. (2010a). ZmPIN1-Mediated Auxin Transport Is Related to Cellular Differentiation during Maize Embryogenesis and Endosperm Development. Plant Physiology **152,** 1373-1390.

Forestan, C., Meda, S., and Varotto, S. (2010b). ZmPIN1-mediated auxin transport is related to cellular differentiation during maize embryogenesis and endosperm development. Plant Physiol. **152,** 1373-1390.

Frey, M., Stettner, C., and Gierl, A. (1998). A general method for gene isolation in tagging approaches: amplification of insertion mutagenised sites (AIMS). The Plant Journal **13,** 717-721.

Fu, Y., Wen, T.J., Ronin, Y.I., Chen, H.D., Guo, L., Mester, D.I., Yang, Y.J., Lee, M., Korol, A.B., Ashlock, D.A., and Schnable, P.S. (2006a). Genetic dissection of intermated recombinant inbred lines using a new genetic map of maize. Genetics **174,** 1671-1683.

Fu, Y., Wen, T.-J., Ronin, Y.I., Chen, H.D., Guo, L., Mester, D.I., Yang, Y., Lee, M., Korol, A.B., Ashlock, D.A., and Schnable, P.S. (2006b). Genetic Dissection of Intermated Recombinant Inbred Lines Using a New Genetic Map of Maize. Genetics **174,** 1671-1683.

Gallavotti, A., Yang, Y., Schmidt, R.J., and Jackson, D. (2008). The relationship between auxin transport and maize branching. Plant Physiology **147,** 1913-1923.

Geisler-Lee, J., and Gallie, D.R. (2005). Aleurone cell identity is suppressed following connation in maize kernels. Plant Physiology **139,** 204-212.

Goll, D.E., Thompson, V.F., Li, H., Wei, W., and Cong, J. (2003). The Calpain system. Physiological Reviews **83,** 731-801.

Gomez, E., Royo, J., Muniz, L.M., Sellam, O., Paul, W., Gerentes, D., Barrero, C., Lopez, M., Perez, P., and Hueros, G. (2009). The Maize Transcription Factor Myb-Related Protein-1 Is a Key Regulator of the Differentiation of Transfer Cells. Plant Cell **21,** 2022-2035.

Gruis, D., Guo, H., Selinger, D., Tian, Q., and Olsen, O.-A. (2006). Surface position, not signaling from surrounding maternal tissues, specifies aleurone epidermal cell fate in maize. Plant Physiol. **141,** 898-909.

Igarashi, D., Ishida, S., Fukazawa, J., and Takahashi, Y. (2001). 14-3-3 proteins regulate intracellular localization of the bZIP transcriptional activator RSG. Plant Cell **13,** 2483-2497.

Jefferson, R.A., Kavanagh, T.A., and Bevan, M.W. (1987). GUS fusions: beta-glucuronidase as a sensitive and versatile gene fusion marker in higher plants. EMBO J **6,** 3901-3907.

Jestin, L., Ravel, C., Auroy, S., Laubin, B., Perretant, M.-R., Pont, C., and Charmet, G. (2008). Inheritance of the number and thickness of cell layers in barley aleurone tissue (Hordeum vulgare L.): an approach using F2–F3 progeny. TAG Theoretical and Applied Genetics **116,** 991.

Jin, P., Guo, T., and Becraft, P.W. (2000). The maize CR4 receptor-like kinase mediates a growth factor-like differentiation response. Genesis **27,** 104-116.

Johnson, K.L., Faulkner, C., Jeffree, C.E., and Ingram, G.C. (2008). The Phytocalpain Defective Kernel 1 Is a Novel Arabidopsis Growth Regulator Whose Activity Is Regulated by Proteolytic Processing. Plant Cell **20,** 2619-2630.

Kawakatsu, T., Yamamoto, M.P., Touno, S.M., Yasuda, H., and Takaiwa, F. (2009). Compensation and interaction between RISBZ1 and RPBF during grain filling in rice. The Plant Journal **59,** 908-920.

Kessler, S., Seiki, S., and Sinha, N. (2002a). *Xcl1* causes delayed oblique periclinal cell divisions in developing maize leaves, leading to cellular differentiation by lineage instead of position. Development **129,** 1859-1869.

Kessler, S., Seiki, S., and Sinha, N. (2002b). Xcl1 causes delayed oblique periclinal cell divisions in developing maize leaves, leading to cellular differentiation by lineage instead of position. Development **129,** 1859-1869.

Kozaki, A., Hake, S., and Colasanti, J. (2004). The maize ID1 flowering time regulator is a zinc finger protein with novel DNA binding properties. Nucleic Acids Research **32,** 1710-1720.

Lee, B.H., Johnston, R., Yang, Y., Gallavotti, A., Kojima, M., Travencolo, B.A.N., Costa, L.D., Sakakibara, H., and Jackson, D. (2009). Studies of aberrant phyllotaxy1 Mutants of Maize Indicate Complex Interactions between Auxin and Cytokinin Signaling in the Shoot Apical Meristem. Plant Physiology **150,** 205-216.

Levy, A.A., and Walbot, V. (1990). REGULATION OF THE TIMING OF TRANSPOSABLE ELEMENT EXCISION DURING MAIZE DEVELOPMENT. Science **248,** 1534-1537.

Lid, S.E., Gruis, D., Jung, R., Lorentzen, J.A., Ananiev, E., Chamberlin, M., Niu, X., Meeley, R., Nichols, S., and Olsen, O.-A. (2002a). The *defective kernel 1* (*dek1*) gene required for aleurone cell development in the endosperm of maize grains encodes a membrane protein of the calpain gene superfamily. Proc Natl Acad Sci USA **99,** 5460-5465.

Lid, S.E., Gruis, D., Jung, R., Lorentzen, J.A., Ananiev, E., Chamberlin, M., Niu, X.M., Meeley, R., Nichols, S., and Olsen, O.A. (2002b). The defective kernel 1 (dek1) gene required for aleurone cell development in the endosperm of maize grains encodes a membrane protein of the calpain gene superfamily. Proceedings of the National Academy of Sciences of the United States of America **99,** 5460-5465.

Liu, S., Chen, H.D., Makarevitch, I., Shirmer, R., Emrich, S.J., Dietrich, C.R., Barbazuk, W.B., Springer, N.M., and Schnable, P.S. (2010a). High-Throughput Genetic Mapping of Mutants via Quantitative Single Nucleotide Polymorphism Typing. Genetics **184,** 19-26.

Liu, S., Chen, H.D., Makarevitch, I., Shirmer, R., Emrich, S.J., Dietrich, C.R., Barbazuk, W.B., Springer, N.M., and Schnable, P.S. (2010b). High-Throughput Genetic Mapping of Mutants via Quantitative Single Nucleotide Polymorphism Typing. Genetics **184,** 19-U51.

Liu, Y.G., Mitsukawa, N., Oosumi, T., and Whittier, R.F. (1995). Efficient isolation and mapping of Arabidopsis thaliana T-DNA insert junctions by thermal asymmetric interlaced PCR. Plant J **8,** 457-463.

McCarty, D.R., Settles, A.M., Suzuki, M., Tan, B.C., Latshaw, S., Porch, T., Robin, K., Baier, J., Avigne, W., Lai, J., Messing, J., Koch, K.E., and Hannah, L.C. (2005). Steady-state transposon mutagenesis in inbred maize. Plant J **44,** 52-61.

McGinnis, K., Chandler, V., Cone, K., Kaeppler, H., Kaeppler, S., Kerschen, A., Pikaard, C., Richards, E., Sidorenko, L., Smith, T., Springer, N., and Wulan, T. (2005). Transgene-induced RNA interference as a tool for plant functional genomics. In Rna Interference, D.R. Engelke and J.J. Rossi, eds (San Diego: Elsevier Academic Press Inc), pp. 1-24.

Miranda, L.T.d. (1980). Inheritance and linkages of multiple aleurone layering. Maize Genetics Cooperation News Letter**,** 15-18.

Morrison, I.N., Obrien, T.P., and Kuo, J. (1978). INITIAL CELLULARIZATION AND DIFFERENTIATION OF ALEURONE CELLS IN VENTRAL REGION OF DEVELOPING WHEAT-GRAIN. Planta **140,** 19-30.

Myers, A.M., James, M.G., Lin, Q., Yi, G., Stinard, P.S., Hennen-Bierwagen, T.A., and Becraft, P.W. (2011). Maize opaque5 Encodes Monogalactosyldiacylglycerol Synthase and Specifically Affects Galactolipids Necessary for Amyloplast and Chloroplast Function. Plant Cell **23,** 2331-2347.

Nelson, O.E., and Chang, M.T. (1974). Effect of multiple aleurone layers on the protein and amino acid content of maize endosperm. Crop Sci. **14,** 374-376.

Neuffer, M.G. (1995). Chromosome breaking sites for genetic analysis in maize. Maydica **40,** 99-116.

Ohtsu, K., Smith, M.B., Emrich, S.J., Borsuk, L.A., Zhou, R.L., Chen, T.L., Zhang, X.L., Timmermans, M.C.P., Beck, J., Buckner, B., Janick-Buckner, D., Nettleton, D., Scanlon, M.J., and Schnable, P.S. (2007). Global gene expression analysis of the shoot apical meristem of maize (Zea mays L.). Plant Journal **52,** 391-404.

Olsen, L.T., Divon, H.H., Al, R., Fosnes, K., Lid, S.E., and Opsahl-Sorteberg, H.G. (2008). The defective seed5 (des5) mutant: effects on barley seed development and HvDek1, HvCr4, and HvSal1 gene regulation. J Exp Bot **59,** 3753-3765.

Olsen, O.-A. (2004a). Dynamics of maize aleurone cell formation: the “surface” rule. Maydica **49,** 37-40.

Olsen, O.A. (2004b). Nuclear endosperm development in cereals and Arabidopsis thaliana. Plant Cell **16,** S214-S227.

Olsen, O.A. (2004c). Dynamics of maize aleurone cell formation: The "surface-"rule. Maydica **49,** 37-40.

Patterson, G.I., Harris, L.J., Walbot, V., and Chandler, V.L. (1991). Genetic Analysis of B-Peru, a Regulatory Gene in Maize. Genetics **127,** 205-220.

Reyes, F.C., Sun, B., Guo, H., Gruis, D.F., and Otegui, M.S. (2010). Agrobacterium tumefaciens-mediated transformation of maize endosperm as a tool to study endosperm cell biology. Plant Physiol **153,** 624-631.

Reyes, F.C., Chung, T., Holding, D., Jung, R., Vierstra, R., and Otegui, M.S. (2011). Delivery of prolamins to the protein storage vacuole in maize aleurone cells. Plant Cell

Robertson, D.S., and Stinard, P.S. (1987). Genetic Evidence of Mutator-Induced Deletions in the Short Arm of Chromosome 9 of Maize. Genetics **115,** 353-361.

Robertson, D.S., Stinard, P.S., and Maguire, M.P. (1994). Genetic evidence of Mutator-induced deletions in the short arm of chromosome 9 of maize. II. wd deletions. Genetics **136,** 1143-1149.

Santoni, V. (2007). Plant plasma membrane protein extraction and solubilization for proteomic analysis. Methods in Molecular Biology **355,** 93-109.

Schnable, P.S., Ware, D., Fulton, R.S., Stein, J.C., Wei, F.S., Pasternak, S., Liang, C.Z., Zhang, J.W., Fulton, L., Graves, T.A., Minx, P., Reily, A.D., Courtney, L., Kruchowski, S.S., Tomlinson, C., Strong, C., Delehaunty, K., Fronick, C., Courtney, B., Rock, S.M., Belter, E., Du, F.Y., Kim, K., Abbott, R.M., Cotton, M., Levy, A., Marchetto, P., Ochoa, K., Jackson, S.M., Gillam, B., Chen, W.Z., Yan, L., Higginbotham, J., Cardenas, M., Waligorski, J., Applebaum, E., Phelps, L., Falcone, J., Kanchi, K., Thane, T., Scimone, A., Thane, N., Henke, J., Wang, T., Ruppert, J., Shah, N., Rotter, K., Hodges, J., Ingenthron, E., Cordes, M., Kohlberg, S., Sgro, J., Delgado, B., Mead, K., Chinwalla, A., Leonard, S., Crouse, K., Collura, K., Kudrna, D., Currie, J., He, R.F., Angelova, A., Rajasekar, S., Mueller, T., Lomeli, R., Scara, G., Ko, A., Delaney, K., Wissotski, M., Lopez, G., Campos, D., Braidotti, M., Ashley, E., Golser, W., Kim, H., Lee, S., Lin, J.K., Dujmic, Z., Kim, W., Talag, J., Zuccolo, A., Fan, C., Sebastian, A., Kramer, M., Spiegel, L., Nascimento, L., Zutavern, T., Miller, B., Ambroise, C., Muller, S., Spooner, W., Narechania, A., Ren, L.Y., Wei, S., Kumari, S., Faga, B., Levy, M.J., McMahan, L., Van Buren, P., Vaughn, M.W., Ying, K., Yeh, C.T., Emrich, S.J., Jia, Y., Kalyanaraman, A., Hsia, A.P., Barbazuk, W.B., Baucom, R.S., Brutnell, T.P., Carpita, N.C., Chaparro, C., Chia, J.M., Deragon, J.M., Estill, J.C., Fu, Y., Jeddeloh, J.A., Han, Y.J., Lee, H., Li, P.H., Lisch, D.R., Liu, S.Z., Liu, Z.J.,

Nagel, D.H., McCann, M.C., SanMiguel, P., Myers, A.M., Nettleton, D., Nguyen, J., Penning, B.W., Ponnala, L., Schneider, K.L., Schwartz, D.C., Sharma, A., Soderlund, C., Springer, N.M., Sun, Q., Wang, H., Waterman, M., Westerman, R., Wolfgruber, T.K., Yang, L.X., Yu, Y., Zhang, L.F., Zhou, S.G., Zhu, Q., Bennetzen, J.L., Dawe, R.K., Jiang, J.M., Jiang, N., Presting, G.G., Wessler, S.R., Aluru, S., Martienssen, R.A., Clifton, S.W., McCombie, W.R., Wing, R.A., and Wilson, R.K. (2009). The B73 Maize Genome: Complexity, Diversity, and Dynamics. Science **326,** 1112-1115.

Sekhon, R.S., Lin, H.N., Childs, K.L., Hansey, C.N., Buell, C.R., de Leon, N., and Kaeppler, S.M. (2011). Genome-wide atlas of transcription during maize development. Plant Journal **66,** 553-563.

Seo, P.J., Ryu, J., Kang, S.K., and Park, C.M. (2011a). Modulation of sugar metabolism by an INDETERMINATE DOMAIN transcription factor contributes to photoperiodic flowering in Arabidopsis. Plant Journal **65,** 418-429.

Seo, P.J., Kim, M.J., Ryu, J.Y., Jeong, E.Y., and Park, C.M. (2011b). Two splice variants of the IDD14 transcription factor competitively form nonfunctional heterodimers which may regulate starch metabolism. Nature Communications **2**.

Settles, A.M., Latshaw, S., and McCarty, D.R. (2004). Molecular analysis of high-copy insertion sites in maize. Nucleic Acids Res **32,** e54.

Settles, A.M., Holding, D.R., Tan, B.C., Latshaw, S.P., Liu, J., Suzuki, M., Li, L., O'Brien, B.A., Fajardo, D.S., Wroclawska, E., Tseung, C.W., Lai, J.S., Hunter, C.T., Avigne, W.T., Baier, J., Messing, J., Hannah, L.C., Koch, K.E., Becraft, P.W., Larkins, B.A., and McCarty, D.R. (2007a). Sequence-indexed mutations in maize using the UniformMu transposon-tagging population. Bmc Genomics **8**.

Settles, A.M., Holding, D.R., Tan, B.C., Latshaw, S.P., Liu, J., Suzuki, M., Li, L., O'Brien, B.A., Fajardo, D.S., Wroclawska, E., Tseung, C.W., Lai, J., Hunter, C.T., 3rd, Avigne, W.T., Baier, J., Messing, J., Hannah, L.C., Koch, K.E., Becraft, P.W., Larkins, B.A., and McCarty, D.R. (2007b). Sequence-indexed mutations in maize using the UniformMu transposon-tagging population. BMC Genomics **8,** 116.

Shen, B., Li, C., Min, Z., Meeley, R.B., Tarczynski, M.C., and Olsen, O.A. (2003a). *sal1* determines the number of aleurone cell layers in maize endosperm and encodes a class E vacuolar sorting protein. Proc Natl Acad Sci U S A **100,** 6552-6557.

Shen, B., Li, C.J., Min, Z., Meeley, R.B., Tarczynski, M.C., and Olsen, O.A. (2003b). sal1 determines the number of aleurone cell layers in maize endosperm and encodes a class E vacuolar sorting protein. Proceedings of the National Academy of Sciences of the United States of America **100,** 6552-6557.

Sheridan, W.F., and Neuffer, M.G. (1982). MAIZE DEVELOPMENTAL MUTANTS - EMBRYOS UNABLE TO FORM LEAF PRIMORDIA. Journal of Heredity **73,** 318-329.

Singleton, W.R. (1946). INHERITANCE OF INDETERMINATE GROWTH IN MAIZE. Journal of Heredity **37,** 61-64.

Stewart, M.L., and Slavin, J.L. (2009). Particle size and fraction of wheat bran influence short-chain fatty acid production in vitro. British Journal of Nutrition **102,** 1404-1407.

Suzuki, M., Kao, C.Y., and McCarty, D.R. (1997). The conserved B3 domain of VIVIPAROUS1 has a cooperative DNA binding activity. Plant Cell **9,** 799-807.

Suzuki, M., Latshaw, S., Sato, Y., Settles, A.M., Koch, K.E., Hannah, L.C., Kojima, M., Sakakibara, H., and McCarty, D.R. (2008). The maize Viviparous8 locus, encoding a putative ALTERED MERISTEM PROGRAM1-like peptidase, regulates abscisic acid accumulation and coordinates embryo and endosperm development. Plant Physiology **146,** 1193-1206.

Tanimoto, M., Tremblay, R., and Colasanti, J. (2008). Altered gravitropic response, amyloplast sedimentation and circumnutation in the Arabidopsis shoot gravitropism 5 mutant are associated with reduced starch levels. Plant Molecular Biology **67,** 57-69.

Tian, Q., Olsen, L., Sun, B., Lid, S.E., Brown, R.C., Lemmon, B.E., Fosnes, K., Gruis, D.F., Opsahl-Sorteberg, H.G., Otegui, M.S., and Olsen, O.A. (2007a). Subcellular localization and functional domain studies of DEFECTIVE KERNEL1 in maize and Arabidopsis suggest a model for aleurone cell fate specification involving CRINKLY4 and SUPERNUMERARY ALEURONE LAYER1. Plant Cell **19,** 3127-3145.

Tian, Q., Olsen, L., Sun, B., Lid, S.E., Brown, R.C., Lemmon, B.E., Fosnes, K., Gruis, D.F., Opsahl-Sorteberg, H.G., Otegui, M.S., and Olsen, O.A. (2007b). Subcellular localization and functional domain studies of DEFECTIVE KERNEL1 in maize and Arabidopsis suggest a model for aleurone cell fate specification involving CRINKLY4 and SUPERNUMERARY ALEURONE LAYER1. Plant Cell **19,** 3127-3145.

Vos, P., Hogers, R., Bleeker, M., Reijans, M., van de Lee, T., Hornes, M., Frijters, A., Pot, J., Peleman, J., Kuiper, M., and et al. (1995). AFLP: a new technique for DNA fingerprinting. Nucleic Acids Res **23,** 4407-4414.

Walbot, V., and Warren, C. (1988). Regulation of Mu element copy number in maize lines with an active or inactive Mutator transposable element system. Mol Gen Genet **211,** 27-34.

Wang, C., Barry, J.K., Min, Z., Tordsen, G., Rao, A.G., and Olsen, O.-A. (2003a). The calpain domain of the maize DEK1 protein contains the conserved catalytic triad and functions as a cysteine proteinase. J. Biol. Chem. **278,** 34467-34474.

Wang, C.X., Barry, J.K., Min, Z., Tordsen, G., Rao, A.G., and Olsen, O.A. (2003b). The calpain domain of the maize DEK1 protein contains the conserved catalytic triad and functions as a cysteine proteinase. Journal of Biological Chemistry **278,** 34467-34474.

Wang, Y., Yin, G., Yang, Q., Tang, J., Lu, X., Korban, S.S., and Xu, M. (2008). Identification and isolation of Mu-flanking fragments from maize. J Genet Genomics **35,** 207-213.

Wisniewski, J.P., and Rogowsky, P.M. (2004a). Vacuolar H+-translocating inorganic pyrophosphatase (Vpp1) marks partial aleurone cell fate in cereal endosperm development. Plant Molecular Biology **56,** 325-337.

Wisniewski, J.P., and Rogowsky, P.M. (2004b). Vacuolar H+-translocating inorganic pyrophosphatase (Vpp1) marks partial aleurone cell fate in cereal endosperm development. Plant Mol Biol **56,** 325-337.

Wolf, M.J., Zuber, M.S., Cutler, H.C., and Khoo, U. (1972a). MAIZE WITH MULTILAYER ALEURONE OF HIGH PROTEIN CONTENT. Crop Science **12,** 440-&.

Wolf, M.J., Cutler, H.C., Zuber, M.S., and Khoo, U. (1972b). Maize with multilayer aleurone of high protein content. Crop Sci. **12,** 440-442.

Wong, A.Y.M., and Colasanti, J. (2007). Maize floral regulator protein INDETERMINATE1 is localized to developing leaves and is not altered by light or the sink/source transition. Journal of Experimental Botany **58,** 403-414.

Yamamoto, M.P., Onodera, Y., Touno, S.M., and Takaiwa, F. (2006). Synergism between RPBF Dof and RISBZ1 bZIP activators in the regulation of rice seed expression genes. Plant Physiol. **141,** 1694-1707.

Yephremov, A., and Saedler, H. (2000). Technical advance: display and isolation of transposon-flanking sequences starting from genomic DNA or RNA. Plant J **21,** 495-505.

Yi, G., Lauter, A.M., Scott, M.P., and Becraft, P.W. (2011). The thick aleurone1 Mutant Defines a Negative Regulation of Maize Aleurone Cell Fate That Functions Downstream of defective kernel1. Plant Physiology **156,** 1826-1836.

Yi, G., Luth, D., Goodman, T.D., Lawrence, C.J., and Becraft, P.W. (2009). High-throughput linkage analysis of Mutator insertion sites in maize. Plant Journal **58,** 883-892.

Yu, C., Zhang, J., and Peterson, T. (2011). Genome rearrangements in maize induced by alternative transposition of reversed *Ac/Ds* termini. Genetics **in press**.

Zhang, J., and Peterson, T. (2004). Transposition of reversed *Ac* element ends generates chromosome rearrangements in maize. Genetics **167,** 1929-1937.

Figure Legends

Figure 1. Analysis of the *thk1* mutant phenotype. A, Mutant kernel (right) shows increased anthocyanin pigmentation and lack of a well-developed embryo. B, C, Longitudinal sections of WT (B) and *thk1* (C) embryos at 12 DAP. D-G, microscopic sections showing WT (D, F) and *thk1* (E, G) aleurone. D, E, Histologically stained sections. Starch grains stained pink with PAS and protein-dense aleurone cells (arrow) stain intensely with Toluidine blue. F, G, Expression of the *Vp1-GUS* transgene as determined by X-gluc histochemical stain. Scale bars = 100 µm

Figure 2. Genetically mosaic kernels with *thk1* sectors. A, The chromosomal basis of *thk1* sector generation. Endosperm cells were heterozygous for the recessive *thk1* mutant and therefore phenotypically normal. The chromosome breaking *Ds1S4* element is located proximal to the wild type *Thk1+* allele. In the presence of an *Ac* element, aberrant *Ds1S4* transposition results in chromosome breakage and loss of the distal chromosome 1S arm containing the *Thk1+* allele, uncovering the *thk1* mutant allele. Such events occur in individual cells occasionally during kernel development, and subsequent mitotic divisions generate clonal sectors of hemizygous *thk1* mutant cells in a

background of otherwise normal endosperm. B, Example of a kernel containing darkly pigmented *thk1* mutant sectors (lower kernel, arrow) compared to a normal unsectored kernel (top). C, D, Kernel cross-sections showing examples of *thk1/-* mutant sectors with adjacent normal endosperm. Sector boundaries appear sharp, consistent with a laterally cell-autonomous function. E, Several small sectors producing one or a few sub-peripheral aleurone cells (arrows). All are in direct contact with the peripheral layer of aleurone cells. Scale bars (B-D)= 200 µm; (E)=50 µm.

Figure 3. Effect of the *thk1* mutant on leaf cells. A, Control leaf with *vp5* sector. The arrow designates a vascular bundle where the right half of the bundle sheath is devoid of well developed chloroplasts due to the carotenoid deficiency conferred by the *vp5* mutation. No morphological defects were observed. The brackets highlight an intermediate vascular bundle with foci of sclerenchyma cells (small thick-walled cells, turquoise stained online) at the adaxial and abaxial poles. B, A *thk1/-* mutant sector covering an extensive area of upper leaf epidermis, including the entire area shown. The cells are enlarged, but only occupy a single cell layer. C, Sector where internal cells show possible epidermal identities. The internal cells have attributes distinct from normal mesophyll or bundle sheath, but which resemble bulliform cells (denoted with asterisks). Also, the lower (abaxial) epidermal cells resemble bulliform cells, which are normally restricted to the upper surface. Cells with clearly recognizable mesophyll or vascular bundle identities are outlined. Scale bars A, B, = 100 µm; C, = 50 µm.

Figure 4. *thk1* is epistatic for multiple pleiotropic *dek1* phenotypes. A, Marker genotyping demonstrated the epistasis of *thk1* over *dek1*. Kernels from an F2 ear segregating for the *thk1* and *dek1-1394* mutants were genotyped for the marker IDP112 (Fu et al., 2006a). DNA from five pooled kernels with *thk1* mutant phenotypes showed two polymorphic alleles. DNA from 12 pooled *dek1* kernels only showed the upper band indicating all were homozygous for the upper allele and that this marker allele is tightly linked to the *dek1-1394* mutant allele. Among 18 individual kernels with *thk1* mutant phenotypes, five were homozygous for the marker allele linked to *dek1-1394* (arrows), indicating that these individuals were likely homozygous for the *dek1* mutation. M=molecular weight marker. B, Zein profiles were examined by HPLC analysis. The *dek1* single mutant (bottom trace) is deficient in zein proteins compared to WT (upper trace), particularly for the gamma zein peaks. Both the *thk1* single mutant and *thk1, dek1* double traces (second and third from the top, respectively) are similar to WT.

Figure 5. Genetic mosaics with *thk1* sectors in *dek1* mutant kernels. A, The chromosomal basis of these mosaics. Kernels were homozygous for the recessive *dek1-1394* mutant allele and heterozygous *thk1/Thk1+.* Breakage and loss of the chromosome arm carrying the *Thk1+* allele resulted in *thk1, dek1/-, -* double mutant sectors in a background of *dek1* single mutant endosperm cells. B, An example of a *dek1* mutant kernel with *thk1* mutant sectors. The purple

sectors are *thk1, dek1*/- - double mutant cells. C, Yellow halos surrounding isolated *thk1* sectors in a *dek1* mutant kernel suggest carotenoids are produced by the *thk1, dek1*/- - double mutant cells, while the surrounding *dek1* single mutant tissue is carotenoid deficient. D, E, Sectioned kernels showing the multiple aleurone phenotype of *thk1* sectors even though cells are also mutant for *dek1.* The red pigment is anthocyanin. Scale bars = 200 µm

Figure 6. Model for *thk1* function in *dek1* regulation of aleurone cell fate. *Thk1*+ functions as a negative regulator of aleurone identity. In the outer layer, DEK1 inhibits THK1 function to derepress aleurone fate. In internal layers, THK1 is not inhibited and therefore represses aleurone fate. In *dek1* mutants, THK1 function would not be inhibited and aleurone fate would be repressed in all cell layers. In *thk1* mutants, there is no repression of aleurone identity in any of the cell layers, permitting the formation of aleurone, independent of DEK1 function.

Supplementary Figures

Fig. S1. Early stage embryo development in WT vs. *thk1.* (A,B) Longitudinal sections through WT (A) and *thk1* (B) endosperm and embryos at 7 DAP. **(C,D)** Higher magnifications of the embryos shown in (A) and (B), respectively. Scale bars (A,B) = 500 µm; (C,D) = 200 µm

Fig. S2. Single celled *thk1* sectors. (A) An aleurone cell with starchy cell(s) between it and the surface aleurone layer, but it has a lateral contact with another aleurone cell that has an uninterrupted chain of aleurone cell

connections to the surface. **(B,C)** Small *thk1* sectors are obvious in *dek1* mutant backgrounds and were always observed to be in the surface layer. Such sectors have not been observed in *dek1-1394* mutant kernels without a *thk1* allele and a chromosome breaking system. Scale bars = 50 μm

Fig. S3. Leaf sectors. (A,B) Examples of leaves creased adaxially and abaxially, respectively. **(C)** Hand sections through a *thk1* sectored leaf. The adaxial (upper) surface shows enlarged cells. Arrows and brackets highlight internal mutant cells apparent because they are devoid of chlorophyll. No obvious epidermal cell types were observed. **(D)** A control leaf containing a *vp5* mutant sector (bracket). The internal cell morphology appears normal and similar to internal mutant cells in (C). **(E,F)** Scanning electron micrographs (SEMs) of *thk1/-* mutant epidermal sectors (brackets) and neighboring normal cells. Scale bars = 100 μm.

Fig. S4. Marker genotyping demonstrates the epistasis of *thk1* over *dek1*. Kernels from an F2 ear segregating for the *thk1* and *dek1-1394* mutants were genotyped for the marker IDP112 (Fu et al., 2006). DNA from five pooled kernels with *thk1* mutant phenotypes showed two polymorphic alleles. DNA from 12 pooled *dek1* kernels only showed the upper band indicating that this marker allele is tightly linked to the *dek1-1394* mutant allele. Among 18 individual kernels with *thk1* mutant phenotypes, five were homozygous for the marker allele linked to *dek1- 1394* (arrows), indicating that these individuals were likely homozygous for the *dek1* mutation. M=molecular weight marker.

Fig. S5. Cross used to generate *thk1* sectors in *dek1* mutant kernels. Five types of progeny kernels were expected and recovered from this cross: WT, *dek1-1394* homozygous mutant, WT with *dek1-1394* sectors, WT with *thk1* sectors, and *dek1-1394* homozygous mutants with *thk1* sectors. Female parents were heterozygous *thk1, dek1*/+ + in coupling linkage. Due to recombination, gametes produced included double mutant, *thk1* or *dek1* single mutants, and WT. The double mutant gametes were required for the desired mosaics containing *thk1* sectors in a *dek1* mutant kernel. The male parent was heterozygous *dek1/ Dek1*+, *Ds1S4*. The majority of gametes produced were either *dek1* or *Dek1+, Ds1S4*. Only in the case of recombination were *dek1, Ds1S4* gametes produced. These were the ones required for the desired mosaics. The

images show examples of all the different sector types.

Fig. S6. *thk1* and *dek1* sectors on the same kernel indicating the occurrence of chromosome rearrangements or interstitial deletions. Darkly pigmented sectors indicate *thk1/-* tissue (magenta arrow) while unpigmented areas are *dek1/-* (white arrow).

Table 1. Summary of genetic mosaic analysis.

Female[a]	# Ears	# WT K	# *dek1* K	# *dek1* sectored K	# *thk* sectored K	# *dek1* K w/ *thk* sectors
thk1,dek1/+, +	10	1684	947	386	930	115
dek1/+	11	2642	1286	1303	0	0
thk1/+	8	2656	0	0	772	0
WT	8	3364	0	0	0	0

[a] All males in these crosses were of the genotype *Thk1+, dek1-1394* / *Thk1+, Dek1+, Ds1S4*.

Table 2. F2 segregation of *dek1* and *thk1* mutant kernel phenotypes

Experiment 1	Obs.[a]	Exp.[b] (9:3:3:1)	Exp. (9:3:4)
WT	1701	1635	1635
dek1-D	484	545	545
thk1	714	545	727
dek1-D; thk1	(7)[c]	182	0
Experiment 2	Obs.	Exp. (9:3:3:1)	Exp. (9:3:4)
WT	793	840	840
dek1-1394	290	280	280
thk1	364	280	373
dek1-1394; thk1	(14)[c]	93	0
Experiment 3	Obs.	Exp. (3:1)	
WT	737	719	
dek1-1394	221	239	

[a] Observed number of kernels for each phenotype.
[b] Expected number of kernels for the given phenotypic segregation ratio (parentheses).
[c] Kernels displayed aborted kernel phenotypes indistinguishable as to their *thk1* or *dek1* phenotypes.

Supplementary Table 1. Genetic mapping of the *thk1* mutation

Marker	Recomb[1]	Position[2]	Primer	Sequence
TIDP6442	0/54*	0.13Mb	TIDP6442F	gaactgtgcaacagacagcc
			TIDP6442R	tgaagcagttgtttgcttgg
104D10-7,8	0/74*	1.00Mb	104D10-7	tgcatgggcttccgacagtgg
			104D10-8	tggtggtcgtggacaggttcg
318G19-3.4	0/82*	1.57Mb	318G19-3	tcccacaattcatctcctgca
			318G19-4	atggagtacgggtgttggct
313O01-3,4	1/184 (0.5%)	2.21Mb	313O01-3	gtgttaagctggcaagatctgaag
			313O01-4	acagagccagaggtgccacc
TIDP5514M**	1/186 (0.5%)	2.43Mb	TIDP5514F	tcaaagccatgaagaaaggc
			121M23-5	tcaataatgcgatgcacgtac
121M23-3,4	1/164 (0.6%)	2.54Mb	121M23-3	cgtgccatcatgttagccacaa
			121M23-4	gaggtccagttgagaacaact
IDP1464	10/118 (8.5%)	4.04Mb	IDP1464F	atccattatgccctagacgg
			IDP1464R	ctttctggcaaaggaagtgc
IDP8147	11/64 (17.2%)	7.24Mb	IDP8147F	tacatacagatgcatgggcg
			IDP8147R	gtgccacctctgtatcatgg

1. Recombinants per chromosome in *thk1* mutant kernels of F2 populations.
2. Distance from the distal end of the chromosome according to RefGen_v2, B73**.**

* The PCR product was absent in all *thk1* kernels of the F2 populations. The number of individuals assayed was half the number of F2 chromosomes indicated.

** TIDP5514 was modified by increasing PCR product size.

Fig. 1

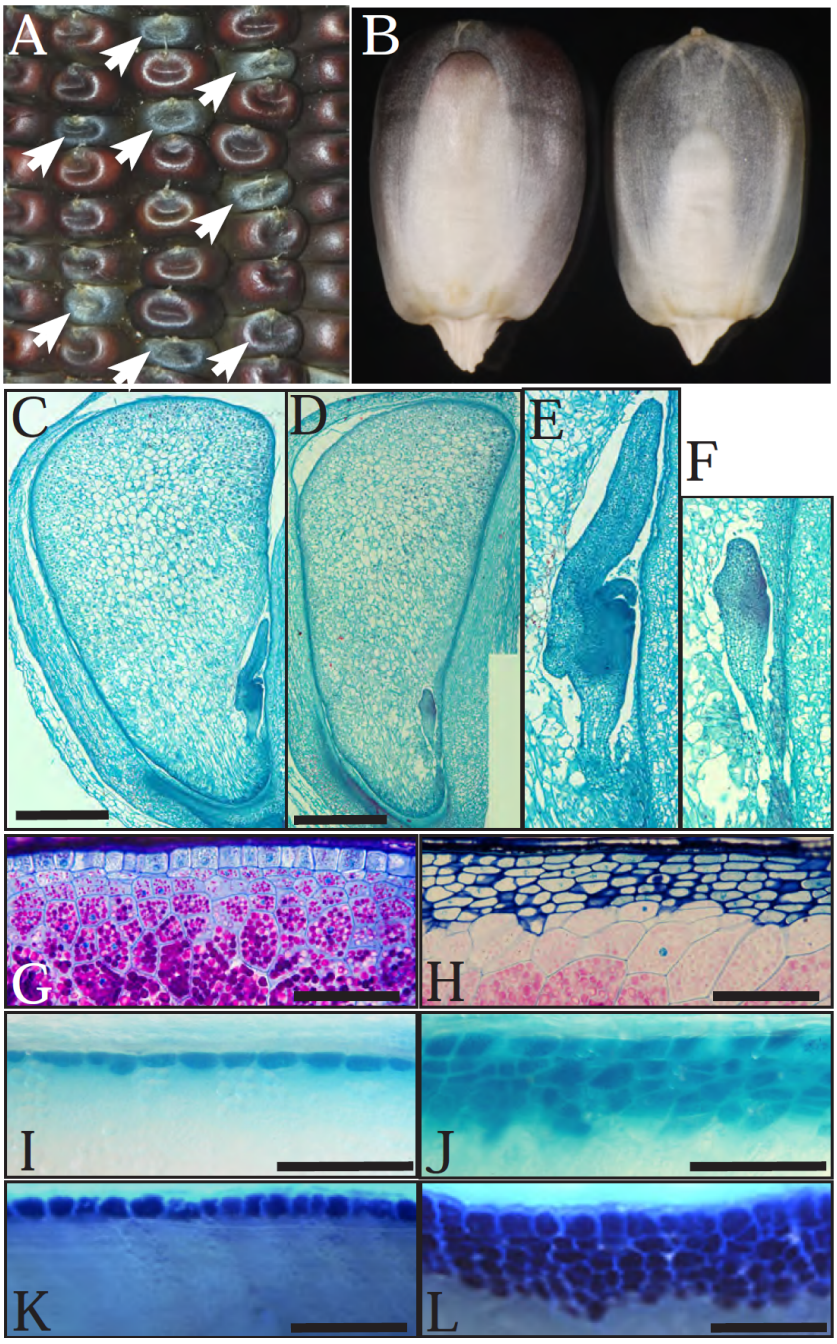

Fig. 2

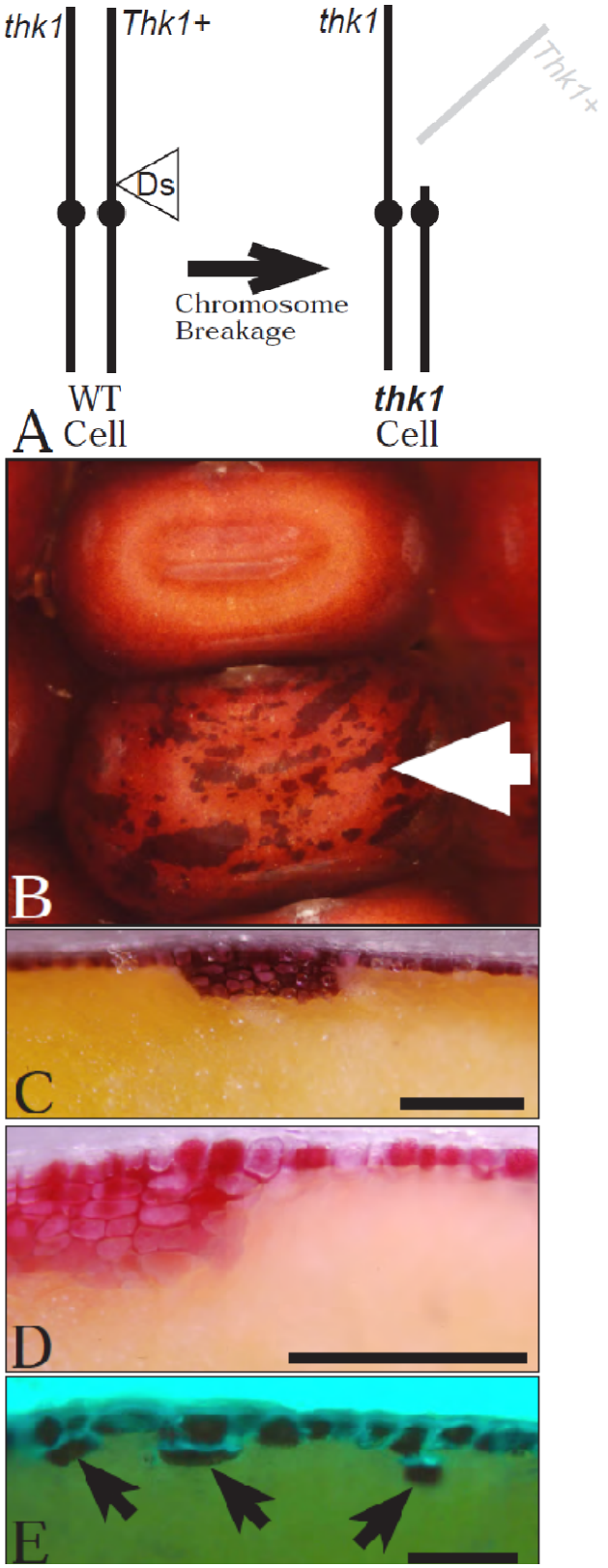
thk1
Thk1+
Ds
Chromosome
Breakage
thk1
Thk1+
WT
Cell
thk1
Cell
A
B
C
D
E

Fig. 3

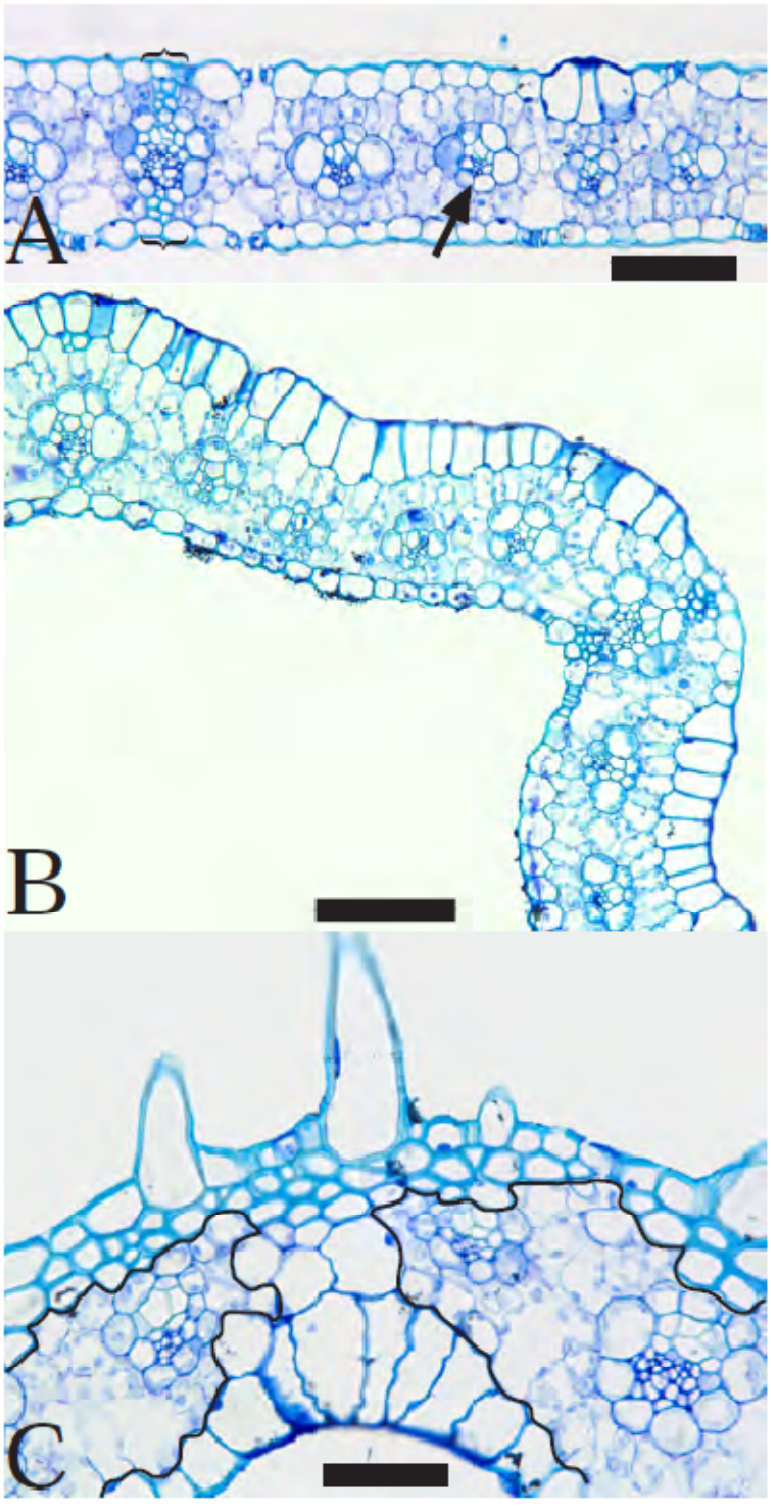

Fig. 4

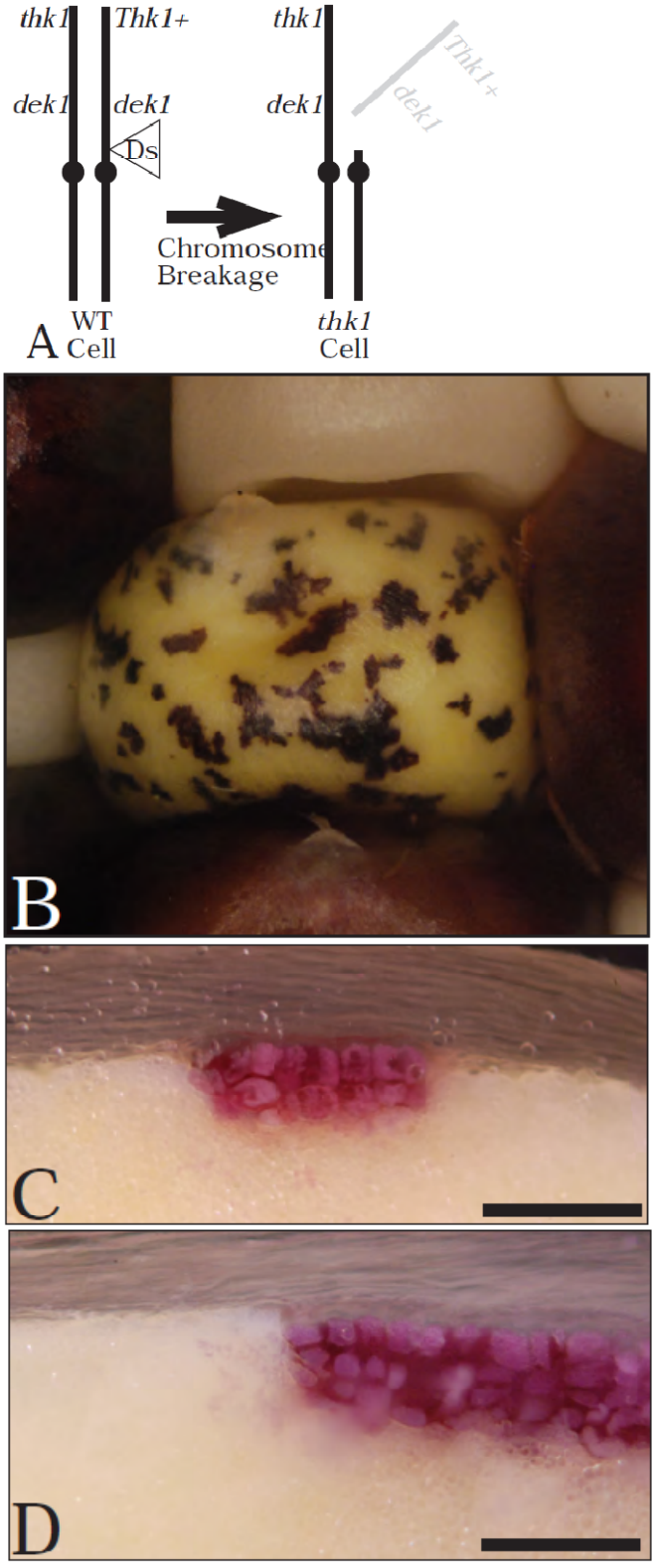
thk1
Thk1+
dek1
dek1
Ds
Chromosome
Breakage
thk1
dek1
Thk1+
dek1
A
WT
Cell
thk1
Cell
B
C
D

Fig. 5

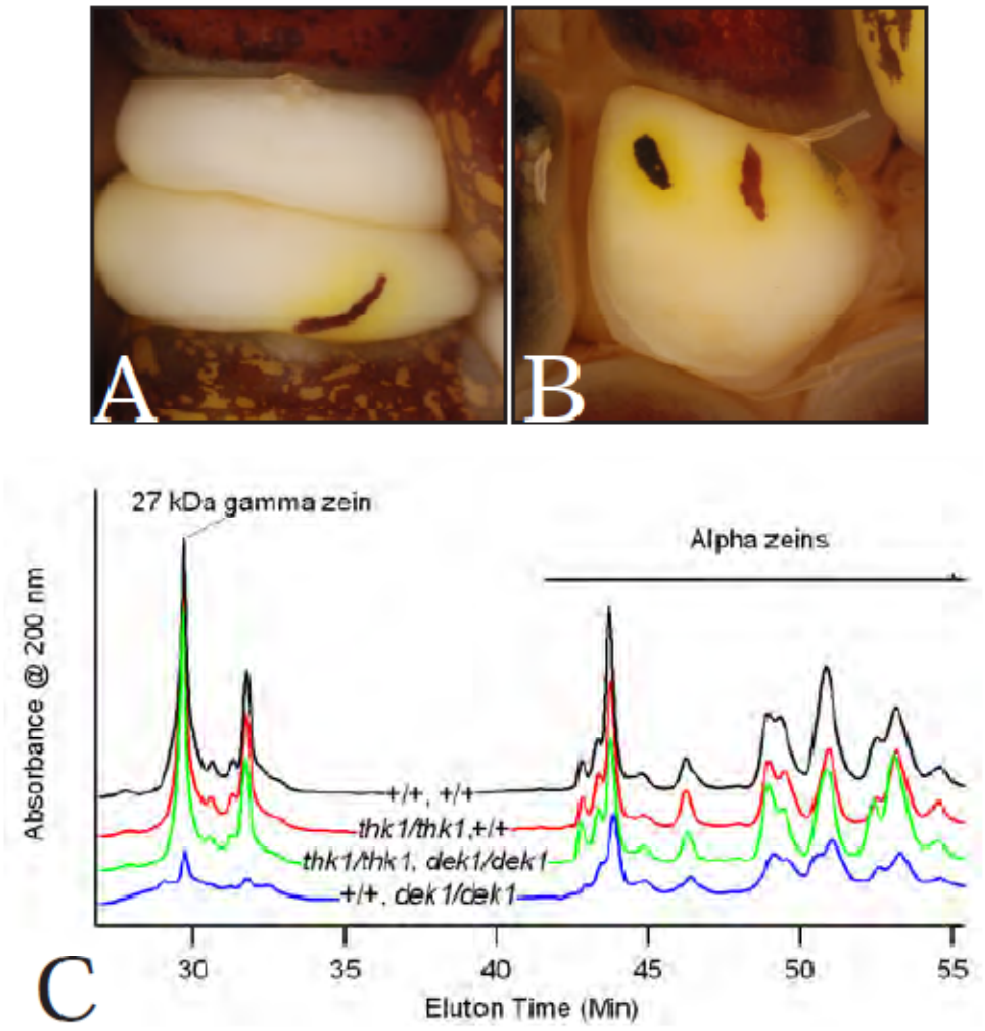
A
B
27 kDa gamma zein
Alpha zeins
Absorbance @ 200 nm
+/+, +/+
thk1/thk1,+/+
thk1/thk1, dek1/dek1
+/+, dek1/dek1
30
35
40
45
50
55
Eluton Time (Min)
C

Fig. 6

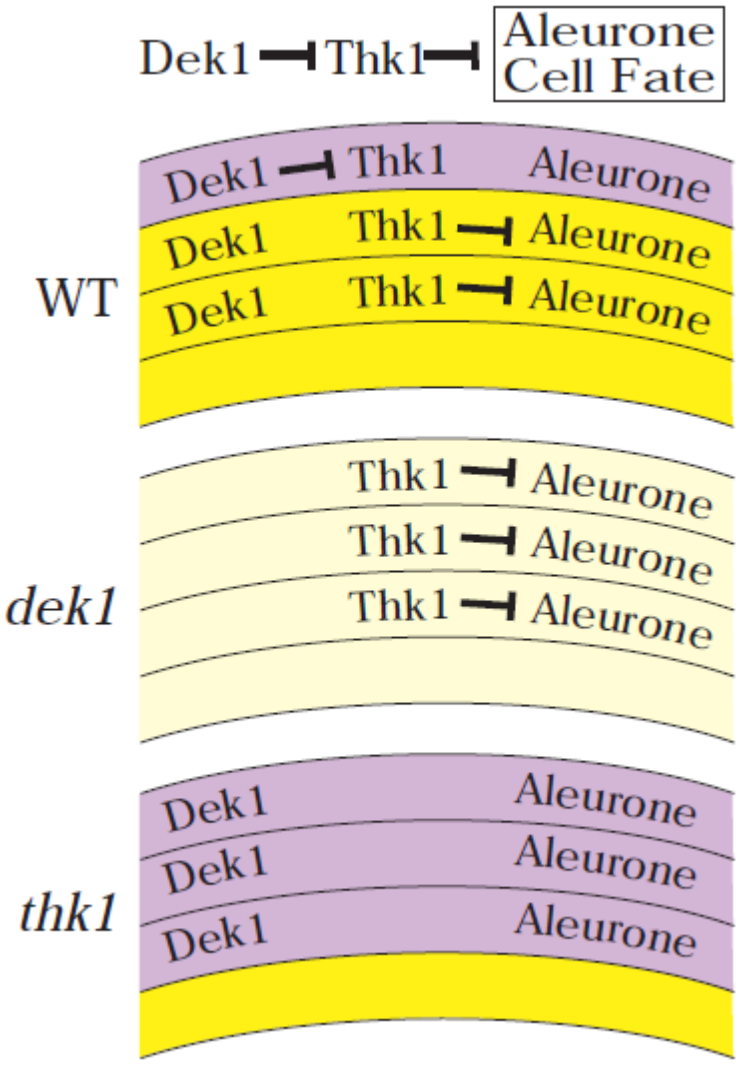
Dek1 ⊣ Thk1 ⊣ Aleurone Cell Fate
WT
Dek1 ⊣ Thk1 Aleurone
Dek1 Thk1 ⊣ Aleurone
Dek1 Thk1 ⊣ Aleurone
dek1
Thk1 ⊣ Aleurone
Thk1 ⊣ Aleurone
Thk1 ⊣ Aleurone
thk1
Dek1 Aleurone
Dek1 Aleurone
Dek1 Aleurone

Fig. S1

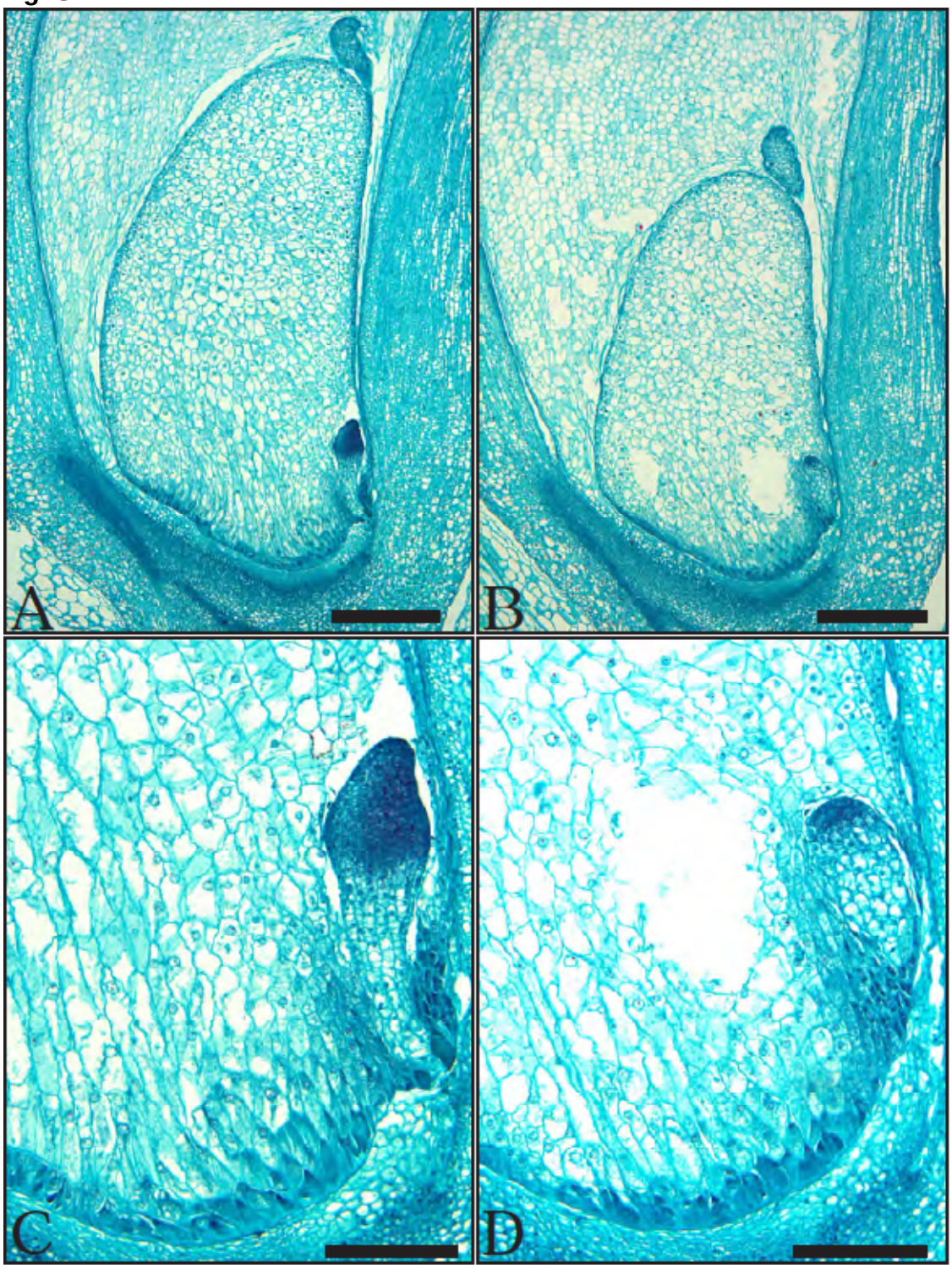

Fig. S2

Fig. S3

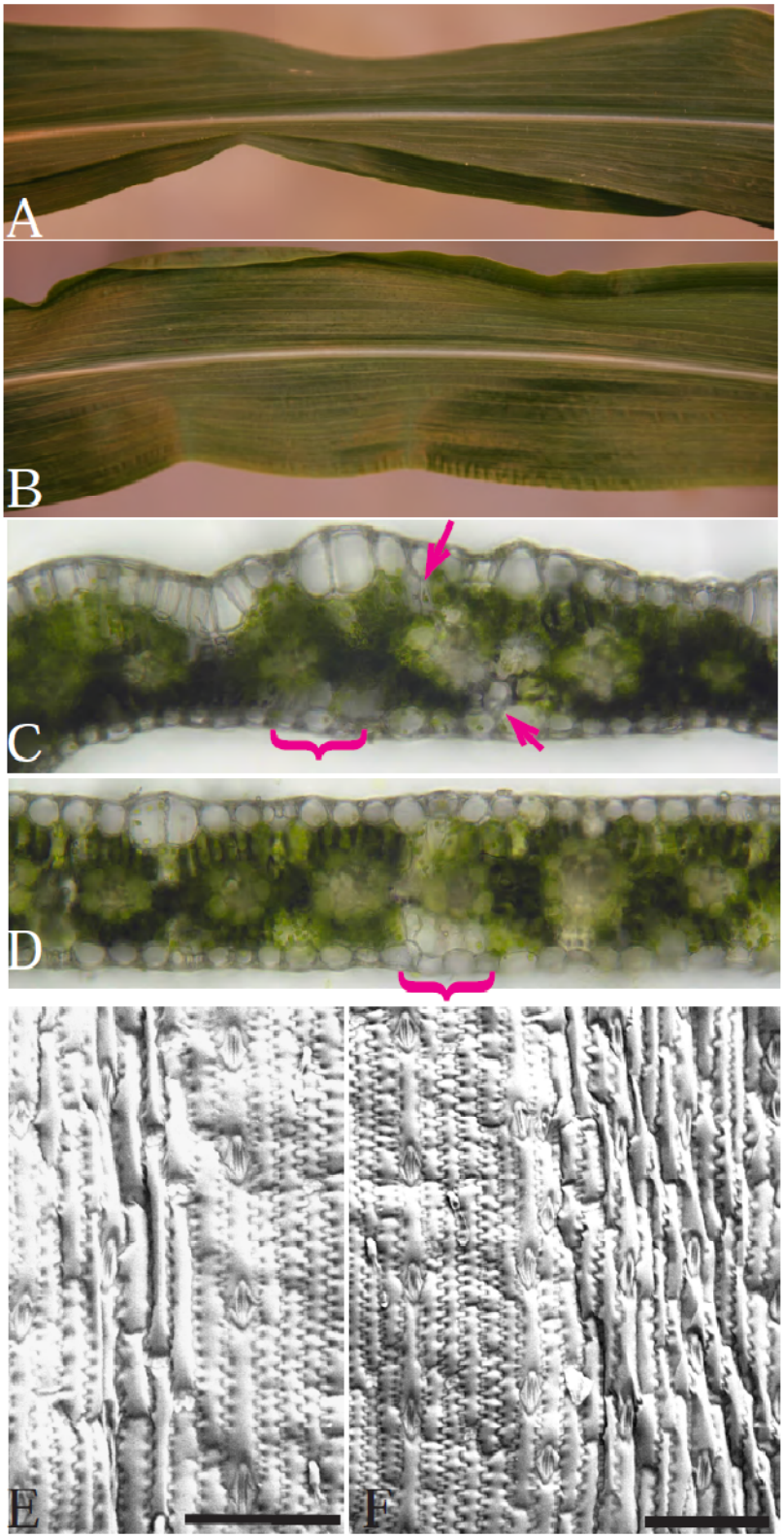

Fig.S4

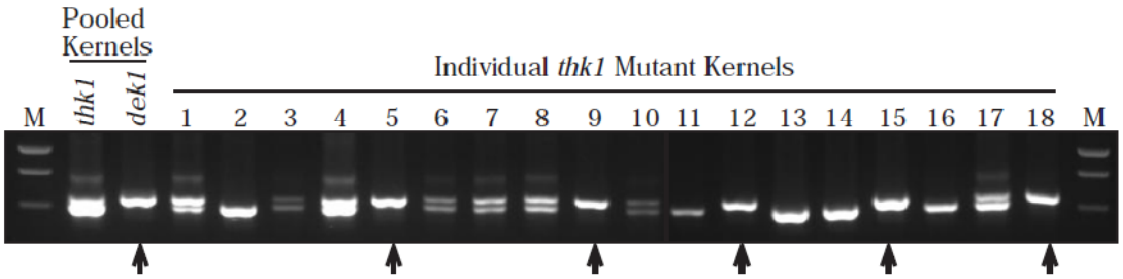
Pooled Kernels
thk1
dek1
Individual thk1 Mutant Kernels
M
1 2 3 4 5 6 7 8 9 10 11 12 13 14 15 16 17 18
M

Fig. S5

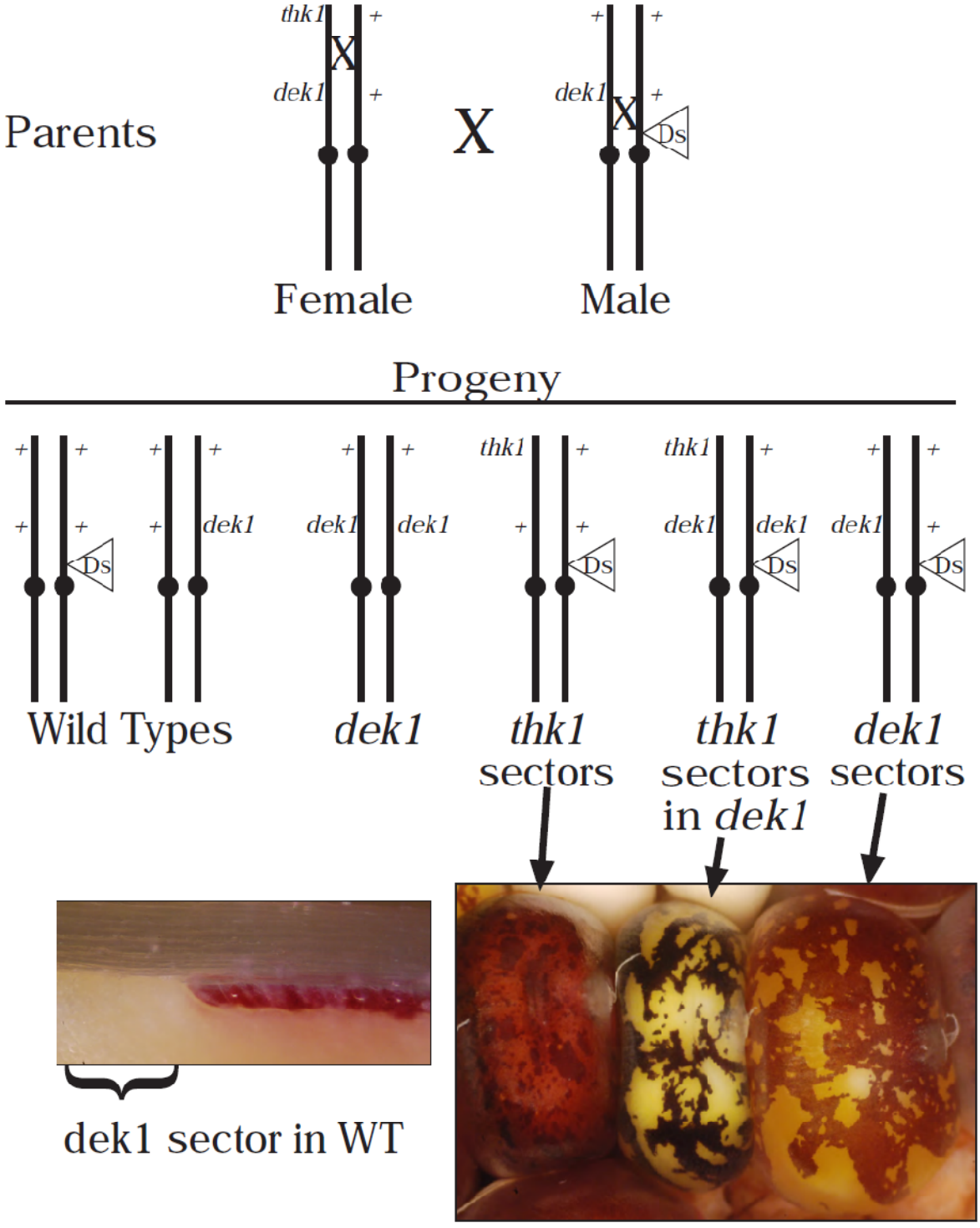
Parents
thk1
dek1
X
Female
X
dek1
Ds
Male
Progeny
Wild Types
dek1
thk1
sectors
thk1
sectors
in dek1
dek1
sectors
dek1 sector in WT

Fig. S6

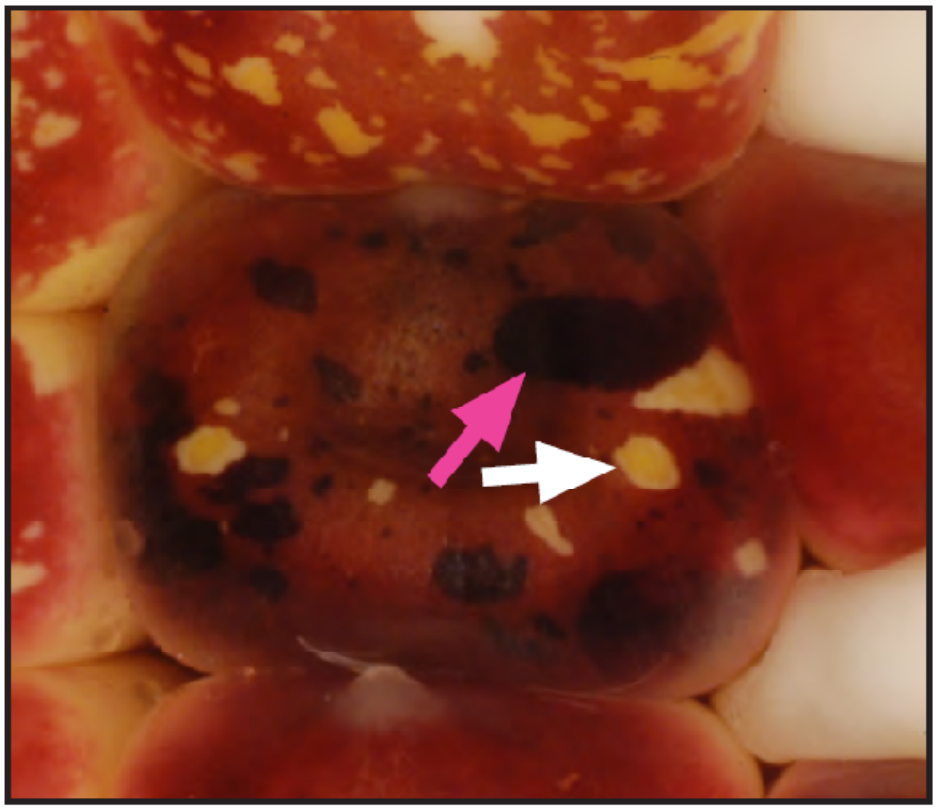

The *naked endosperm* genes encode duplicate ID domain transcription factors required for maize aleurone differentiation

Gibum Yi[1,2], Anjanasree K Neelakanda[1] and Philip W. Becraft[1,2,3]

A paper to be submitted to *Plant Cell*

[1.] Genetics, Development and Cell Biology Dept. Iowa State University, Ames, IA 50011
[2.] Interdepartmental Plant Biology Program, Iowa State University, Ames, IA 50011
[3.] Agronomy Dept., Iowa State University, Ames, IA 50011

Abstract

The outermost layer of the endosperm is a specific cell type called the aleurone which is one of the grain quality determining factors because of its high content in lipid, minerals and high quality proteins compared to starchy endosperm. The aleurone layer is also an attractive system to study cell fate determination because of the simplicity and plasticity of aleurone cell fate. Here we report the identification of *naked endosperm (nkd)* genes which are involved in aleurone differentiation in maize. The *nkd* mutant shows defects in aleurone cell identity and has approximately 3 outer cell layers instead of the single in WT. However these outer cells do not contain dense granular cytoplasm typical of normal aleurone and have sporadic expression of a *Vp1* promoter GUS transgene, which is an aleurone identity marker. The *nkd* mutant phenotype shows 15:1 segregation ratio in F_2 populations suggesting two recessive genes are involved in this phenotype. We performed map-based cloning and found two homologous genes in syntenic regions. The INDETERMINATE1 domain containing transcription factors *ZmIDDveg9* and *ZmIDD9* correspond to the *nkd1* and *nkd2* mutant genes on chromosomes 2 and 10, respectively. Independent

Ds transposon insertion alleles of *nkd1* and *nkd2*, *nkd1-Ds* and *nkd2-Ds* respectively, failed to complement the original *nkd* mutant. A *Nkd2*-RNAi line, in which both of *nkd* genes were knocked down, also showed the *nkd* mutant phenotype. The *nkd* transcripts were most abundant in developing kernels around 11 to16 days after pollination. The NKD proteins have putative nuclear localization signals as other IDD genes and GFP fusion proteins showed nuclear localization. The mutant phenotype and gene expression pattern suggest NKD functions in aleurone cell fate acquisition and differentiation.

Introduction

Cereal grains are essential for human beings as a food source and for value added industrial materials. The cereal grain is mainly composed of two products of double fertilization; the embryo and endosperm. The endosperm, comprising 70-90% of a grain, is the major source of nutrients and is an important breeding target for enhanced grain quality as people look for food with improved nutrition. Maize is a major cereal crop and a model system for seed biology. Maize endosperm has a contains four specialized cell types; starchy endosperm, aleurone, basal endosperm transfer layer, and embryo surrounding region (Becraft, 2001; Olsen, 2004c). The aleurone is the outermost layer of the endosperm, just beneath the pericarp. The aleurone layer accumulates storage molecules such as lipids, minerals and proteins as the seeds mature. In particular genotypes of maize, anthocyanin pigments specifically accumulate in the aleurone. Aleurone cells survive grain desiccation, while starchy endosperm

undergoes programmed cell death. At germination, the aleurone layer secretes hydrolases to digest storage molecules (starch and proteins) in the starchy endosperm. Accumulating reports show the aleurone provides important health benefits such as anti-cancer and anti-obesity activity (Fenech et al., 2005; Stewart and Slavin, 2009; Borowicki et al., 2010).

In addition to its practical importance, maize aleurone has experimental advantages as a system for studying cell fate decisions in endosperm development (reviewed in Becraft, 2011). Most cereal grains, including maize, have a single cell layer of aleurone. Barley has multiple layers, while one maize landrace was reported to have multilayer aleurone (Wolf et al., 1972a). Aleurone differentiation involves a single cell fate decision with starchy endosperm. Because the aleurone is the outmost layer in the endosperm, it is inferred that a positional signal must be involved in this cell fate decision (Olsen, 2004b). Cells in the periphery of the endosperm retain the plasticity to become either aleurone or starchy endosperm until the very last cell division in endosperm development (Becraft and Asuncion-Crabb, 2000b). Thus, the positional cues that specify aleurone identity are present throughout development.

The anthocyanin of the aleurone has historically been used as a great marker for maize genetics (Levy and Walbot, 1990). Anthocyanin biosynthesis which occurs after aleurone cells are differentiated is relatively well understood. However, the molecular mechanism of aleurone cell differentiation is not well understood. Observation of many aleurone mutants and cell lineage studies proposed that a positional cue and hierarchical genetic pathway controlled

aleurone cell fate (Becraft and Asuncion-Crabb, 2000b; Olsen, 2004b; Wisniewski and Rogowsky, 2004b). The *Cr4*, *Dek1* and S*al1* genes are the known players in aleurone differentiation pathway. *Dek1* is a positive regulator of aleurone cell fate and its loss of function mutant shows absence of aleurone layer (Sheridan and Neuffer, 1982; Becraft and Asuncion-Crabb, 2000b; Becraft et al., 2002b; Lid et al., 2002a). DEK1 is a calpain protease with membrane targeting signal and extracytosolic loop region (Lid et al., 2002a; Wang et al., 2003b; Johnson et al., 2008). A strong allele such as *dek1-388* eliminates aleurone completely while a weaker *dek1-D*, shows mosaic aleurone (Becraft et al., 2002b). *Crinkly4* is also a positive regulator. CR4 is a receptor like kinase, and *cr4* mutants show similar aleurone phenotypes to *dek1*(Becraft et al., 1996a). *Dek1* and/or *Cr4* may work as receptors for positional cues which induce and maintain aleurone cell specification. The *sal1*mutant has multiple aleurone layers, and the gene encode a Class E vacuolar sorting protein (Shen et al., 2003b). *Sal1*is hypothesized to act as a negative regulator of *Cr4* and/or *Dek1* (Shen et al., 2003b; Tian et al., 2007a). A negative regulator of aleurone cell fate *thk1* was recently reported (Yi et al., 2011). The loss of function mutant makes four to five layers of aleurone. The *thk1* is epistatic to *dek1* and double mutant sectors generated by chromosomal breakage in a *dek1* single mutant (aleuroneless) background show multiple layers of aleurone. Although a number of aleurone mutants were cloned and studied, the molecular mechanisms by which these protein specify aleurone identity are not understood and the molecules for positional the cue are also unknown.

Geisler-Lee *et al*. showed that aleurone cell identity was suppressed in a sandwich of endosperm cells within connated maize kernels induced in a transgenic line with the *SAG12* promoter deriving isopentenyl transferase, a cytokinin synthesizing enzyme. Nonconnated kernels in this line showed mosaic aleurone suggesting cytokinins influence aleurone development (Geisler-Lee and Gallie, 2005). Expression of the auxin transporter, ZmPIN1 is preferentially localized in the aleurone of normal kernels and treatment of developing kernels with the auxin transport inhibitor N-1-naphthylphthalamic acid (NPA) induced alterations in aleurone cell layer number (Forestan et al., 2010a; Becraft and Yi, 2011b). This shows that auxin may be an aleurone cell fate determinant.

The *vp1* gene is the most upstream known regulator of the anthocyanin biosynthesis pathway. VP1 is a required regulator for seed maturation and is controlled by abcisic acid (ABA) (Cao et al., 2007). ABA and gibberellic acid (GA) play major antagonistic roles in switching phase between seed maturation and dormancy versus germination and vivipary. VP1 is a transcription factor containing a B3-domain which binds the CATGCA, DNA element (Suzuki et al., 1997). The *vp1* gene is specifically expressed in embryo and aleurone cells allowing a *Vp1* promoter derived GUS reporter to be used for an aleurone marker.

Here we report a novel aleurone differentiation mutant, *naked endosperm* (*nkd*). Mutations in the duplicated INDETERMINATE1 Domain (ID domain, IDD) genes *iddveg9* and *idd9* cause the *nkd* phenotype. Gene function was confirmed by identification of an independent mutant allele and by RNAi induced gene

knock down. We propose that NKD proteins function as transcription factors controlling aleurone cell differentiation.

Results

The nkd genes are required for aleurone cell fate and cell differentiation

The *naked endosperm* (*nkd*) mutant maize kernels show aleuroneless or mosaic aleurone phenotypes as reported (Becraft and Asuncion-Crabb, 2000). In sections, *nkd* mutants have multiple (2-5) layers of peripheral endosperm cells that lack starch granules or other features of starchy endosperm. Yet, most of these cells do not have typical aleurone cell characteristics such as thick walls, dense cytoplasm, accumulation of anthocyanin pigments, or expression of the *Vp1pro-GUS* marker gene. Cells with typical aleurone features do form sporadically within the peripheral layers. Aleurone cells are more likely to form around the silk scar region, following a pattern that has been described for several mosaic aleurone mutants (Becraft et al., 1996a; Becraft and Asuncion-Crabb, 2000b; Becraft et al., 2002b; Becraft and Yi, 2011b).

Because the peripheral layers are distinct from starchy endosperm and sporadically acquire aleurone cell characteristics, the *nkd* mutant was interpreted as affecting the aleurone cell differentiation process (Becraft and Asuncion-Crabb, 2000b). However, the multiple layers of cells distinct from starchy endosperm, in contrast to the normal single layer of aleurone, indicate that *nkd* function is also required to restrict the number of peripheral cell layers. Therefore *nkd* appears

required for dual functions in the endosperm periphery, regulating cell fate specification and for cell differentiation.

Other pleiotropic aspects of nkd mutants

The endosperms of *nkd* mutant kernels often display an opaque phenotype instead of the normal translucency. Defects in several endosperm components can result in an opaque phenotype including deficiencies or imbalances in zein storage proteins. HPLC analysis showed no detectable difference in zein profiles between normal and mutant kernels (not shown) thus the basis of the endosperm opacity remains unknown.

Mutant kernels are also pale yellow or sometimes nearly white, indicating they are carotenoid deficient. There is also a propensity for vivipary in *nkd* mutant seeds. The disrupted expression of the *Vp1pro*-GUS marker indicates that the *nkd* functions upstream of *vp1* in the endosperm. When mutant embryos were stained for GUS activity, no qualitative difference in staining was detected (not shown). *Vp1* expression was therefore assayed by quantitative RT-PCR and found to be decreased in mutant kernels compared to wild type (WT; Fig. 4F).

Seed weight is decreased in the mutant. Hundred-kernel seed weights were measured for *nkd* mutant and WT in 5 samples from a segregating F_2 population. The mutant seed weight (26.8 +/-1.28 g) was only 73% of WT (36.5g +/-0.95g). Thus the *nkd* mutant seed appears to have reduced grain filling for which the basis is not clear (Fig.1L).

The *nkd* mutant seed showed decreased germination rates. Germination rates were assayed by planting triplicates of 230 WT and 230 *nkd* mutant kernels from F_2 populations. In the field, mutants showed 72% germination compared to 96% in WT, while in the greenhouse 80% of mutants germinated compared to 97.4% in WT (Fig. 1I). Seedling survival rate was lower in the mutant. Only 75% of geminated *nkd* plants remained viable 45 days after planting while 93% of WT survived (Fig. 1J). Approximately a quarter of the mutant plants were poorly developed and arrested at the 2-3 leaf stage. Mutant plants that survived to maturity were morphologically normal and produced the same number of nodes as wild type, although they grew slowly and showed a delay of 5 days to anthesis.

Map based cloning of the nkd genes

The *nkd* mutants show a 15:1 F_2 segregation ratio, which suggests that two unlinked recessive genes determine this phenotype. Because only the double homozygous mutant shows a phenotype it is likely that these two genes perform redundant functions. Crosses with B-A translocation lines (Beckett, 1978b) revealed that one of the *nkd* genes, designated *nkd1*, is located on the short arm of chromosome 2 (ch2S). A *nkd* mutant was crossed to translocation line TB-2Sb and hypoploid F_1 plants were self-pollinated. The F_2 showed a 3:1 segregation ratio compared to the 15:1 ratio observed for translocation lines involving other chromosome arms.

An F_2 mapping population was generated by crossing a *nkd* mutant to the H99 inbred line, and genomic DNA from 62 *nkd* F_2 seedlings was isolated. IDP

makers (Fu et al., 2006b) at 10cM intervals on ch2S, were tested for linkage and *nkd1* localized to about an 11 cM interval between IDP7746 and IDP1612. We increased the number of F_2 individuals to 170, and extracted genomic DNA directly from the kernels. To develop markers for fine mapping we used B73 genomic DNA sequence (Schnable et al., 2009) to design primers at the 5' and 3'UTRs of annotated genes. These primer pairs were screened for polymorphisms evident as size differences on agarose gels between the *nkd* and H99 parents. Markers polymorphic between parents were applied to the F_2 population. About 20% of designed primers were polymorphic in 1-2% agarose gels. Finally *nkd1* was mapped between markers 266H09-9/10 and 166I20-1/5. These markers have 5 recombinants out of 328 chromosomes and two recombinants out of 332 chromosomes respectively. The interval between these two markers was 385 kb in length in B73. According to *Zea mays* version 53.4a (AGPv1; maizesequence.org), there were 31 annotated genes in this region, 10 of which had no supporting evidence (i.e. no maize EST). 18 of them had weak support such as a single EST, mostly from LCM-dissected SAM tissue (Emrich et al., 2007; Ohtsu et al., 2007). The remaining three genes with strong support putatively encoded a *MuDR* transposase, a C2H2 zinc finger protein, and a DEAD-like helicase. Only two of these genes have homologues in *Sorghum* and only the C2H2 zinc finger protein gene has fully covered EST evidence.

To map the *nkd2* locus, we used the Sequenom MassARRAY ® system in a genome-wide assay of SNP markers that are polymorphic between B73 and Mo17 (Fu et al., 2006b; Liu et al., 2010a). The *nkd* mutant arose in a mongrel

genetic background; therefore, we used two different mapping populations to maximize SNP polymorphisms: BC_3F_2 for B73 and BC_2F_2 for Mo17. Bulked segregant analysis (BSA) was performed by mixing 12 WT and 12 *nkd* kernels each from 4 different ears (Total 48 WT and 48 mutants). Results showed linked SNP makers clustered on ch2 and ch10. Linkage to the *nkd* phenotype was confirmed with analysis of IDP markers on the ch10. The *nkd2* region on the long arm of chromosome10 (ch10L) was narrowed down to the interval between IDP8526 and IDP8334, which is approximately 1.7 Mb in B73 genome sequence.

According to the hypothesis that *nkd1* and *nkd2* genes are duplicate factors, we compared the entire annotated gene sets in the *nkd1* and *nkd2* regions. Only the C2H2 zinc finger gene from the *nkd1* region had a homologue in the *nkd2* interval. Therefore these two genes were considered as likely candidates. The genes are *ZmIDDveg9* (*nkd1*, GRMZM2G129261) and *ZmIDD9* (*nkd2*, GRMZM5G884137).

Sequence analysis of nkd1 and nkd2 mutant genes

The *nkd* mutant arose fortuitously in a mongrel genetic background during an unrelated genetic screen. To understand the nature of the mutations, the *nkd1* and *nkd2* mutant genes were PCR amplified, cloned and sequenced. For *nkd* , a total of 10876 bp (-3584 bp 5’ from the start codon to +1365 bp 3’ of the stop codon) were sequenced and 65 sequence differences (40 SNPs, 15 deletions, 10 insertions) were detected relative to the B73 sequence. One mutation caused an amino acid change that is likely to be significant. A C to T transition caused an

amino acid substitution (CAC→TAC, His→Tyr) at residue 102. This histidine is part of the C2H2 motif located on the first zinc finger of the IDD domain and is highly conserved among the IDD family (Colasanti et al., 2006). Other changes include a 13bp deletion in intron 2 and a 26 bp deletion 3' of the transcribed region. The 26 bp deletion was found to exist in the progenitor population (Data not shown) suggesting it is not a causal mutation.

For *nkd2*, 9219 bp (-3233 bp 5' from the start codon to +876 bp 3' of the stop codon) were sequenced. 73 sequence differences (44 SNPs, 14 deletions, 15 insertions) were detected. Of note was a copia-like retrotransposon insertion in the first exon. The insertion site showed well conserved 5bp (CACCG) target site duplication and long terminal repeats.

Genetic confirmation of the nkd genes

To test the hypothesis that the candidate genes corresponded to *nkd1* and *nkd2*, public resources were searched and a *Ds* transposon insertion allele (B.S08.0002) for *nkd1* was identified from the *Ac/Ds* project (Ahern et al., 2009). This mutant is henceforth referred to as *nkd1-Ds* while the original reference allele is designated *nkd1-R*. The *nkd1-Ds* heterozygotes (homozygous *Nkd2*+) were self pollinated and crossed as pollen donors to plants with the genotype *nkd1*/+; *nkd2*/ *nkd2*. Surprisingly one fourth of the seeds from this cross showed the *nkd* mutant phenotype. Since *nkd2* was uniformly heterozygous in the progeny, we hypothesized that the 3:1 segregation ratio follows the *nkd1* genotype and that kernels with *nkd1-Ds*/*nkd1* would have mutant phenotype.

Twelve WT and twelve mutant kernels were genotyped and all kernels showing a *nkd* mutant phenotype carried one original *nkd1-R* allele and one *nkd1-Ds* allele, while all the WT kernels had at least one *Nkd1*+ allele.

The failure of the independent *nkd1-Ds* allele to complement the original *nkd1* mutant confirmed the identity of *nkd1* as *IDDveg9.* Furthermore, these results also suggested there may be a dosage requirement for *nkd* gene function and that the *nkd1-R* allele may be hypomorphic, while *nkd1-Ds* is likely to be a stronger loss-of-function allele. Consistent with this, self pollinating *nkd1-Ds/+* showed 3:1 segregation with WT and a weak mutant phenotype; mutant kernels were opaque and rough textured.

Two independent *Ds* insertion alleles for *nkd2* (B.W06.0297, I.W06.0766) were available from the *Ac/Ds* project (Ahern et al., 2009) and named *nkd2-Ds0297*, *nkd2-Ds0779* respectively, while the original reference allele is designated *nkd2-R*. The *nkd2-0297* has a *Ds* insertion in the first intron (-499bp) and *nkd2-Ds0779* at -1215 bp in the putative promoter region. Each of these alleles was crossed to a *nkd1* single mutant, the resulting F1 was self pollinated, and the F_2 showed about 15:1 segregation ratios (757 WT : 42 *nkd* for *nkd2-Ds0297;*1062 WT : 84 *nkd* for *nkd2-Ds0766)*. From the non visible *nkd1-R* kernel phenotype and the 15 : 1 ratio, the *nkd* phenotype of these can be explained by *nkd1-R, nkd2-Ds* alleles double mutation. Therefore independent mutations in the *IDD9* gene fail to complement the *nkd1-R* mutant, confirming the identity of *nkd2* as *IDD9*.

RNAi suppression with nkd2 confers a *nkd* mutant phenotype

Maize transgenic RNAi lines were developed using *nkd2* (*IDD9*) so as to downregulate *nkd* gene expression and examine the resultant phenotype. The ID domain encoded by exons 1-3 is highly conserved, so to minimize the likelihood of targeting other members of the IDD family, only the fourth exon was used for the RNAi construct. The *nkd2* fourth exon shares 87% nucleotide identity with *nkd1* but is unique among other IDD genes in maize. We obtained T2 seeds from 5 independent events (G1, G7, G9, G11, and G14) which were crossed to three different inbreds (B73, W22, H99). Lines from 3 events showed aleurone phenotypes mimicking the original *nkd* mutant (Fig. 3B). One line (G7) showed a strong phenotype that segregated 354:281 (WT: mutant). Each of these three independent lines was analyzed for inheritance of the transgene and co-segregation with the mutant phenotype. All individuals showing the *nkd*-like aleurone phenotype carried the transgene however, some kernels carrying the transgene showed normal phenotypes, possibly due to transgene silencing.

The independent lines G7-1 and G9-2 were selected for *Nkd* expression analysis using real time RT-PCR. In both lines, a reduction in both *Nkd2* and *Nkd1* transcript abundance was observed in transgenic seedlings with respect to the control, untransformed siblings (FIG. 4E). This could be attributed to the conservation in nucleotide sequence of the fourth exon between the two maize paralogs leading to concomitant transcript downregulation. The G7-1 line showed the strongest mutant seed phenotype as well as the strongest suppression of *Nkd* expression, as compared to the other events. The recapitulation of the *nkd*

mutant seed phenotype by RNAi suppression further supports the identification of the *nkd1* and *nkd2* genes as *IDDveg9* and *IDD9*, respectively. Because the original report of the *nkd* mutant (Becraft et al., 2000) predated the first report of the IDD gene family (Colasanti et al., 2006), we use the *nkd1* and *nkd2* designations.

Characteristics of the IDD proteins encoded by the nkd genes

The predicted proteins encoded by the *nkd* genes contain ID domains, consisting of four C2H2 zinc fingers, that define the IDD family (Colasanti et al., 2006). The founding member of IDD gene family, INDETERMINATE1 (ID1), shows a late flowering phenotype and is the only gene of this family with known mutant phenotype in maize (Singleton, 1946; Colasanti et al., 1998; Colasanti et al., 2006). The two *nkd* genes showed high homology (81% identity/ 84% positive) in overall amino acid sequence. The predicted NKD1 protein contains 588 amino acids with a calculated molecular weight of 61 kD. NKD2 contains 599 amino acids with a molecular weight of 62 kD. In addition to the ID domains, these proteins contain predicted N-terminal nuclear localization signals, and 2 conserved motifs of unknown function in the C-terminal domain (Colasanti et al., 2006).

nkd gene expression

Transcript levels of *nkd1* and *nkd2* were examined by RT-PCR. A basal level of *nkd* gene expression was detected in all tissue we tested. However the expression level was very low in root and tassel. The *nkd* genes were most abundantly expressed in kernels and showed higher expression in endosperm than in embryo. The *nkd1* gene expression gradually increased from 7 DAP (days after pollination) and peaked about 15 DAP, whereas *nkd2* peaked at 11 DAP.

Transcript levels in *nkd* mutants were examined by real time RT-PCR. As shown in Figure 4D, *nkd1* transcript levels were decreased in *nkd1-R* single mutant and *nkd1-R; nkd2-R* double mutant, but increased expression was observed in the *nkd2-R* single mutant. The *nkd2* transcript levels were decreased in *nkd1-R; nkd2-R* double mutants, but expression levels in *nkd2-R* single mutants were similar to WT. Both *nkd1* and *nkd2* were more highly expressed in each other's mutant backgrounds than in WT suggesting that compensatory mechanisms might regulate transcript levels. No *nkd1* transcript was detected in *nkd1-Ds* mutants suggesting this likely represents a null allele (Fig. 4C).

Nuclear localization of NKD-GFP fusion proteins

Both predicted NKD proteins have putative nuclear localization signals (KKKR) as do other IDD proteins. To experimentally verify the nuclear localization of the NKD1 and 2 proteins, NKD-GFP translational fusion constructs were generated for both proteins and transiently expressed in onion bulb

epidermal cells. As expected, the fusion proteins showed localization in nuclei as ascertained by accumulation of green fluorescence (Fig. 5).

Discussion

In this study, we identified the *nkd1* and *nkd2* genes by map-based cloning as duplicated members of the IDD family. Because of the mongrel genetic background in which the mutation arose, and the high levels of sequence polymorphisms compared to the B73 sequence, it was not possible to unequivocally identify the causal lesions. However, a H→Y substitution in the highly conserved C2H2 motif of the first zinc finger of *nkd1* and a retrotransposon insertion in the first exon of *nkd2* are likely candidates. An independent *nkd1-Ds* allele failed to complement original *nkd* mutant phenotype and *nkd2-Ds0297, nkd2-Ds0766* alleles similarly failed to complement the *nkd1* mutant. Furthermore, the mutant phenotype was reproduced by generating *nkd2*-RNAi transgenic lines, confirming the correct identity of these genes.

The *nkd* mutant showed 2-5 layers of undifferentiated aleurone cells as well as floury, opaque endosperm. As previously reported (Becraft and Asuncion-Crabb, 2000b), the original mutant segregated 15:1 in the F_2 due to the duplicated genes, with only the double homozygous mutant showing a phenotype. A single mutant homozygote for the *nkd1-Ds* allele showed rough textured endosperm and undifferentiated aleurone-like cells and careful examination of the original *nkd1-R* single mutant showed a subtle effect on aleurone layer

number with sporadic development of double layers. These phenotypes of *nkd1* mutants were enhanced as doses of the *nkd2* mutant allele were added. The *nkd1-Ds* allele, which has a *Ds* transposon insertion within coding sequences of the fourth exon, is thought to be a null mutant and showed a stronger phenotype than the *nkd1-R* reference allele. However the *nkd2* single mutant did not show any phenotypic defect. This might be explained by the higher expression level of *nkd1* transcript (Fig. 4D) or perhaps the *nkd2* allele is not a null and retains sufficient function for normal development.

The *nkd1* and *nkd2* genes are located in a duplicated region of the genome. Interestingly, the syntenic regions of chromosomes 2 and 10 that contain *nkd1* and *nkd2* also contain the duplicate maize floricaula/leafy homologs (Bomblies et al., 2003; Colasanti et al., 2006). Other cereals including sorghum and rice only have one copy of the *nkd* (IDD9) gene, whereas this clade of IDD proteins is absent from Arabidopsis (Colasanti et al., 2006).

NKD1 and NKD2 have conserved ID domains with two C2H2 and two C2HC zinc finger motifs, consistent with their DNA binding activity and roles as transcription factors (Kozaki et al., 2004; Colasanti et al., 2006). The *nkd1* gene corresponds to *ZmIDDveg9*, although it is misannotated in the B73 genome assembly v2. *ZmIDDveg9* was cloned by screening a cDNA library generated from the vegetative apex using a probe consisting of the region coding the ID domain in the *id1* (Colasanti et al., 2006). They showed by electrophoretic mobility shift assay (EMSA) that ZmIDDveg9 binds the same DNA sequence elements as ID1, albeit with somewhat different properties. The *ZmIDDveg9*

transcript was detected in the apical region and immature leaf by RNA blot but they did not examine kernel samples. In the same study, NKD2 was described as ZmIDD9. Because the *nkd* mutant (Becraft and Asuncion-Crabb, 2000b) was reported prior to the description of the IDD family (Colasanti et al., 2006), we chose to refer to these factors as NKD1 and NKD2.

The expression profile portrayed for *nkd1* by public microarray data available at PLEXDB (Sekhon et al., 2011; Dash et al., 2012) was consistent with the results of this study. Transcripts for *nkd1*were detected in most tissues examined but most abundantly in kernels. In kernels, *nkd1* is expressed at higher levels in endosperm than in embryo. During kernel development, the expression level gradually increased from 6 to 16 DAP and then plateaued until 24 DAP (Sekhon et al., 2011).

The IDD gene family has high conservation in the putative nuclear localization signal (KKKR) as well as the zinc finger motifs of the ID domain. ID1 was nuclear localized in a transfection assay of onion epidermal cells (Wong and Colasanti, 2007). Here, nuclear localization was demonstrated for NKD proteins by detecting NKD-GFP fusion proteins in nuclei of onion epidermal cells in a transfection assay (Fig. 5I-M). Thus, we conclude that NKDs are nuclear localized proteins, and very likely function as transcription factors.

In the *nkd1*mutant, *nkd2* transcripts were elevated compared to WT, whereas in the *nkd2* mutant *nkd1* transcripts were elevated (Fig. 4D). This suggests a feedback mechanism is involved in compensatory regulation of *nkd* genes. By aligning promoter regions of *nkd1* and *nkd2* genomic sequences, it

was found that approximately 1.3 kb of *nkd1* and 1 kb of *nkd2* are conserved with 75% identity, suggesting conserved regulatory functions. We can also find two motifs that resemble the consensus binding sequence defined for ID1 and shown to bind NKD1/IDDveg9 (Colasanti et al., 2006). For *nkd1*, TTTTGTTGTTTT and TTTTGTTAATCT occur at position -563 with a 58 bp interval, while for *nkd2* TTTTGTTGTCTT, TTTTGTTTAATC occur at position -528 with a 60 bp interval. Thus it is an intriguing possibility that these genes might autoregulate, or be controlled by other IDD family members.

The *indeterminate1* gene is the only other IDD family member with a known mutant in maize. The loss of function mutant of *id1* causes late flowering or the complete inability to flower in maize (Colasanti et al., 1998). Mutants of IDD8 in *Arabidopsis* also show delayed flowering time (Seo et al., 2011a). This could be related to altered sugar metabolism as sugar levels and 2 sucrose synthase gene transcript levels were altered in *idd8* mutants, IDD8 directly binds the SUS4 promoter and is itself transcriptionally regulated by sugar levels. The *nkd* mutant also showed delayed flowering time without any change in total leaf number. It is not yet clear whether late flowering is simply due to slow growth or other flowering time gene regulation.

The complete B73 sequence (Schnable et al., 2009) reveals the IDD gene family in maize contains 17 members, instead of the 13 originally identified by cDNA cloning (Colasanti et al., 2006). In Arabidopsis there are 16 IDD genes and phylogentic analysis shows that there are monocot and dicot-specific clades

(Colasanti et al., 2006). Although IDD proteins share high similarity in their N-terminal ID domains, other parts of the proteins vary substantially. This suggests the functions of IDD genes are also likely to be diverse and genetic studies in *Arabidopsis* support this. Five Arabidopsis *idd* mutants have been linked with gene functions through mutant phenotype. In addition to *idd8*, *idd14* also affected carbohydrate metabolism, showing inhibited starch metabolism (Seo et al., 2011b). The *SHOOT GRAVITROPHISM5 (SGR5)* gene turned out allelic to AtIDD15 (Tanimoto et al., 2008). AtIDD1 was recently reported as ENHYDROUS, functioning to promote seed germination (Feurtado et al., 2011). Functional relationships among the IDD genes in dicots and monocots remains to be elucidated.

The molecular mechanism of *nkd* genes' functions remain to be studied. Studying downstream genes of *nkd* will provide new understanding in aleurone differentiation and will give more opportunities to improve cereal grain quality.

Materials and Methods

Plant materials

The *nkd* mutant was crossed to H99 and Mo17 and following F_2 populations were used for mapping and germination rate observation. The *nkd* mutant backcrossed to B73 and Mo17 inbreds three times was used for sequenom assays. The RT-PCR and western analysis was performed using B73

BC5 introgressed *nkd* mutant and WT B73. The *nkd1-Ds* allele was identified in stock # B.S08.0002 and *nkd2-Ds0297*, *nkd2-Ds0766* was identified in stock # B.W06.0297, I.W06.0766 from the *Ac/Ds* project (Ahern et al., 2009).

Genetic mapping

Genomic DNA for mapping was extracted from seedling or seed as described (Yi et al., 2011).

The IDP markers were used for mapping as described (Fu et al., 2006b). Additional PCR markers were developed by PCR amplifying 3' or 5' UTR regions of predicted gene models and identifying size polymorphisms between parents by running amplification products on 2% agarose gels. The primers for polymorphic markers are listed on Table1.

Sequencing

For each *nkd1* and *nkd2* loci, six fragments of around 2 kb were amplified from *nkd* mutant genomic template DNA. Primers are listed supplementary Table 1. The PCR amplicons were cloned by StrataClone PCR Cloning Kit™ (Agilent, USA) and sequenced at Iowa State University DNA facility. At least 3 different clones were sequenced per fragment and compared with the B73 reference genome sequence. Only when all three clones showed the same difference with reference sequence, it was considered as valid.

Subcellular localization of GFP fusion protein

Full length CDS of *nkd1* and *nkd2* were amplified from cDNA clones (Zm-BFc0139A11 and Zm-BFb0091K24 from Arizona Genomic Institute) by PCR with primers 2ZNF-Xba1,

2ZNF-BamH1 for *nkd1* and 10ZNF-Xba1, 10ZNF-BamH1 for *nkd2* (supplementary Table1). XbaI and BamHI digested PCR products were then cloned into the pJ4GFP-XB (Igarashi et al., 2001) and confirmed by sequencing. Gold particles coated with 1ug of each plasmid DNA was bombarded into onion epidermal cell and incubated 3 hours at room temperature. The slides were observed with Olympus BX-60 microscope equipped with a Chromatek GFP filter and a Jenoptik C-5 camera.

RT-PCR

RNA extraction and cDNA synthesis was performed as described (Myers et al., 2011). The ubiqitin primers (Lee et al., 2009) were used for both RT-PCR and real time RT-PCR as a control. PCRs parameters included 94^{o}C 4 min followed by 30-35 cycles of 94 ^{o}C 30 sec, 55 ^{o}C 30 sec, 72 ^{o}C 60 sec and a 72 ^{o}C 10 min final extension. PCR products were then visualized in 1% agarose gel electrophoresis. The existing *vp1* primers (Cao et al., 2007) used for RT-PCR and newly designed VP1-RT3 and VP1-RT4 were used for real time RT-PCR. Quantified RT PCR was performed with a Mx4000 (Stratagen) real time PCR machine and iQ™ SYBR Green Supermix (Bio-Rad). Primers were listed in supplementary Table 1.

RNAi lines

The *nkd2* fourth exon was PCR amplified from B73 template DNA using 2 sets of primers tailed with different pairs of restriction enzyme sites. Primers 10ZNF3EF-Avr2/10ZNF3ER-Asc1 and 10ZNF3EF-Xma1/10ZNF3ER-Spe1 are listed in supplementary Table 1. These fragments were cloned into pMCG1005 (McGinnis et al., 2005) in sense and antisense directions with corresponding restriction enzyme digestion and ligation and their sequences confirmed. The vector was transformed into EHA101 by freezing thawing method and construct-containing clones were confirmed by plasmid isolation and PCR. Agrobacterium mediated transformation was performed at Plant Transformation Facility (PTF, Iowa State University). The RNAi plantlets were recovered and crossed to inbred lines for analysis.

Transgenic line genotyping was done by PCR using the forward primer specific to the waxy intron (Waxy GK-1) and the reverse primer complementary to the *Nkd2* fourth exon (10ZNF-13). Amplification was performed with Go Taq green master mix (Promega) at an annealing temperature of 52 ^{o}C, with other parameters as described above. As an internal control, primers specific to the endogenous *Nkd1* gene (291F22-5 and 2ZNF-5) were employed with an annealing temperature of 55 ^{o}C. The amplicon sizes were around 500 bp and 900 bp respectively for the transgene and the endogenous gene. For expression analysis, RNA was isolated from 1 week old seedlings using RNeasy Plant Mini kit (Qiagen). All primer sequences are listed in supplementary Table 1.

Acknowledgements

The authors thank members of the Becraft lab for helpful discussions of the manuscript. Thanks to Julie Meyer, Jordon Pace for their contributions to the genetic mapping. This research was supported by NSF grant IOS-1121738. The following Iowa State University facilities provided technical assistance: the Microscopy and NanoImaging Facility assisted with some of the microscopic preparations, the Genomic Technologies Facility provided the mass array SNP genotyping and the Plant Transformation Facility generated transgenic RNAi lines.

References

Ahern, K.R., Deewatthanawong, P., Schares, J., Muszynski, M., Weeks, R., Vollbrecht, E., Duvick, J., Brendel, V.P., and Brutnell, T.P. (2009). Regional mutagenesis using Dissociation in maize. Methods **49,** 248-254.

Beckett, J.B. (1978). B-A TRANSLOCATIONS IN MAIZE .1. USE IN LOCATING GENES BY CHROMOSOME ARMS. Journal of Heredity **69,** 27-36.

Becraft, P.W. (2001). Cell fate specification in the cereal endosperm. Seminars in Cell & Developmental Biology **12,** 387-394.

Becraft, P.W., and Asuncion-Crabb, Y. (2000). Positional cues specify and maintain aleurone cell fate in maize endosperm development. Development **127,** 4039-4048.

Becraft, P.W., and Yi, G. (2011). Regulation of aleurone development in cereal grains. Journal of Experimental Botany **62,** 1669-1675.

Becraft, P.W., Stinard, P.S., and McCarty, D.R. (1996). CRINKLY4: A TNFR-like receptor kinase involved in maize epidermal differentiation. Science **273,** 1406-1409.

Becraft, P.W., Li, K.J., Dey, N., and Asuncion-Crabb, Y. (2002). The maize dek1 gene functions in embryonic pattern formation and cell fate specification. Development **129,** 5217-5225.

Bomblies, K., Wang, R.L., Ambrose, B.A., Schmidt, R.J., Meeley, R.B., and Doebley, J. (2003). Duplicate FLORICAULA/LEAFY homologs zfl1 and zfl2 control inflorescence architecture and flower patterning in maize. Development **130,** 2385-2395.

Borowicki, A., Stein, K., Scharlau, D., Scheu, K., Brenner-Weiss, G., Obst, U., Hollmann, J., Lindhauer, M., Wachter, N., and Glei, M. (2010). Fermented wheat aleurone inhibits growth and induces apoptosis in human HT29 colon adenocarcinoma cells. British Journal of Nutrition **103,** 360-369.

Cao, X.Y., Costa, L.M., Biderre-Petit, C., Kbhaya, B., Dey, N., Perez, P., McCarty, D.R., Gutierrez-Marcos, J.F., and Becraft, P.W. (2007). Abscisic acid and stress

signals induce viviparous1 expression in seed and vegetative tissues of maize. Plant Physiology **143,** 720-731.

Colasanti, J., Yuan, Z., and Sundaresan, V. (1998). The indeterminate gene encodes a zinc finger protein and regulates a leaf-generated signal required for the transition to flowering in maize. Cell **93,** 593-603.

Colasanti, J., Tremblay, R., Wong, A.Y.M., Coneva, V., Kozaki, A., and Mable, B.K. (2006). The maize INDETERMINATEI flowering time regulator defines a highly conserved zinc finger protein family in higher plants. Bmc Genomics **7**.

Dash, S., Van Hemert, J., Hong, L., Wise, R.P., and Dickerson, J.A. (2012). PLEXdb: gene expression resources for plants and plant pathogens. Nucleic Acids Research **40,** D1194-D1201.

Emrich, S.J., Barbazuk, W.B., Li, L., and Schnable, P.S. (2007). Gene discovery and annotation using LCM-454 transcriptome sequencing. Genome Research **17,** 69-73.

Fenech, M., Noakes, M., Clifton, P., and Topping, D. (2005). Aleurone flour increases red-cell folate and lowers plasma homocyst(e)ine substantially in man. British Journal of Nutrition **93,** 353-360.

Feurtado, J.A., Huang, D.Q., Wicki-Stordeur, L., Hemstock, L.E., Potentier, M.S., Tsang, E.W.T., and Cutler, A.J. (2011). The Arabidopsis C2H2 Zinc Finger INDETERMINATE DOMAIN1/ENHYDROUS Promotes the Transition to Germination by Regulating Light and Hormonal Signaling during Seed Maturation. Plant Cell **23,** 1772-1794.

Forestan, C., Meda, S., and Varotto, S. (2010). ZmPIN1-Mediated Auxin Transport Is Related to Cellular Differentiation during Maize Embryogenesis and Endosperm Development. Plant Physiology **152,** 1373-1390.

Fu, Y., Wen, T.J., Ronin, Y.I., Chen, H.D., Guo, L., Mester, D.I., Yang, Y.J., Lee, M., Korol, A.B., Ashlock, D.A., and Schnable, P.S. (2006). Genetic dissection of intermated recombinant inbred lines using a new genetic map of maize. Genetics **174,** 1671-1683.

Gallavotti, A., Yang, Y., Schmidt, R.J., and Jackson, D. (2008). The relationship between auxin transport and maize branching. Plant Physiology **147,** 1913-1923.

Geisler-Lee, J., and Gallie, D.R. (2005). Aleurone cell identity is suppressed following connation in maize kernels. Plant Physiology **139,** 204-212.

Gomez, E., Royo, J., Muniz, L.M., Sellam, O., Paul, W., Gerentes, D., Barrero, C., Lopez, M., Perez, P., and Hueros, G. (2009). The Maize Transcription Factor Myb-Related Protein-1 Is a Key Regulator of the Differentiation of Transfer Cells. Plant Cell **21,** 2022-2035.

Igarashi, D., Ishida, S., Fukazawa, J., and Takahashi, Y. (2001). 14-3-3 proteins regulate intracellular localization of the bZIP transcriptional activator RSG. Plant Cell **13,** 2483-2497.

Johnson, K.L., Faulkner, C., Jeffree, C.E., and Ingram, G.C. (2008). The Phytocalpain Defective Kernel 1 Is a Novel Arabidopsis Growth Regulator Whose Activity Is Regulated by Proteolytic Processing. Plant Cell **20,** 2619-2630.

Kozaki, A., Hake, S., and Colasanti, J. (2004). The maize ID1 flowering time regulator is a zinc finger protein with novel DNA binding properties. Nucleic Acids Research **32,** 1710-1720.

Lee, B.H., Johnston, R., Yang, Y., Gallavotti, A., Kojima, M., Travencolo, B.A.N., Costa, L.D., Sakakibara, H., and Jackson, D. (2009). Studies of aberrant phyllotaxy1 Mutants of Maize Indicate Complex Interactions between Auxin and Cytokinin Signaling in the Shoot Apical Meristem. Plant Physiology **150,** 205-216.

Levy, A.A., and Walbot, V. (1990). REGULATION OF THE TIMING OF TRANSPOSABLE ELEMENT EXCISION DURING MAIZE DEVELOPMENT. Science **248,** 1534-1537.

Lid, S.E., Gruis, D., Jung, R., Lorentzen, J.A., Ananiev, E., Chamberlin, M., Niu, X.M., Meeley, R., Nichols, S., and Olsen, O.A. (2002). The defective kernel 1 (dek1) gene required for aleurone cell development in the endosperm of maize grains encodes a membrane protein of the calpain gene superfamily. Proceedings of the National Academy of Sciences of the United States of America **99,** 5460-5465.

Liu, S., Chen, H.D., Makarevitch, I., Shirmer, R., Emrich, S.J., Dietrich, C.R., Barbazuk, W.B., Springer, N.M., and Schnable, P.S. (2010). High-Throughput Genetic Mapping of Mutants via Quantitative Single Nucleotide Polymorphism Typing. Genetics **184,** 19-U51.

McGinnis, K., Chandler, V., Cone, K., Kaeppler, H., Kaeppler, S., Kerschen, A., Pikaard, C., Richards, E., Sidorenko, L., Smith, T., Springer, N., and Wulan, T. (2005). Transgene-induced RNA interference as a tool for plant functional genomics. In Rna Interference, D.R. Engelke and J.J. Rossi, eds (San Diego: Elsevier Academic Press Inc), pp. 1-24.

Morrison, I.N., Obrien, T.P., and Kuo, J. (1978). INITIAL CELLULARIZATION AND DIFFERENTIATION OF ALEURONE CELLS IN VENTRAL REGION OF DEVELOPING WHEAT-GRAIN. Planta **140,** 19-30.

Myers, A.M., James, M.G., Lin, Q., Yi, G., Stinard, P.S., Hennen-Bierwagen, T.A., and Becraft, P.W. (2011). Maize opaque5 Encodes Monogalactosyldiacylglycerol Synthase and Specifically Affects Galactolipids Necessary for Amyloplast and Chloroplast Function. Plant Cell **23,** 2331-2347.

Ohtsu, K., Smith, M.B., Emrich, S.J., Borsuk, L.A., Zhou, R.L., Chen, T.L., Zhang, X.L., Timmermans, M.C.P., Beck, J., Buckner, B., Janick-Buckner, D., Nettleton, D., Scanlon, M.J., and Schnable, P.S. (2007). Global gene expression analysis of the shoot apical meristem of maize (Zea mays L.). Plant Journal **52,** 391-404.

Olsen, O.A. (2004a). Nuclear endosperm development in cereals and Arabidopsis thaliana. Plant Cell **16,** S214-S227.

Olsen, O.A. (2004b). Dynamics of maize aleurone cell formation: The "surface-"rule. Maydica **49,** 37-40.

Santoni, V. (2007). Plant plasma membrane protein extraction and solubilization for proteomic analysis. Methods in Molecular Biology **355,** 93-109.

Schnable, P.S., Ware, D., Fulton, R.S., Stein, J.C., Wei, F.S., Pasternak, S., Liang, C.Z., Zhang, J.W., Fulton, L., Graves, T.A., Minx, P., Reily, A.D., Courtney, L., Kruchowski, S.S., Tomlinson, C., Strong, C., Delehaunty, K., Fronick, C., Courtney, B., Rock, S.M., Belter, E., Du, F.Y., Kim, K., Abbott, R.M., Cotton, M., Levy, A., Marchetto, P., Ochoa, K., Jackson, S.M., Gillam, B., Chen, W.Z., Yan, L., Higginbotham, J., Cardenas, M., Waligorski, J., Applebaum, E., Phelps, L., Falcone, J., Kanchi, K., Thane, T., Scimone, A., Thane, N., Henke, J., Wang, T., Ruppert, J., Shah, N., Rotter, K., Hodges, J., Ingenthron, E., Cordes, M., Kohlberg, S., Sgro, J., Delgado, B., Mead, K., Chinwalla, A., Leonard, S., Crouse, K., Collura, K., Kudrna, D., Currie, J., He, R.F., Angelova, A., Rajasekar, S., Mueller, T., Lomeli, R., Scara, G., Ko, A., Delaney, K., Wissotski, M., Lopez, G., Campos, D., Braidotti, M., Ashley, E., Golser, W., Kim, H., Lee, S., Lin, J.K., Dujmic, Z., Kim, W., Talag, J., Zuccolo, A., Fan, C., Sebastian, A., Kramer, M., Spiegel, L., Nascimento, L., Zutavern, T., Miller, B., Ambroise, C., Muller, S., Spooner, W., Narechania, A., Ren, L.Y., Wei, S., Kumari, S., Faga, B., Levy, M.J., McMahan, L., Van Buren, P., Vaughn, M.W., Ying, K., Yeh, C.T., Emrich, S.J., Jia, Y., Kalyanaraman, A., Hsia, A.P., Barbazuk, W.B., Baucom, R.S., Brutnell, T.P.,

Carpita, N.C., Chaparro, C., Chia, J.M., Deragon, J.M., Estill, J.C., Fu, Y., Jeddeloh, J.A., Han, Y.J., Lee, H., Li, P.H., Lisch, D.R., Liu, S.Z., Liu, Z.J., Nagel, D.H., McCann, M.C., SanMiguel, P., Myers, A.M., Nettleton, D., Nguyen, J., Penning, B.W., Ponnala, L., Schneider, K.L., Schwartz, D.C., Sharma, A., Soderlund, C., Springer, N.M., Sun, Q., Wang, H., Waterman, M., Westerman, R., Wolfgruber, T.K., Yang, L.X., Yu, Y., Zhang, L.F., Zhou, S.G., Zhu, Q., Bennetzen, J.L., Dawe, R.K., Jiang, J.M., Jiang, N., Presting, G.G., Wessler, S.R., Aluru, S., Martienssen, R.A., Clifton, S.W., McCombie, W.R., Wing, R.A., and Wilson, R.K. (2009). The B73 Maize Genome: Complexity, Diversity, and Dynamics. Science **326,** 1112-1115.

Sekhon, R.S., Lin, H.N., Childs, K.L., Hansey, C.N., Buell, C.R., de Leon, N., and Kaeppler, S.M. (2011). Genome-wide atlas of transcription during maize development. Plant Journal **66,** 553-563.

Seo, P.J., Ryu, J., Kang, S.K., and Park, C.M. (2011a). Modulation of sugar metabolism by an INDETERMINATE DOMAIN transcription factor contributes to photoperiodic flowering in Arabidopsis. Plant Journal **65,** 418-429.

Seo, P.J., Kim, M.J., Ryu, J.Y., Jeong, E.Y., and Park, C.M. (2011b). Two splice variants of the IDD14 transcription factor competitively form nonfunctional heterodimers which may regulate starch metabolism. Nature Communications **2**.

Shen, B., Li, C.J., Min, Z., Meeley, R.B., Tarczynski, M.C., and Olsen, O.A. (2003). sal1 determines the number of aleurone cell layers in maize endosperm and encodes a class E vacuolar sorting protein. Proceedings of the National Academy of Sciences of the United States of America **100,** 6552-6557.

Sheridan, W.F., and Neuffer, M.G. (1982). MAIZE DEVELOPMENTAL MUTANTS - EMBRYOS UNABLE TO FORM LEAF PRIMORDIA. Journal of Heredity **73,** 318-329.

Singleton, W.R. (1946). INHERITANCE OF INDETERMINATE GROWTH IN MAIZE. Journal of Heredity **37,** 61-64.

Stewart, M.L., and Slavin, J.L. (2009). Particle size and fraction of wheat bran influence short-chain fatty acid production in vitro. British Journal of Nutrition **102,** 1404-1407.

Suzuki, M., Kao, C.Y., and McCarty, D.R. (1997). The conserved B3 domain of VIVIPAROUS1 has a cooperative DNA binding activity. Plant Cell **9,** 799-807.

Suzuki, M., Latshaw, S., Sato, Y., Settles, A.M., Koch, K.E., Hannah, L.C., Kojima, M., Sakakibara, H., and McCarty, D.R. (2008). The maize Viviparous8 locus, encoding a putative ALTERED MERISTEM PROGRAM1-like peptidase, regulates abscisic acid accumulation and coordinates embryo and endosperm development. Plant Physiology **146,** 1193-1206.

Tanimoto, M., Tremblay, R., and Colasanti, J. (2008). Altered gravitropic response, amyloplast sedimentation and circumnutation in the Arabidopsis shoot gravitropism 5 mutant are associated with reduced starch levels. Plant Molecular Biology **67,** 57-69.

Tian, Q., Olsen, L., Sun, B., Lid, S.E., Brown, R.C., Lemmon, B.E., Fosnes, K., Gruis, D.F., Opsahl-Sorteberg, H.G., Otegui, M.S., and Olsen, O.A. (2007). Subcellular localization and functional domain studies of DEFECTIVE KERNEL1 in maize and Arabidopsis suggest a model for aleurone cell fate specification involving CRINKLY4 and SUPERNUMERARY ALEURONE LAYER1. Plant Cell **19,** 3127-3145.

Wang, C.X., Barry, J.K., Min, Z., Tordsen, G., Rao, A.G., and Olsen, O.A. (2003). The calpain domain of the maize DEK1 protein contains the conserved catalytic triad and functions as a cysteine proteinase. Journal of Biological Chemistry **278,** 34467-34474.

Wisniewski, J.P., and Rogowsky, P.M. (2004). Vacuolar H+-translocating inorganic pyrophosphatase (Vpp1) marks partial aleurone cell fate in cereal endosperm development. Plant Molecular Biology **56,** 325-337.

Wolf, M.J., Zuber, M.S., Cutler, H.C., and Khoo, U. (1972). MAIZE WITH MULTILAYER ALEURONE OF HIGH PROTEIN CONTENT. Crop Science **12,** 440-&.
Wong, A.Y.M., and Colasanti, J. (2007). Maize floral regulator protein INDETERMINATE1 is localized to developing leaves and is not altered by light or the sink/source transition. Journal of Experimental Botany **58,** 403-414.
Yi, G., Lauter, A.M., Scott, M.P., and Becraft, P.W. (2011). The thick aleurone1 Mutant Defines a Negative Regulation of Maize Aleurone Cell Fate That Functions Downstream of defective kernel1. Plant Physiology **156,** 1826-1836.

Figure legends

Figure 1. Anaylysis of the *nkd* mutant phenotype. **A.** *nkd* mutants show 15:1 F_2 segregation. **B.** *nkd* mutant kernels show sporadic pigmentation. Wild type (**F, G, H**) endosperm contains a single layer of aleurone cells while the *naked endosperm (nkd)* mutant (**C, D, E**) disrupts aleurone differentiation. The peripheral layer of *nkd* mutant is distinct from starchy endosperm but has not differentiated the typical attributes of aleurone, including dense cytoplasm, thick cell walls and cuboidal shape. **C, F.** Histological section with starch grains stained pink with PAS. Protein-dense aleurone is darkly stained with toluidine blue. **D, G.** Scanning electron microscopy. **E, H.** Expression of a *Vp1*-GUS reporter specifically in aleurone cells. The *Vp1-GUS* reporter shows sporadic expression in *nkd* mutant. **I, J.** Wild type and *nkd* mutants from segregating F_2 kernels were planted and germination rate and survival rate were measured in the field. Only 72% of *nkd* mutants germinated (96% in WT) and 76% of germinated *nkd* mutants survived (over 93% in WT) after 39 days. **K.** The difference of flowering time was 5 days between *nkd2* and *nkd* double mutants ($P<.001$). However *nkd1* and *nkd* mutant did not show a significant difference. The number of total leaves did not have any significant difference. **L.** Weight of

100 kernels for *nkd* mutant was significantly less than wild type. (P<.001). Scale bars = 100 µm.

Figure 2. *nkd* gene structure and alleles. *nkd1-R* allele has an amino acid change (H→Y) at residue 102. The *nkd1-Ds* allele has a *Ds* insertion in the 4th exon. The *nkd2-R* allele contains a copia-like retrotransposon insertion in the first exon.

Figure 3. *nkd1-Ds* and *Nkd2*-RNAi show *nkd* mutant phenotypes **A.** *nkd1-Ds*/+ self-pollinated ear showed 3:1 segregation for kernels with weak *nkd* phenotypes and rough textured opaque endosperm, associated with *nkd1-Ds* homozygotes . Arrows indicate mutant kernels. **B.** *Nkd2*-RNAi line (G7-1) shows 1:1 ratio of WT : *nkd* phenotype. Mutant kernels show wrinkled endosperm. **C.** Section of *nkd1-Ds* homozygous kernel shows irregular double layer aleurone **D.** *Nkd2*-RNAi mutant kernel section shows, irregular double layer aleurone. **E.** Different *nkd* mutants show different levels of *nkd* phenotypes in terms of doubled aleurone. Degree of *nkd* phenotype strength was measured as % of double layered aleurone. Kernels were scored by counting about 150 aleurone cells across the crown of the kernel and calculating the ratio of secondary aleurone cells as a percent. *nkd1-R* sometimes showed multiple layers of aleurone. *nkd1-Ds* allele has a stronger phenotype than *nkd1-R*. The phenotype became stronger when *nkd2-R* was added.

Figure 4. Transcript expression analysis **A.** The *nkd1* transcript was detected in all tissues tested. However abundance was very low in root and

tassel. It was most highly expressed in kernels. The *nkd2* transcript was detected in leaf tissues and ear and most highly in kernels. **B.** The *nkd* transcript expression pattern in developing kernels. Both *nkd* transcripts were highly expressed at 11 days after pollination after which *nkd2* declined. **C.** The *nkd1* transcript was not detected in 11 DAP *nkd1-Ds* homozygous kernels suggesting it could be a null allele. **D.** *nkd1, nkd2* transcript levels were quantified by real time RT- PCR. In *nkd* mutant both *nkd1* and *nkd2* transcripts were decreased. Higher expression of *nkd1* in *nkd2* mutant suggests potential feedback regulation of the *nkd* genes. **E.** *Nkd2*-RNAi shows reduced transcript level for both *nkd1* and *nkd2* in independent events, G7-1 and G9-2. **F.** Reduced *vp1* transcript level in *nkd* mutant suggests NKD is required to regulate *vp1*.

Figure 5. Nuclear localization of NKD proteins. **A-F.** Subcellular localization of NKD-GFP fusion proteins showed nuclear localization of NKD. **A, D.** Empty vector GFP control. **B, E.** NKD1-GFP. **C, F.** NKD2-GFP. **A-C.** DIC optics. **D-F.** GFP fluorescence. Arrows indicate nuclei. Scale bars = 100 µm.

Supplementary figure legends

Figure S1. Complementation test with *nkd1-Ds* allele. **A.** Cross performed for the complementation test. Note that all the progeny are *nkd2*/+ heterozygous from the cross maternal *nkd2/nkd2* and paternal +/+. Four different progeny genotypes can be identified by marker analysis. WT *Nkd1-B73* can be distinguished from *nkd1-R* and *Nkd1-W22* by susceptibility to *Hin*dIII digestion of

the PCR product produced by primer pair 1/2. The *Ds* insertion allele was detected by PCR with *Ds* specific primer 3 and gene specific primer 1. **B.** Ears derived from the designated cross segregated 3:1 for WT : mut. 12WT kernels and 12 mutant kernels were selected for genotyping. **C.** Genotyping for 12 WT and 12 *nkd* kernels. All the mutant kernels inherited *nkd1-R,* as indicated by lack of *Hin*dIII digestion of the maternal allele, and *nkd1-Ds* as indicated by amplification with the Ds-specific primer 3. All the WT kernels inherited either the *Nkd1-B73* maternal allele, the *Nkd1-W22* paternal allele or both.

Table S1. Primers used in this study

Primer	Sequence	Used for
491I18-7h99f	CAGCTAAAAGTGGGAGCGCGC	Mapping
491I18-7h99r	TGCTAGTGCTAGTGCTACCTAT	Mapping
190B15-6	ACGTGCCTCTGACATGTGGGTCAC	Mapping
190B15-7	CCGATCTCTTGCGATGCATCGAG	Mapping
266H09-9	CGTGAGCTGGACATTTTACAG	Mapping
266H09-10	GTGCATACGGGTCTTCATAGTAC	Mapping
166I20-1	AGAACGAGAAGGGGACCTCATAA	Mapping
166I20-5	TCCCTCCATTCCATTGATTAAGATG	Mapping
2ZNF-Xba1*	acgt*tctagA*TGGCATCGAATTCATCGGCG	GFP fusion
2ZNF-BamH1*	tgac*ggatcc*TGGCATCCTGCCTCCGTTGAAG	GFP fusion
10ZNF-Xba1*	acgt*tctagA*TGGCGTCGAATTCACCGGCG	GFP fusion
10ZNF-BamH1*	tgac*ggatcc*TGGCATCCTGCCTCCATTGAAG	GFP fusion
10ZNF3EF-Avr2*	agg*cctagg*GAGGGACAGCTTCATCACG	RNAi
10ZNF3ER-Asc1*	tca*ggcgcgcc*TCATGGCATCCTGCCTCCA	RNAi
10ZNF3EF-Xma1*	tca*cccggg*GAGGGACAGCTTCATCACG	RNAi
10ZNF3ER-Spe1*	agg*actagt*TCATGGCATCCTGCCTCCA	RNAi
291F22-5	CATATATGAGTCTGCGGGTG	RT PCR
291F22-7	TGCTGCCGCAGATGTCGGCGACA	RT PCR
291F22-8	TCGGTCATGGCATCCTGCCTCCG	RT PCR, Sequencing
2ZNF-5	GATTCCGGTCGTGCATGCACACTGC	RT PCR
2ZNF-8	CTGTGTGACATGGAGCACGAGGT	RT PCR
10ZNF-12	TACCGCTGCGACTGCGGCACGC	RT PCR
10ZNF-13	AGGCTTGTTGGCCTGCAGCTGAA	RT PCR
10ZNF-17	CGACATGGCGGAGCGCGAGGG	RT PCR
10ZNF-2	TCTGTCATGGCATCCTGCCTCCA	RT PCR
Nkd2F209	CTCTGACTAATGGAGCAGTAAGCTG	RT PCR
Nkd2R317	CAACAAGAACGAGACCAGCAGAAT	RT PCR
VP1-RT3	CTTCAGATAAGCGGCAGGG	RT PCR
VP1-RT4	CCAAAACCTGTACCGCATG	RT PCR
Waxy GK-1	CCAGTTCAAATTCTTTTAGGCTCACC	RT PCR
N1atgB-F*	tgac*ggatcc*GGGACAGCTTCATCACACACCG	Antibody, Sequencing
N1atgE-R*	acgt*gaattc*TCATGGCATCCTGCCTCCGTTG	Antibody
N2atgB-F*	tgac*ggatcc*GGGACAGCTTCATCACGCACCG	Antibody, Sequencing
N2atgE-R*	acgt*gaattc*TCATGGCATCCTGCCTCCATTG	Antibody
N1intr3-1	AGGTAGTAACGGCGTGTGTGAGT	Sequencing
N1intr3-2	ACTCACACACGCCGTTACTACCT	Sequencing
2ZNFg-1	GATGTTTCCATTTGGGGCCAGCCATTTTAT	Sequencing
2ZNFg-2	GGTGAAAAAGGTCCCTTCATGCTTGTCAAA	Sequencing
2ZNF-1	ACCCCGACGCTGAGGTGATCGCG	Sequencing
2ZNF-2	CTGGAGAAGAGTGTGCCGCAGTCGCAT	Sequencing
2ZNF-9	TCGGGAGGAAGTGATGGCATCGAATTCATCGG	Sequencing
291F22-6	CCGATGAATTCGATGCCATCACTT	Sequencing
NKD1U-1	CGTGCAGGATGCTCACTATGTTGGC	Sequencing
NKD1U-2	GGCTGGCCCCAAATGGAAACATC	Sequencing
10ZNF-1	ATGGCGTCGAATTCACCGGCGGC	Sequencing
10ZNFg-2	ACCTCCATCTTCCCAAAATAAATGCAAGTGCA	Sequencing
10ZNF-18	GCCGCCGGTGAATTCGACGCCAT	Sequencing

N2intr2-1	TCTTTCCTCCCTATCTAGTTCGAGGTG	Sequencing
N2intr2-2	CACCTCGAACTAGATAGGGAGGAAAGA	Sequencing
N2ex4-1	GTTAGCAAAGAAACCCAGGCTGAAG	Sequencing
NKD2U-1	GCCATGCGTGTTACGTACGTGC	Sequencing
NKD2U-3	GTGTACGCTTGCTATACTCCGAC	Sequencing
NKD2U-6	TGGATGTGGTTTTGACAAACA	Sequencing
copiaLRT-1	CATAGTCACAGCGATTCCAGTC	Sequencing

* Additional sequences were written in lower case and restriction enzyme sites are *italic*.

Fig. 1

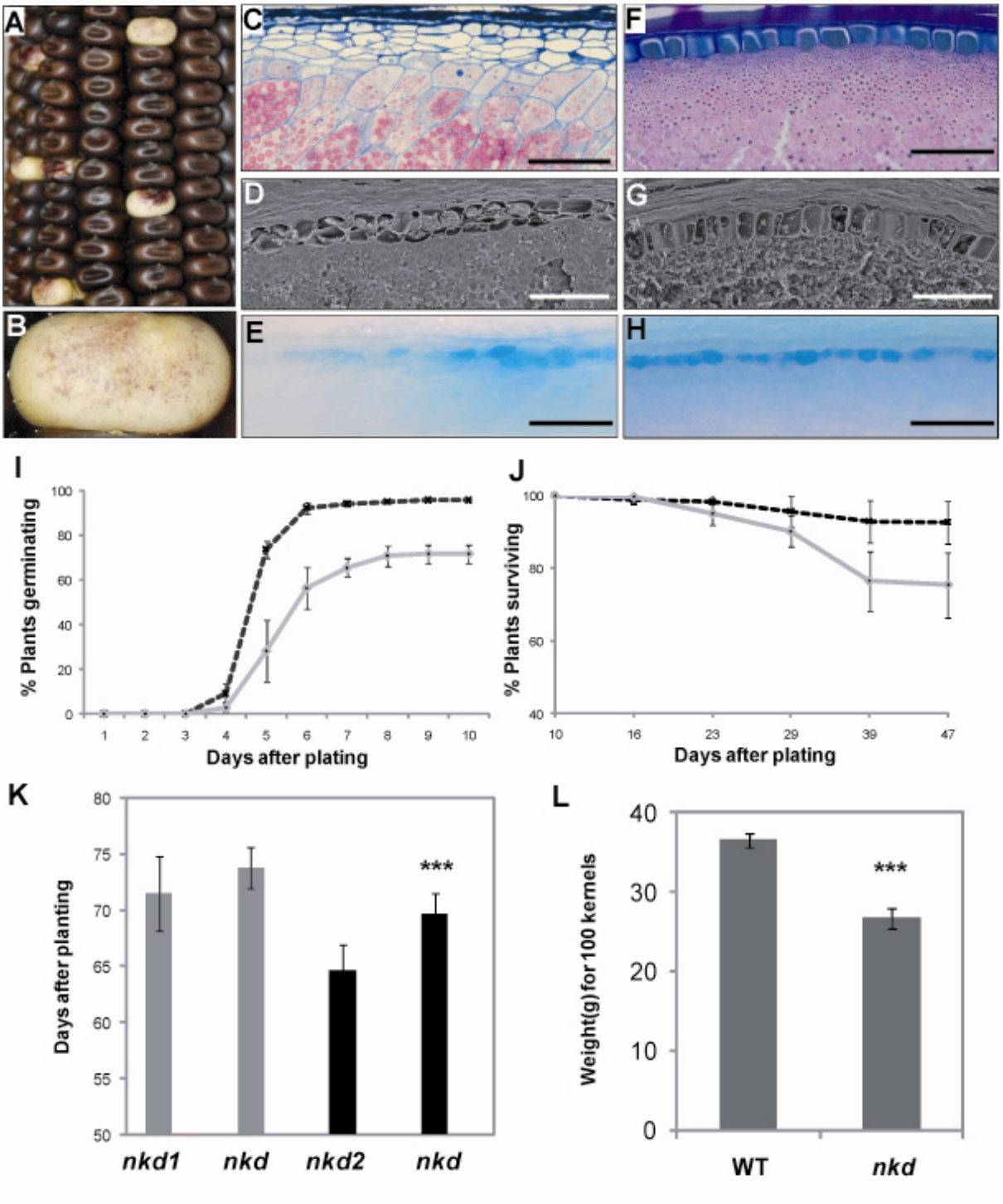
A
B
C
D
E
F
G
H
I
% Plants germinating
Days after plating
J
% Plants surviving
Days after plating
K
Days after planting
***
nkd1
nkd
nkd2
nkd
L
Weight(g) for 100 kernels
***
WT
nkd

Fig. 2

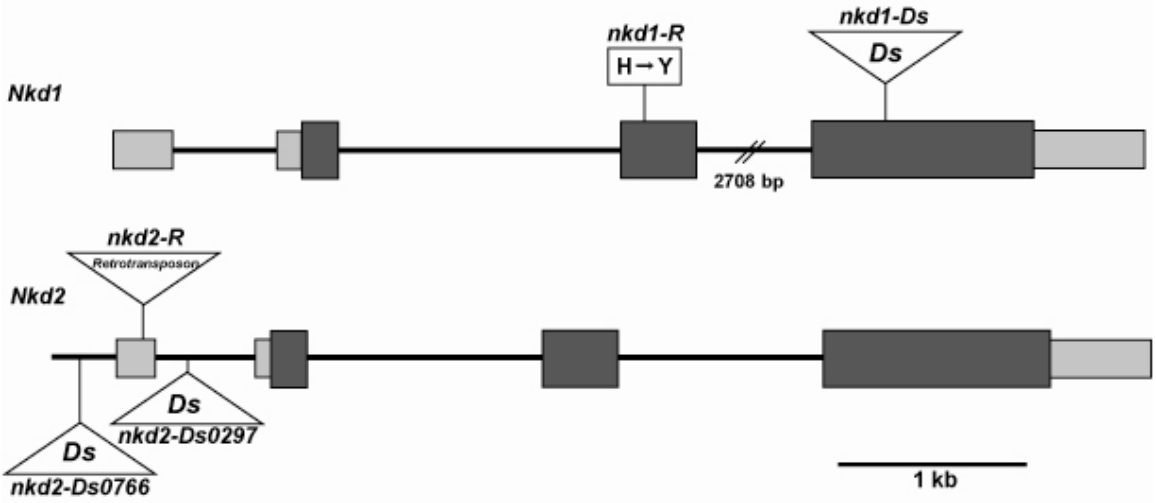
nkd1-R
H→Y
nkd1-Ds
Ds
Nkd1
2708 bp
nkd2-R
Retrotransposon
Nkd2
Ds
nkd2-Ds0297
Ds
nkd2-Ds0766
1 kb

Fig. 3

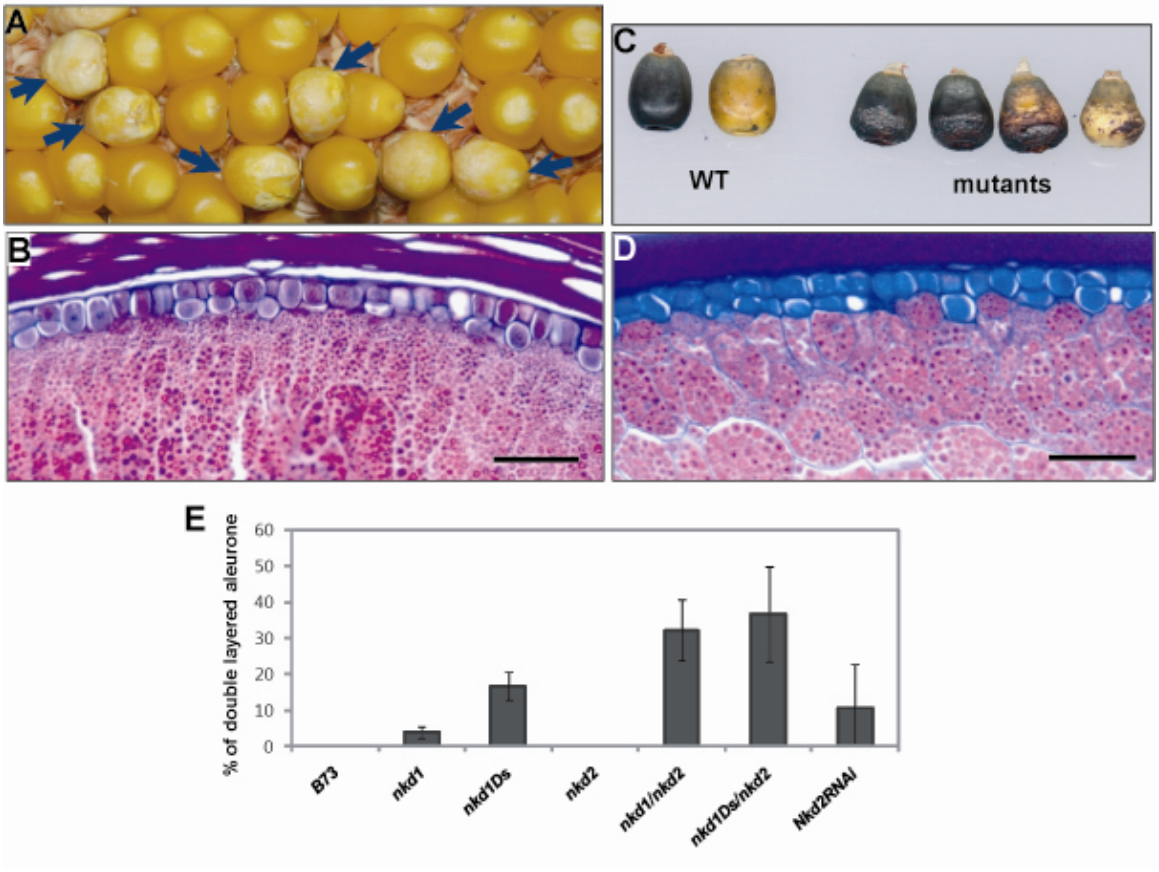
A
C
WT
mutants
B
D
E
% of double layered aleurone
60
50
40
30
20
10
0
B73
nkd1
nkd1Ds
nkd2
nkd1/nkd2
nkd1Ds/nkd2
Nkd2RNAi

Fig. 4

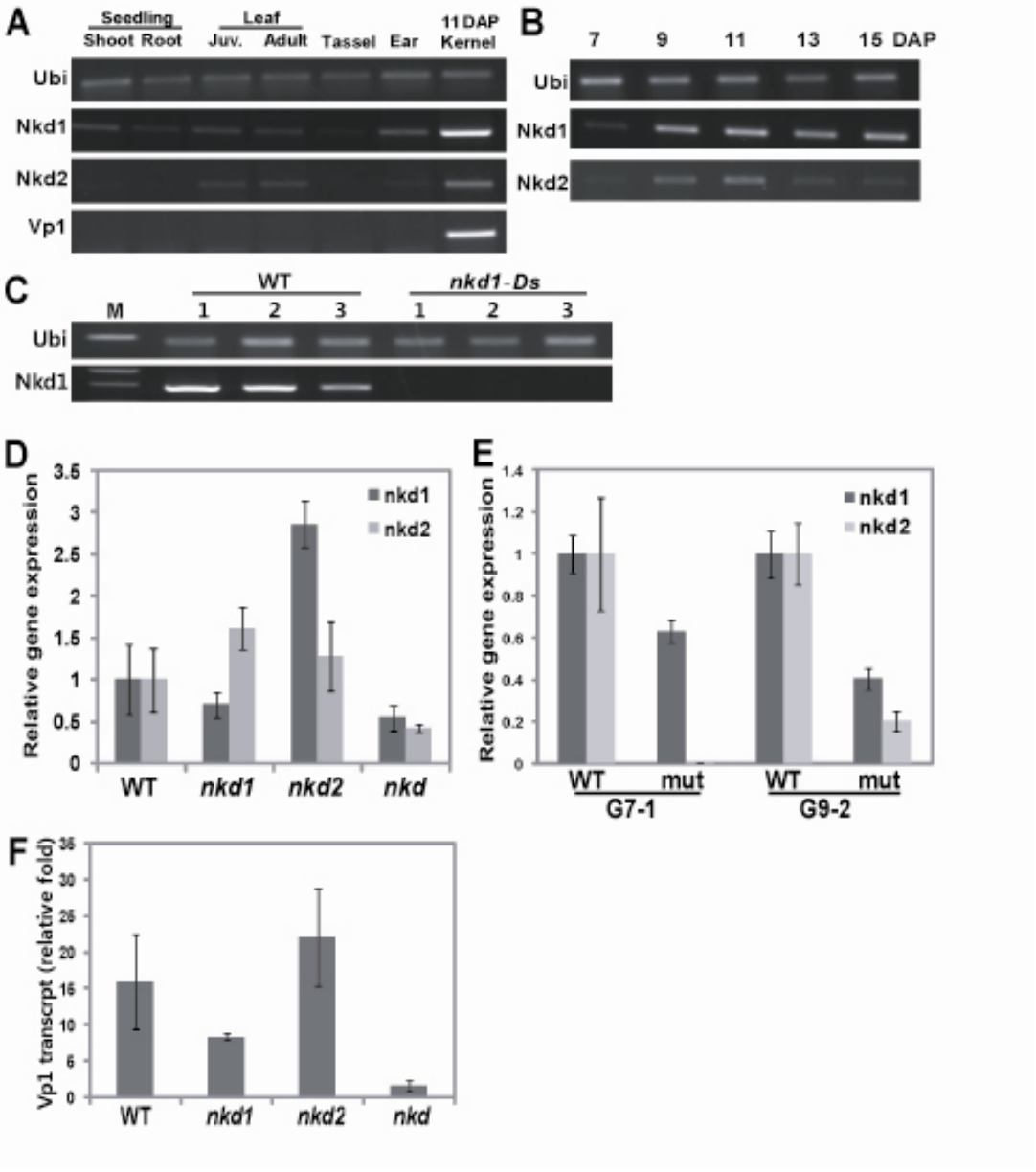
A
Seedling
Shoot Root
Leaf
Juv. Adult
Tassel
Ear
11 DAP Kernel
Ubi
Nkd1
Nkd2
Vp1
B
7 9 11 13 15 DAP
Ubi
Nkd1
Nkd2
C
WT
nkd1-Ds
M 1 2 3 1 2 3
Ubi
Nkd1
D
Relative gene expression
nkd1
nkd2
WT nkd1 nkd2 nkd
E
Relative gene expression
nkd1
nkd2
WT mut WT mut
G7-1 G9-2
F
Vp1 transcrpt (relative fold)
WT nkd1 nkd2 nkd

Fig. 5

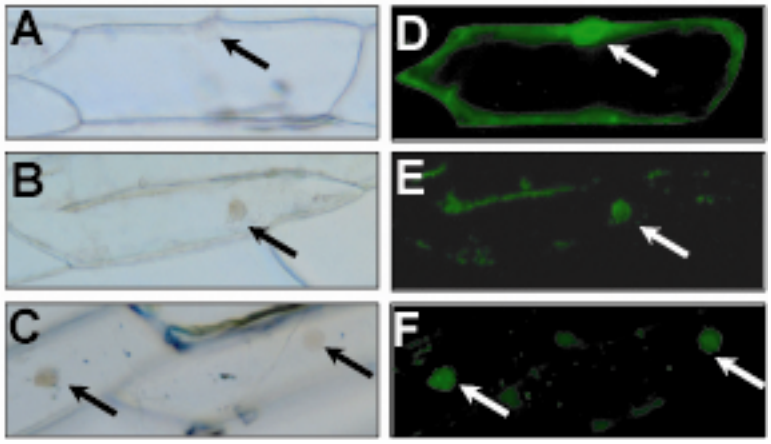

Fig. S1

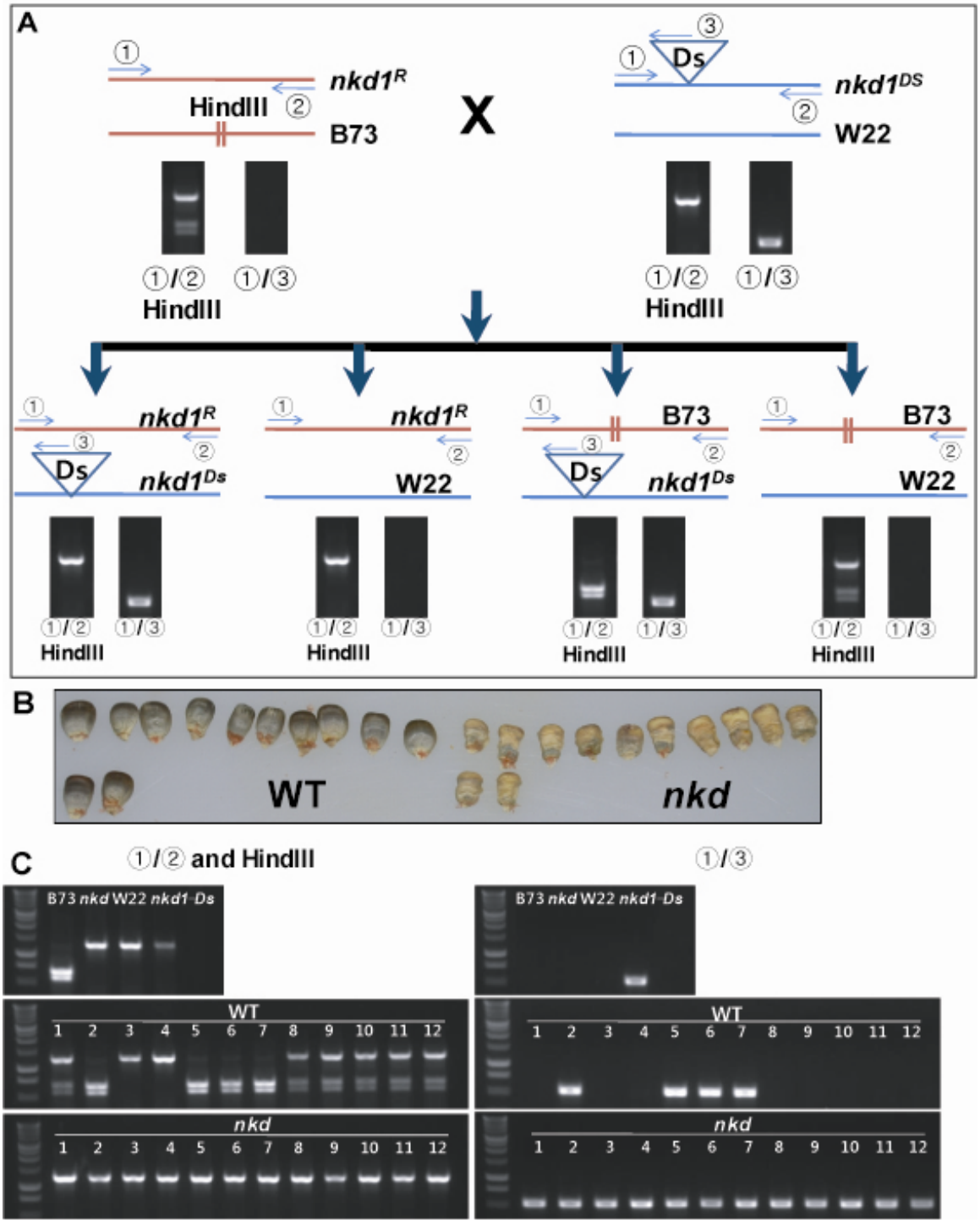
A
nkd1R
HindIII
B73
X
Ds
nkd1DS
W22
①/②
①/③
HindIII
B
WT
nkd
C
①/② and HindIII
①/③
B73 nkd W22 nkd1-Ds
WT
nkd
1 2 3 4 5 6 7 8 9 10 11 12

CHAPTER 5. General conclusions

The main questions of this thesis are how the cells get the aleurone cell fate and how the cells differentiate to aleurone in maize endosperm. Previous studies suggest that positional signals specify aleurone cell fate and it remains plastic throughout development. After the cell gets aleurone cell fate, following genetic hierarchy controls aleurone cell differentiation (Becraft and Asuncion-Crabb, 2000; Becraft and Yi, 2011). Studies of the aleurone development mutant would give us a better understanding of the aleurone cell development. With the convenience of the aleurone anthocyanin marker, it is possible to do an efficient screening for aleurone mutants with large scale mutagenesis. For high throughput screening of aleurone mutants we developed improved method for detecting *Mu* insertion site which was described in chapter 2. And the studies about two novel aleurone mutants were presented in the following chapter 3 and 4.

In chapter 2, the 96-well based method for *Mu* insertion cloning named MuTA was developed (Yi et al., 2009). Mutant specific *Mu* insertion can be determined by bulked segregant analysis (BSA) approach. Genomic DNA from four mutants and four wild type plants was digested with four different 4-6 cutter restriction enzymes and adapters were ligated. After two round of TAIL-PCR with the adapter primers and the *Mu* specific primers, PCR products were labeled with the four different fluorescent markers. Mixture of four fluorescent labeled PCR products were size analyzed by a capillary sequencer. If the mutant

specific DNA fragments were found, the *Mu* franking sequence was obtained by cloning and sequencing of the PCR product. We tested this method with fifteen *Mu* induced endosperm mutants and we could identify co-segregating *Mu* insertion from seven of them. One of the mutants was successfully cloned and characterized and published (Myers et al., 2011).

In chapter 3, the *thk1* mutants which have multiple layers of aleurone were characterized (Yi et al., 2011). The *thk1* mutant was embryo lethal with arrested embryo development after transition stage. The multiple layers of aleurone showed clear aleurone identities such as shape, lack of starch accumulation, thick cell wall with auto fluorescence and expression of *Vp1*-GUS transgene. The *thk1* locus was located on chromosome 1 short arm by bulked segregants analysis and about 2 Mb of deletion at the distal end of chromosome1 short arm was detected. This result suggests that the *thk1* phenotype could be a multiple gene effect. The *thk1* sectors were generated with *Ds* induced chromosome breakage. The *thk1* sectors showed sharp boundaries and no *thk1* sector which is surrounded by starchy endosperm cell was detected. We concluded that the additional aleurone cell should be connected to epidermal aleurone cell to receive the positional signal and the signal is more likely to be cell autonomous. Genetic interaction with *dek1* which is a positive regulator of aleurone cell fate was studied. Double mutant phenotype which was not distinguishable with *thk1* single mutant reveals that *thk1* is epistatic to *dek1*. This epistasis was found not only in the extra aleurone cell layer number but also in the pleotrophic phenotypes such as zein composition. The *thk1* and *dek1* double

mutant sectors which were generated with *Ds* induced chromosome breakage confirmed that that *thk1* is down stream of *dek1* in the genetic hierarchy. Several multilayered aleurone mutant were reported in maize such as *sal1*, *Xcl*, *Mal* etc. (Miranda, 1980; Kessler et al., 2002; Shen et al., 2003). However *thk1* mutant has more number of aleurone layers which is stable and well differentiated with normal starchy endosperm. We are trying to clone this gene with several mutagenesis methods such as EMS, uniform *Mu* and *Ds* transposon remobilization (Settles et al., 2007; Ahern et al., 2009). We have obtained five EMS alleles and one *Mu* allele, characterization of this putative *thk1* allele is underway.

In chapter 4, the *nkd* mutant which has multiple layer of undifferentiated aleurone was studied. Multiple layers of aleurone phenotype and undifferentiated aleurone of *nkd* mutant suggest that *nkd* genes function both in aleurone cell fate acquisition and differentiation. IDD9 (GRMZM2G12926, *nkd1*) and IDDveg9 (GRMZM5G884137, *nkd2*) were turned out to be the mutant genes for *nkd* by positional cloning. The complementation test with independent *nkd1-Ds* allele and phenotype of *Nkd2*- RNAi confirmed that the genes were correct. As a member of IDD gene family which is characterized with its four zinc finger DNA binding motif and putative nuclear localization signal, we assumed the *Nkd* genes function as transcription factors. The GFP fused NKD protein were biolistically introduced into onion epidermal cell and show nuclear localization. The effort to identify downstream genes which are directly regulated by *nkd* is

under way. Downstream genes of *nkd* gene will unveil the molecular regulation of aleurone cell fate determination and aleurone cell differentiation.

References

Ahern, K.R., Deewatthanawong, P., Schares, J., Muszynski, M., Weeks, R., Vollbrecht, E., Duvick, J., Brendel, V.P., and Brutnell, T.P. (2009). Regional mutagenesis using Dissociation in maize. Methods **49,** 248-254.

Becraft, P.W., and Asuncion-Crabb, Y. (2000). Positional cues specify and maintain aleurone cell fate in maize endosperm development. Development **127,** 4039-4048.

Becraft, P.W., and Yi, G. (2011). Regulation of aleurone development in cereal grains. Journal of Experimental Botany **62,** 1669-1675.

Kessler, S., Seiki, S., and Sinha, N. (2002). Xcl1 causes delayed oblique periclinal cell divisions in developing maize leaves, leading to cellular differentiation by lineage instead of position. Development **129,** 1859-1869.

Miranda, L.T.d. (1980). Inheritance and linkages of multiple aleurone layering. Maize Genetics Cooperation News Letter**,** 15-18.

Myers, A.M., James, M.G., Lin, Q., Yi, G., Stinard, P.S., Hennen-Bierwagen, T.A., and Becraft, P.W. (2011). Maize opaque5 Encodes Monogalactosyldiacylglycerol Synthase and Specifically Affects Galactolipids Necessary for Amyloplast and Chloroplast Function. Plant Cell **23,** 2331-2347.

Settles, A.M., Holding, D.R., Tan, B.C., Latshaw, S.P., Liu, J., Suzuki, M., Li, L., O'Brien, B.A., Fajardo, D.S., Wroclawska, E., Tseung, C.W., Lai, J.S., Hunter, C.T., Avigne, W.T., Baier, J., Messing, J., Hannah, L.C., Koch, K.E., Becraft, P.W., Larkins, B.A., and McCarty, D.R. (2007). Sequence-indexed mutations in maize using the UniformMu transposon-tagging population. Bmc Genomics **8**.

Shen, B., Li, C.J., Min, Z., Meeley, R.B., Tarczynski, M.C., and Olsen, O.A. (2003). sal1 determines the number of aleurone cell layers in maize endosperm and encodes a class E vacuolar sorting protein. Proceedings of the National Academy of Sciences of the United States of America **100,** 6552-6557.

Yi, G., Lauter, A.M., Scott, M.P., and Becraft, P.W. (2011). The thick aleurone1 Mutant Defines a Negative Regulation of Maize Aleurone Cell Fate That Functions Downstream of defective kernel1. Plant Physiology **156,** 1826-1836.

Yi, G., Luth, D., Goodman, T.D., Lawrence, C.J., and Becraft, P.W. (2009). High-throughput linkage analysis of Mutator insertion sites in maize. Plant Journal **58,** 883-892.

ACKNOWLEDGEMENTS

The last five years was the happiest time in my life. First of all, I got the name ‘scientist’ which has been my dream from when I was a kid. I still have questions that ‘Am I a scientist right now?’ or ‘From when I was a scientist?’ However it is clear at least that I passed an important checkpoint to be a scientist. Secondly, I could do research and study which I always liked to do without major concerns. Third, in the last five years my twin babies were grown up to be 5-year old boys.

All of these were possible with the help of lots of people. I would like to thank all of them but I am also worry that I may miss any of them in this acknowledgments.

My advisor, Dr. Becraft, he supported and encouraged me all the time. And to me, he is the role model as a scientist and as a teacher. I deeply thank him. I also thank other members of my POS committee: Drs. Diane Bassham, Erik Vollbrecht, Paul Scott, and Yanhai Yin for their invaluable guidance and encouragement.

I was lucky to work with such nice lab members both past and present, especially Joonbae Seo, Gokhan Kir, Dr. Yongsun Moon, Dr. Anjanasree Neelakanda, Bryan Gontarek, Dr. Antony Chettoor and undergraduate students; Jordon Pace, Maradi Pho. I also thank my Plant Biology Major classmates.

I thank my father in law, Nakjoong Sung, who passed away in 2010, I am sorry that we could not spend more time together when he was fighting with the cancer. I also thank my mother in law.

I thank my parents Bongsung Lee, Jungsuk Han, for their thoughtfulness.

My wife, Guiyoung Sung, she is the greatest. She takes care of two boys and me with love and patience. I thank her for all the support, encouragement, and understanding.

I dedicate this thesis to my wife and parents.